THE SPICY, THE EVERLASTING AND THE UNEXPECTED: INVESTIGATING THREE COMPOUNDS THAT SUPPRESS MACROPHAGES AND MYOFIBROBLASTS TO REDUCE BIOMATERIAL-INDUCED FIBROSIS

THE SPICY, THE EVERLASTING AND THE UNEXPECTED: INVESTIGATING THREE COMPOUNDS THAT SUPPRESS MACROPHAGES AND MYOFIBROBLASTS TO REDUCE BIOMATERIAL-INDUCED FIBROSIS

By

TICH H TRUONG, B.Eng.Biosci.

A Thesis

Submitted to the School of Graduate Studies

in Partial Fulfillment of the Requirements

for the Degree

Master of Applied Science

McMaster University
© Copyright by Tich H Truong, December 2016

Master of Applied Science (2016)
Department of Chemical Engineering

McMaster
University
Hamilton, Ontario

TITLE: The Spicy, the Everlasting and the Unexpected: Investigating Three Compounds That Suppress Macrophages and Myofibroblasts to Reduce Biomaterial-Induced Fibrosis

AUTHOR: Tich H Truong, B.Eng.Biosci.
(McMaster University)

SUPERVISOR: Professor Kim. S. Jones

NUMBER OF PAGES: xx, 119

Lay Abstract

Capsaicin, prostaglandin E_2 (PGE2) and polydopamine were used to reduce scar tissue development around implanted polymers. Biomedical devices implanted in the body can undergo severe scar tissue formation, or fibrosis, and fail. Fibrosis is described by the accumulation of collagen and encapsulation of an implanted polymer. Macrophages regulate fibrosis by secreting pro-fibrotic compounds and myofibroblasts produce unregulated amounts of collagen. In this thesis, capsaicin, PGE2 and polydopamine were incorporated into implants to target macrophage and myofibroblast activity and reduce fibrosis in mice. Capsaicin and PGE2, released from a degradable polymer, altered macrophages to secrete anti-fibrotic compounds and decreased collagen by 40% and 55%, respectively. Polydopamine surface modified implants gave an unexpected result and suppressed overall cell activity to reduce fibrosis by 30%. The research conducted shows the potential of these compounds to reduce fibrosis and extend the lifetime of implantable devices.

ABSTRACT

Capsaicin, prostaglandin E_2 (PGE2) and polydopamine (PDA) were used to target macrophage and myofibroblast activity to reduce biomaterial-induced fibrosis. The lifetime and efficacy of implantable biomedical devices are determined by the foreign body response. Immediately after implantation, proteins nonspecifically adsorb onto the material and initiate inflammation. Macrophages recruited to the site can differentiate into M1 and M2 phenotypes and upregulate inflammation and fibrosis which interferes with the intended function. M1 macrophages secrete pro-inflammatory mediators that induce chronic inflammation and promote myofibroblast differentiation while M2 macrophages are wound healing cells that suppress inflammation and regulate fibroblast activity. The fibrotic tissue is developed by myofibroblasts which produce collagen in an unregulated fashion. Collagen thickening and biomaterial encapsulation decreases efficacy and sensitive of biomedical devices. We investigated the *in vitro* and *in vivo* effects of capsaicin, PGE2 and polydopamine surface modification on macrophages and myofibroblasts. Capsaicin and PGE2 reduced poly(lactic-co-glycolic) acid (PLGA)-induced fibrosis by promoting M2 macrophage phenotype to secrete anti-inflammatory IL-10 and suppressing myofibroblast marker α-smooth muscle actin (α-SMA). Capsaicin decreased collagen by 40% and upregulated IL-10 secretion by 35% while PGE2 reduced collagen by 55% after 14 days of implantation and 40% less collagen after 42 days. PDA was used to bind an anti-fibrotic compound to the surface of a poly(dimethyl siloxane) (PDMS-PDA) to reduce fibrosis. However, PDMS-PDA controls gave an unexpected result by reducing fibrosis to the same extent as anti-fibrotic compound bound PDMS-

PDA. PDA modification reduced cellularity by 50% and significantly decreased collagen thickness by 30%. Overall, our results showed that biomaterial-induced fibrosis can be reduced by promoting M2 macrophage activity and inhibiting myofibroblast differentiation. This research demonstrates three compounds that have potential to reduce fibrosis and extend the lifetime and efficacy of implantable biomedical devices.

ACKNOWLEDGMENTS

First and foremost, I would to thank my supervisor Dr. Kim Jones for her support and guidance throughout my graduate studies. She was always available for my questions and even took time out of her day to assist me with animal experiments. She offered me inspirational and honest advice throughout my studies, especially when I made the decision to transfer to the PhD program but then changed my mind and transferred back to the MASc program. I truly appreciated the freedom she gave me to design my own projects and experiments. She offered me many experiences and opportunities that I think many Master's students would be envious of. I am indebted to you and look forward to having your guidance as I continue my career.

I would like to thank the undergraduate students whom I had the opportunity to work with. Thank you Kimia Sorouri, Anthony Saraco, Ugonwa Echendu and Emma Buller. Thank you Kimia and Anthony for your tremendous amount of work and innovation. Without your efforts, I would not be able to complete two additional and amazing projects for my Master's degree.

I would like to thank Sonia Padwal, Limin Liu and Dr. Peter Margetts for welcoming me into their lab to collaborate on a project. Thank you for helping me with the many unfamiliar bioassays and teaching me about the world of myofibroblasts.

I would like to thank all of the graduate students in the Ghosh, Hoare, Sheardown and Thompson labs. Thank you for being friendly towards me and making me feel like I was part of a family. As the sole student in the Jones lab, I truly appreciated the entertaining outings and sporting events we have done together.

Most importantly, I would like to thank my family for their constant support and endless encouragement. To my parents, thank you for trying to understand my work. I know you did not appreciate not seeing me very often because I was constantly staying late in the lab, but thank you for enduring it. To my brothers, thank you for your advice and motivation for my work.

TABLE OF CONTENTS

LIST OF FIGURES

LIST OF TABLES

LIST OF ABBREVIATIONS AND SYMBOLS

α-SMA	alpha-smooth muscle actin
ANOVA	analysis of variance
bFGF	basic fibroblast growth factor
C57BL/6	multipurpose mouse model (black coat)
CCAC	Canadian Council on Animal Care
cDNA	complimentary deoxyribonucleic acid
DAPI	4’,6-diamidino-2-phenylindole
ddH_2O	double distilled water
DMEM	Dulbecco’s Modified Eagle Medium
DMSO	dimethyl sulfoxide
DNase	deoxyribonuclease
E-cadherin	cadherin-1
ECM	extracellular matrix
EDTA	ethylenediaminetetracetic acid
ELISA	enzyme-linked immunosorbent assay
EndMT	endothelial-mesenchymal transition
EMT	epithelial-mesenchymal transition
FBS	fetal bovine serum
FDA	Food and Drug Administration
Fg	fibrinogen

GAPDH	glyceraldehyde 3-phosphate dehydrogenase
H&E	hematoxylin and eosin
HK-2	human kidney epithelial cells
HPLC	high performance liquid chromatography
HPR	horseradish peroxidase
HSD	honest significance difference
IFNγ	interferon gamma
iNOS	inducible nitric oxide synthase
IL-1β	interleukin-1 beta
IL-1R	interleukin-1 receptor
IL-4	interleukin-4
IL-6	interleukin-6
IL-8	interleukin-8
IL-10	interleukin-10
IL-12	interleukin-12
IL-13	interleukin-13
IL-18	interleukin-18
IL-23	interleukin-23
LPS	lipopolysaccharide
mRNA	messenger ribonucleic acid
MIRC	McMaster Immunology Research Centre
NF-κB	nuclear transcription factor-kappa B

NO	nitric oxide
PBS	phosphate buffered saline
PD	peritoneal dialysis
PDA	polydopamine
PDGF	platelet-derived growth factor
PDMS	polydimethylsiloxane
PDMS-PDA	polydopamine surface modified polydimethylsiloxane
PFA	paraformaldehyde
PGE2	prostaglandin E_2
PLGA	poly(lactic-co-glycolic) acid or poly(D,L-lactic-co-glycolic) acid
PPARγ	peroxisome proliferator-activated receptor gamma
PSR	picrosirius red
PVDF	poly(vinylidene fluoride)
qPCR	quantitative polymerase chain reaction
RAW 264.7	murine macrophage-like cell line
RBC	red blood cell
RNA	ribonucleic acid
RNase	ribonuclease
rRNA	ribosomal ribonucleic acid
SDS-PAGE	sodium dodecyl sulfate polyacrylamide gel electrophoresis
SEM	standard error of the mean
STAT3	signal transducer and activator of transcription 3

TBST	tris-buffered saline and Tween 20 (Polysorbate 20)
TCPS	tissue cultured polystyrene Petri dish
TGF-β1	transforming growth factor beta-1
TNF-α	tumor necrosis factor alpha
WBC	white blood cell

DECLARATION OF ACADEMIC ACHIEVEMENT

The research performed for this thesis was completed by the author, with the guidance and consultation of Dr. Kim S. Jones, with the following exceptions:

- In Chapter 3, the concept of delivering prostaglandin E_2 to treat poly(lactic-co-glycolic) acid-induced fibrosis was conceived by Kimia Sorouri. Ms. Sorouri performed the *in vitro* proof of concept E-cadherin immunoblotting assay, *in vitro* proof of concept E-cadherin quantitative PCR assay, *in vitro* α-smooth muscle actin (α-SMA) fluorescence staining assay and *in vitro* α-SMA fluorescence microscopy.

- In Chapter 3, E-cadherin immunoblotting assay was optimized by Manreet Padwal. Ms. Padwal optimized primary and secondary antibody concentrations to maximize densitometry results.

- In Chapter 4, the concept of modifying polydimethylsiloxane (PDMS) surfaces with polydopamine was conceived by Anthony Saraco. Mr. Saraco developed the polydopamine surface modification protocol and performed the *in vivo* animal experiment and staining for the fluorescence DAPI assay.

- In Chapter 4, the radiolabelled fibrinogen adsorption experiment was conducted by Darren Sandejas.

CHAPTER 1: LITERATURE REVIEW

1.1 INTRODUCTION & SCOPE OF PROJECT

When biomaterials are implanted as part of a prosthetic device, tissue engineered construct, sensor, or as a drug delivery device, uncontrollable scar formation around the biomaterial can develop and interfere with function. The fibrotic response is thought to depend on protein adsorption and macrophage and myofibroblast interaction with the biomaterial. Proteins adsorbed non-specifically to the biomaterial can act as pathogen associated molecular patterns (PAMPs) and trigger an inflammatory response from macrophages. Macrophages are capable of differentiating into two phenotypes, M1 and M2, which have been shown to dictate the extent of inflammation and fibrosis. M1 macrophages secrete proinflammatory mediators that exacerbate the immune response while M2 macrophages secrete mediators that suppress inflammation and regulate fibroblast activity. Regulating fibroblast activity is important because fibroblasts can differentiate into myofibroblasts and produce uncontrolled amounts of extracellular matrix (ECM) proteins and cause scar tissue formation. This thesis focuses on regulating macrophage and myofibroblast activity by delivering two drugs, capsaicin and prostaglandin E_2 (PGE2), and doing a surface modification technique. Macrophage and myofibroblast markers were analysed to determine macrophage phenotype changes and/or reversal of myofibroblast differentiation.

1.2 CONTRIBUTORS TO FIBROTIC RESPONSES TO BIOMATERIALS

A biomaterial is an engineered material that interacts with a biological system.[1,2] Biomaterials have become a popular solution to a wide range of medical problems. These materials can be designed for permanent and temporary applications with different physical properties, such as chemical inertness, toughness and degradation rate.[1,3] Metals and non-degradable polymers have been the popular choice for permanent applications. For example, titanium alloys are used for dental implants and femoral stems and poly(dimethylsiloxane) (PDMS) is used for breast implants.[1] Degradable polymers, such as poly(lactic-co-glycolic) acid, are frequently used for temporary applications because they ideally degrade into nontoxic monomers that are safely excreted from the body.[1] Polymers can be manufactured with a wide range of physical properties that metal alloys do not possess. Soft polymers, such as silicones, are used for tissue augmentation and transparent polymers, such as poly(methyl methacrylate) (PMMA), are used for ophthalmic devices.[1]

Almost all biomaterials elicit a response when interacting with a biological system.[1,3–5] Immediately after implantation, proteins adsorb non-specifically onto the material and initiate the acute inflammatory and/or immune response **(Figure 1.1)**.[1,3,6] Damaged cells, from surgery, produce chemokines and danger signals to promote polymorphonuclear leukocyte (PMN) migration to the site. PMNs are active for a few days, are capable of phagocytosis and are producers of inflammatory cytokine mediators that recruit monocytes that differentiate into macrophages.[3] The chronic inflammation stage starts with the arrival of macrophages that produce additional inflammatory

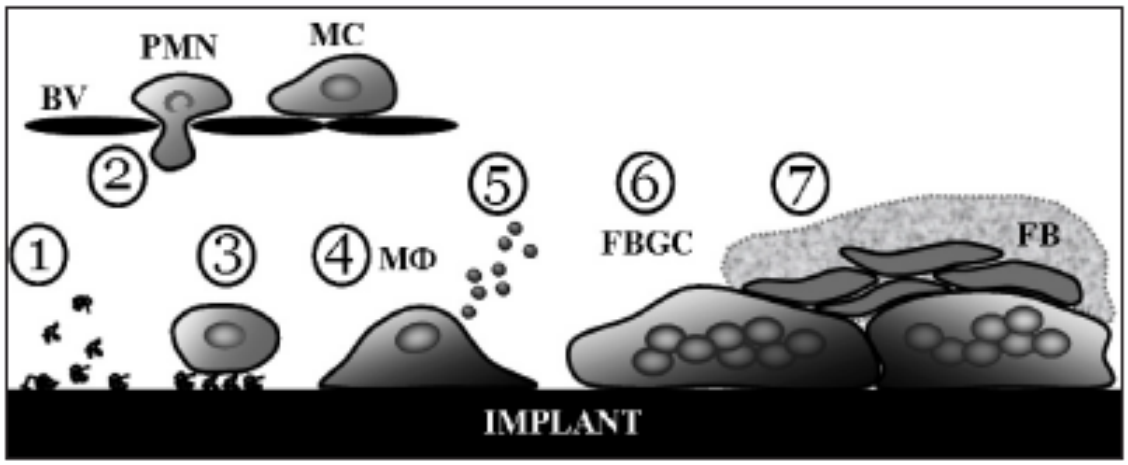

Figure 1.1. Classic stages in the foreign body response. (1) Nonspecific protein adsorption initiates the (2) inflammatory response and (3) promotes monocyte-derived (4) macrophages to migrate to the implant. (5) Macrophages produce inflammatory mediators and fuse into (6) foreign body giant cells in an attempt to phagocytose the foreign material. (7) Chronic inflammation and unsuccessful removal of the material is resolved with fibrous encapsulation which walls off the foreign immune response from healthy tissue. Reprinted with permission from SAGE Publishing.[†]

mediators and attempt to phagocytose the biomaterial.

These cells change phenotype depending on microenvironment conditions and the presence of certain cytokines that upregulate the immune response.[2,3,6,7] In the classic foreign body response, macrophage activity lasts for two weeks but excessive inflammatory stimulation can lead to prolonged and uncontrollable inflammation that can lead to organ failure or autoimmune diseases. Unable to remove large implants or particles, monocytes and macrophages fuse to form multinucleated cells, termed foreign body giant cell (FBGCs). FBGCs can be as large as 1 mm in diameter, can be present for the lifetime of the implanted material and can produce toxic radicals and reactive oxygen species (ROS) in an attempt to break down the foreign material.[3] However, the degradation mediators are destructive to surrounding healthy tissue so a fibrous capsule is

[†] Reprinted from Anti-Inflammatory Polymeric Coatings for Implantable Biomaterials and Devices, 2, A.W. Bridges, A.J. Garcia, 984-994, Copyright 2008, with permission from SAGE Publishing.

formed around the implant. Fibroblasts and myofibroblasts produce extracellular matrix (ECM) proteins, such as collagen-1, to create a fibrous capsule that separates the foreign body and normal host tissue.[3,6] At this stage, the implant is thought to be in a homeostatic environment with the immune response and will remain in the body indefinitely.[2,3,7] However, the classic foreign body response does not occur often and exacerbation of any of these stages can lead to chronic inflammation and/or excess scar tissue formation which results in failure of the biomaterial and/or host injury.

1.2.1 Nonspecific protein adsorption

Protein adsorption is the first event to occur to a biomaterial.[3] Rapid adsorption of nonspecific proteins trigger a slew of reactions that are detrimental to the implant. These reactions include the clotting cascade, thrombosis, leukocyte recruitment and activation of the innate immune system.[8–10] Certain adsorbed proteins undergo the Vroman effect in which proteins are constantly adsorbing onto the surface and being displaced by proteins with higher surface affinity.[10] Clotting proteins, chemokines and cytokines quickly accumulate on the surface and attract leukocytes and many other adsorbed proteins that have the potential to interact with cells and activate the immune system.[3]

In blood contacting environments, platelets and fibrinogen immediately adsorb onto the material. Platelets quickly accumulate to initiate thrombus formation to attract leukocytes. Leukocytes initiate acute inflammation by activating the proinflammatory mediator tumor necrosis factor-alpha (TNF-α).[8] Cell migration is also driven by protein gradients. Liu *et al.* have shown that an increasing fibronectin and vascular endothelial growth factor (VEGF) gradient stimulated endothelial cell migration in a directional manner.[11]

Fibrinogen is synthesized in the liver, is important in clot formation[8,9] and upregulating macrophage activity, has a high surface affinity and adsorbs onto biomaterials.[12,13] Fibrinogen is adsorbed in a multistage fashion because the protein undergoes rearrangement and/or reorientation.[14] However, fibrinogen adsorption is limited by the displacement reaction[9] where it is displaced by high molecular weight kininogen within 5-10 minutes of incubation in human plasma.[8–10] In the clotting cascade, fibrinogen is catalyzed into fibrin polymers, by thrombin, and used to form clots.[15] Patients with a high concentration of soluble fibrinogen are associated with increased risk of atherosclerosis[16] and fibrinogen adsorption is also associated with acute inflammation. Biomaterials with a lot of fibrinogen adsorbed have a high population of adherent macrophages and leukocytes[13] and fibrinogen has been shown to induce proinflammatory IL-4 secretion from monocytes.[17]

There are many methods of reducing protein adsorption including selecting different bulk materials and changing surface chemistry. Metal materials have been shown to be more susceptible to clotting or thromboembolic events[1] whereas silicones and polyurethanes are preferred materials for highly blood contacting environments, such as venous catheters for hemodialysis, because of relatively good blood compatibility.[1] A few surface modifications include removal of hydroxyl groups to decrease complement system activation and precoating surfaces with a nonreactive protein, such as albumin, to reduce platelet and leukocyte adhesion.[8,18] Biomolecules, such as heparin, can also be bound to the surface to reduce thrombus formation[8,19] and hydrophilic polymers, such as

poly(ethylene glycol) (PEG) and poly(acrylamide) chains, can be bound to increase hydrophilicity and steric hindrance to decrease protein adsorption.[20]

1.2.2 Macrophage

Macrophages have phenotypic plasticity that changes depending on signals from the microenvironment.[1] Two phenotypes that are of interest in this thesis are the M1 and M2 macrophage phenotypes which have been shown to mediate the inflammatory and fibrotic response **(Figure 1.2)**.[2,7]

Macrophages are phagocytic cells that are responsible for clearing cellular debris,

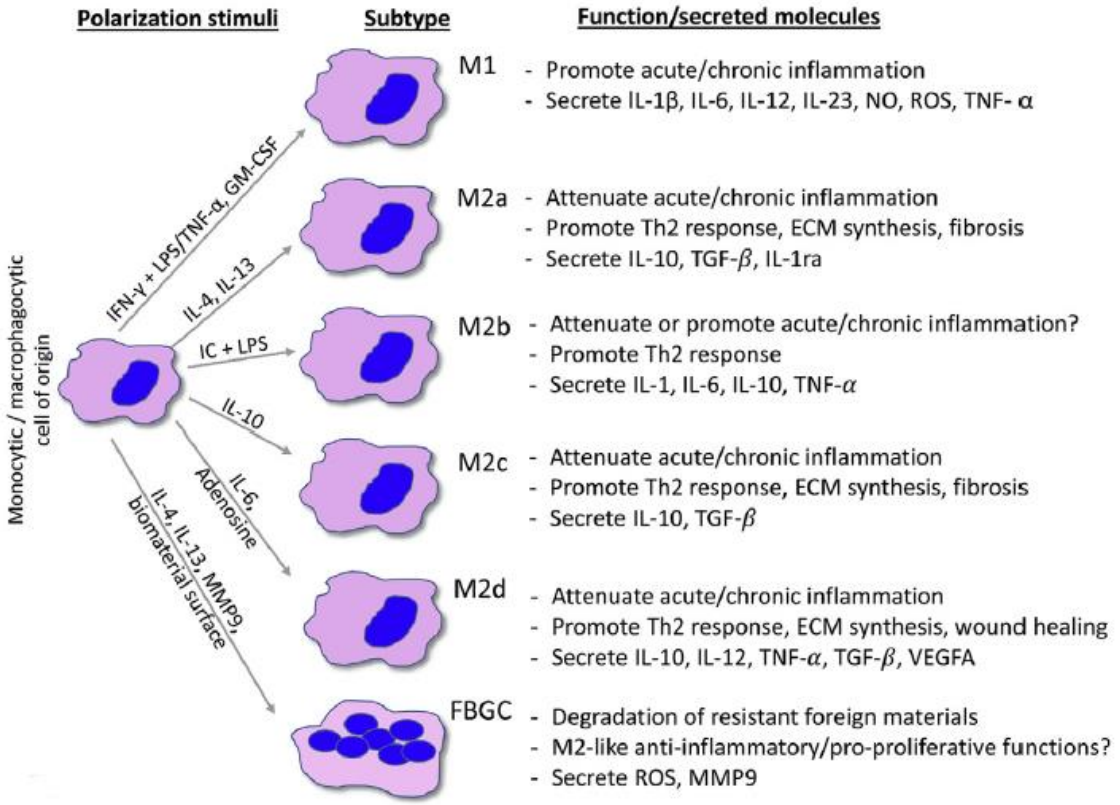

Figure 1.2. Macrophages are derived from monocytes and can differentiate into M1 and M2. M2 macrophages can be divided into subgroups according to different markers that are secreted. Reprinted with permission from Elsevier.‡

‡ Reprinted from Macrophage Reaction Against Biomaterials in the Mouse Model – Phenotypes, Functions and Markers, 43, R. Klopfleisch, 3-13, Copyright 2016, with permission from Elsevier.

removing pathogens, dying and dead cells, and participating in wound healing, tissue remodeling and immune protection.[1] Macrophages are primarily differentiated from monocytes and reside in tissue for years[1] whereas monocytes arise from bone marrow hemopoietic stem cells and can be found circulating in peripheral blood. Promptly after surgical insult and biomaterial implantation, chemokines produced by resident cells signal monocyte migration to the inflammation or immune stimulation sites where they differentiate into tissue-specific macrophage phenotypes. These polarized macrophages can produce interleukin 1-beta (IL-1β), IL-6, IL-8 and TNF-α to mediate a biomaterial response.[3]

1.2.2.1 M1 phenotype

M1, or "classically activated", macrophages are effector macrophages that have enhanced phagocytosis abilities compared to resting macrophages. Two events are required for monocytes to differentiate into M1 macrophages: interferon gamma (IFNγ) stimulation and TNF-α priming **(Figure 1.2)**.[21]

IFNγ reduces monocyte sensitivity to cytokine signals and TNF-α priming upregulates NF-κB-mediated inflammation. IFNγ is produced in low concentrations by natural killer T cells and macrophages stimulated with IL-2 and IL-12.[21] Macrophages activate TNF-α when pathogen-associated molecular patterns (PAMPs) bind to their surface pathogen recognition receptors (PRRs).[22] The most common PAMP is lipopolysaccharide (LPS), which is a major component found on bacterial cell membranes. Other antigen presenting cells, such as dendritic cells, can produce TNF-α to stimulate macrophages.[21,22]

Activated M1 macrophages can be identified by the high expression of inducible nitric oxide synthase (iNOS) and high production of IL-12 and IL-23.[23] iNOS is catalyzed by arginine and upregulates production of nitric oxide and ROS.[21] These cells produce proinflammatory cytokines that upregulate the inflammatory response. Such cytokines include TNF-α, IL-1β, IL-4, IL-6, IL-8, IL-12, IL-18 and IL-23 which activates nuclear factor-kappa B (NF-κB) and upregulates production of inflammatory mediators.[5,21,23] Lastly, M1 macrophages can recruit and modulate fibroblast activity by secreting basic fibroblast growth factor (bFGF), platelet-derived growth factor (PDGF), IL-1 and TNF-α.[5,23] Recruited fibroblasts assist with wound healing and tissue regeneration but persistent fibroblast stimulation by macrophages can promote myofibroblast differentiation. There is recent evidence that suggests that macrophages can differentiate into myofibroblasts, however this was only shown *in vitro*.[24,25]

M1 activity can be suppressed by using glucocorticosteriods that inhibit iNOS, COX-2, and TNF-α production.[21] Glucocorticosterids bind to the immunoreceptor tyrosine-based inhibitory motif and prevent further proinflammatory mediators from being produced.[21] An alternative approach is to activate the peroxisome proliferator-activated receptor gamma (PPARγ) pathway with IL-4; this has been shown to decrease production of proinflammatory mediators such as iNOS, TNF-α, IL-1β and IL-12.[21,23]

1.2.2.2 M2 phenotype

Macrophages with a phenotype that differs from M1 are termed M2, or "alternatively activated", macrophages. Unlike M1 macrophages, M2 macrophages can be divided into sub categories based on observed cytokine production and chemokine secretion when stimulated with certain cytokines **(Figure 1.2)**.[1,23] In this thesis, M2

macrophages will refer to the predominant M2c subset which is IL-10 driven,[26,27] plays a critical role in immune suppression and regulation and is the most commonly identified phenotype in immune *in vivo* models.[2,7,21,23,28]

M2 macrophages require two events in order to be activated: contact with an immune complex and stimulation with IL-4.[21] Activated M2 macrophages are distinguished from M1 macrophages by their high production of arginase-1 and IL-10.[21,28,29] Arginase-1 uses the same arginine substrate as iNOS, thus upregulation of arginase-1 outcompetes iNOS to downregulate nitric oxide production. Arginase-1 is essential for collagen production, extracellular matrix formation and tissue repair. Argianse-1 is used to convert arginine to ornithine and ornithine is used to produce proline and polyamines essential for ECM protein production.[21] M2 macrophages mediate the inflammatory response by producing anti-inflammatory cytokines IL-4, IL-10 and IL-13.[21] IL-4 upregulates arginase-1 expression and production of IL-1 and IL-10 from macrophages in a feedback mechanism. IL-10, the main anti-inflammatory cytokine produced, has been shown to suppress TNF-α activity in M1 macrophages[30] and IL-13 activates M2a differentiation and promotes fibroblast activity.[31]

1.2.2.3 Controversy on "good" and "bad" phenotypes

In the inflammation research field, M1 macrophages are often considered the undesirable, or "bad", phenotype because of their secretion of proinflammatory chemokines while M2 macrophages are the desirable, or "good", phenotype because of their proangiogenic and anti-inflammatory capabilities. However, in the fibrosis research field the good and bad phenotypes are reversed where it is preferred to suppress M2 macrophages because they have been shown to modulate and upregulate myofibroblast

activity, such as in renal fibrosis renal fibrosis,[24,32] and M1 activity is beneficial because it drives the inflammatory response to regulate fibroblast activity.[27] Macrophage phenotype was previously described as a dichotomy between the proinflammatory M1 phenotype and the profibrotic M2 phenotype; however, this extreme spectrum is only seen *in vitro* and rarely seen *in vivo*. In reality, macrophage phenotypes transition quickly and are expressed as a continuum of M1 and M2. This gave rise to the term phenotype plasticity, where a spectrum of M1 and M2 phenotypes can be expressed at once.[33] As such, this has led to controversy on which phenotype is desirable for certain applications and diseases.

The cellular environment can dictate the macrophage response. Contrary to the pro-fibrotic phenotype M2 macrophages are identified as, they can release mediators that upregulate inflammation. In asthmatic research, IL-33 stimulated M2 macrophages have been shown to cause severe inflammation by upregulating IL-4 and IL-13 secretion[34] and M2 macrophages activate and promote angiogenesis and metastasis in cancer, promoting inflammation instead of resolving it.[35]

Timing of macrophage phenotype can play an important role on the response. Historically, it is preferred to minimize inflammation immediately. Nonsteroidal anti-inflammatory drugs (NSAIDs) are an effective method to suppress M1 activity and reduce inflammation in atherosclerosis[36] and chronic spinal inflammation.[37] However, in biomaterial research, the early appearance of M2 macrophages has been shown to reduce acute inflammation and promote biomaterial integration with minimal fibrosis.[38] The subtype of M2 macrophages might be important here.

1.2.3 Myofibroblast

Myofibroblasts contribute to wound healing by exerting traction forces and producing ECM to restore a mechanically sound scar.[39] Two stimuli are required for myofibroblast proliferation: mechanical resistance of ECM and transforming growth factor-beta 1 (TGF-β1) stimulation.[40] Recent research has also shown that substrate stiffness might play a role in stimulating differentiation.[39,40] Activated myofibroblasts are commonly identified by upregulated alpha-smooth muscle actin (α-SMA), which provides cells with cytoskeletal smooth muscle cell abilities.[40] The contractile ability can be described as a cyclic lockstep where a repeated sequence of attaching and pulling of collagen fibers increases tissue tension and stiffness.[39] This mechanism is essential to close wounds but excessive ECM secretion and persistent contractile forces often causes tissue deformation and failure of the biomaterial.[5,39,40]

TGF-β1 has been shown to be the main inducing agent for myofibroblast differentiation. TGF-β1 stimulates cells to differentiate through epithelial-mesenchymal transition (EMT) or endothelial-mesenchymal transition (EndMT).[40] This event is evident by epithelial cells losing epithelial cadherin (E-cadherin) expression and upregulating α-SMA activity. Although TGF-β1 is the main inducer of myofibroblast differentiation, there are studies that have shown that anti-TGF-β1 compounds were ineffective at countering myofibroblast differentiation.[39] This suggests that myofibroblasts are activated by alternative pathways that have yet to be elucidated.

The origin of myofibroblasts has been an interesting topic for the past decade.[40] Myofibroblasts can be derived from numerous cell types including fibroblasts, epithelial

cells, endothelial cells and fibrocytes, but the origin depends on the tissue that is to be repaired **(Figure 1.3)**. Local fibroblasts and fibrocytes are common origins in skin wound

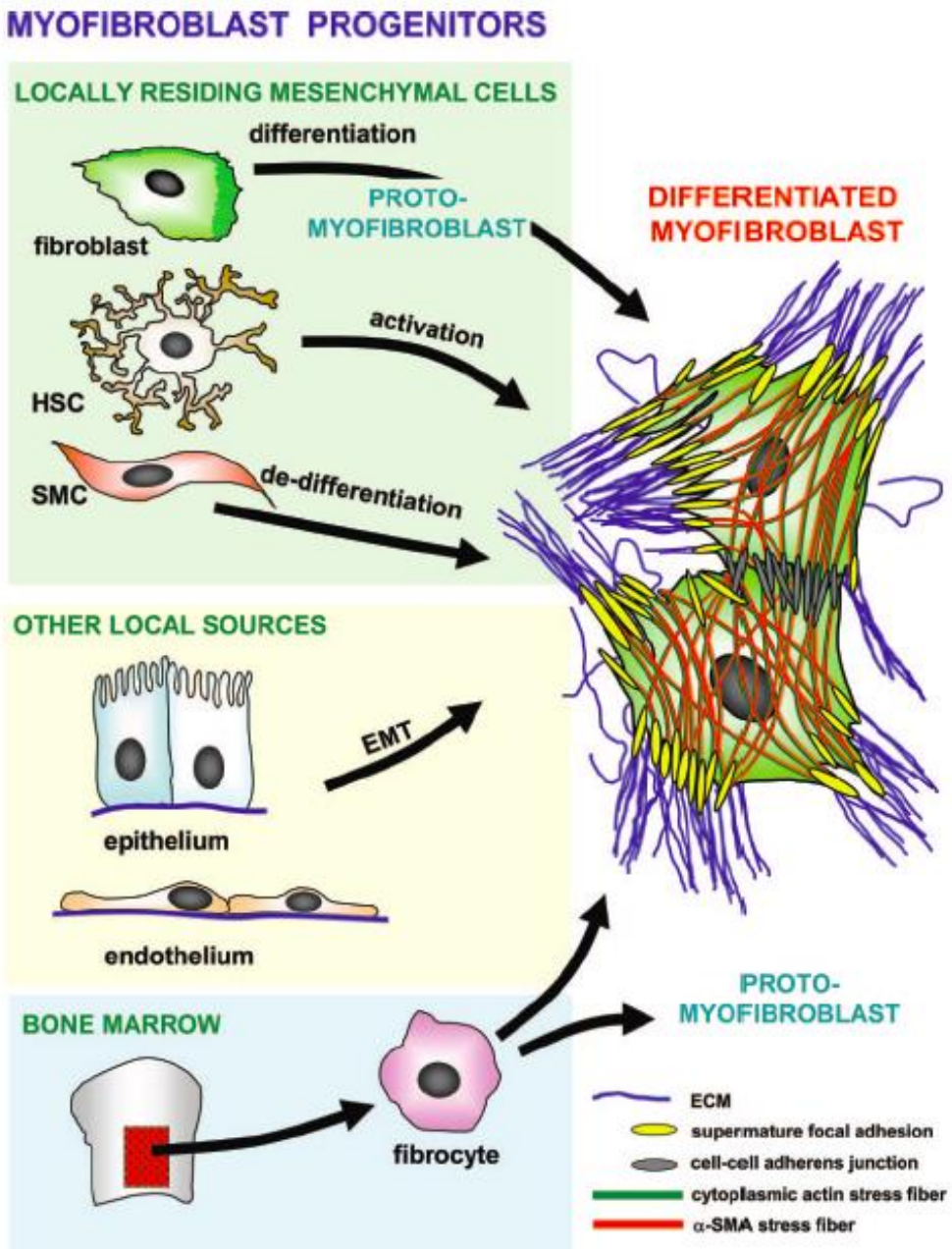

Figure 1.3. Myofibroblasts come from many different origins. Progenitor cells from bone marrow have shown to be a source of myofibroblasts in lung fibrosis. Reprinted with permission from Elsevier.[§]

[§] Reprinted from The Myofibroblast One Function, Multiple Origins, 170, B. Hinz, S.H. Phan, V.J. Thannickal, A. Galli, ML. Bochaton-Piallat, G. Gabbiani, 1807-1816, Copyright 2007, with permission from Elsevier.

healing while pericytes and smooth muscle cells are common origins in vessel repair.[39] In renal fibrosis, myofibroblasts are derived from local fibroblasts, circulating fibrocytes, local pericytes and resident epithelial cells while in lung fibrosis, bone marrow progenitors and lung epithelium are sources of myofibroblasts.[40] As such, for implantable biomaterials, the origin of myofibroblasts would depend on the location in which the biomaterial is implanted.

1.2.4 Other contributors

In addition to nonspecific protein adsorption, macrophages and myofibroblasts, there are non-cell based contributors to inflammation and fibrosis, such as the patient's health. A patient's immune response is dependent on the patient's physical characteristics such as their general health, physical mobility and life style features.[1] The patient's age also affects their immune response where it is well established that young and elderly individuals have a weakened immune system with a slower macrophage response compared to young adults.[41]

Chemical and physical properties of biomaterials, such as bulk material, surface chemical composition and degradation profile, can contribute to the immune response.[1] Leachables can elicit an immune response by recruiting macrophages that will phagocytose the small particles.[1] This response can be beneficial for temporary applications, such as tissue engineering scaffolds, but be detrimental for permanent applications like implanted ocular lenses.

The immune response is also affected by surface properties of the biomaterial. Biomaterial surface topography has also shown to have an effect where monocytes favour an M2 phenotype when cultured on 2D scaffolds, and an M1 phenotype when cultured on

3D scaffolds.[42] Smooth surfaces tend to have a thin layer of macrophages forming whereas rough and porous surfaces will have a thick layer of macrophages forming.[3] The hydrophobic-hydrophilic surface balance of the material can also affect the immune response where nonspecific protein adsorption occurs more readily on hydrophobic surfaces than hydrophilic surfaces.[1] Lastly, the sterility and cleanliness of the surface can have an effect where presence of microorganisms and endotoxins will upregulate macrophage activity through PRR activation.[1] These are a few of the many contributors of inflammation and fibrosis but this thesis will focus on protein adsorption, macrophages and myofibroblasts which are believed to be the main contributors.

1.3 POLY(LACTIC-CO-GLYCOLIC) ACID

Poly(lactic-co-glycolic) acid (PLGA) is a versatile polymer that has many desirable characteristics for use as an implantable biomaterial. Its degradation into nontoxic components allows it to be used as an FDA approved suture material[43,44] and as a degradable system **(Figure 1.4)**.[1] PLGA can be broken down by tissue enzymes, superoxides and free radicals, but degradation is primarily driven by hydrolysis.[1] Ester linkages are hydrolysed to make lactic acid and glycolic acid which are both easily used as an energy source or excreted from the body. The water soluble monomers, dimers or

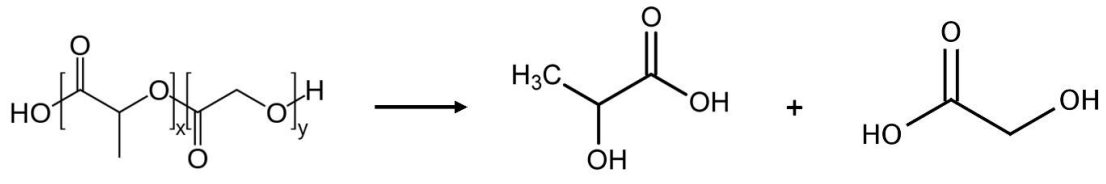

Figure 1.4. Poly(lactic-co-glycolic) acid (PLGA) degrades into lactic acid and glycolic acid under hydrolysis. PLGA degradation rate is dependent on the ratio of lactic acid and glycolic acid where a higher ratio of lactic acid to glycolic acid results in slower degradation.

oligomers of respective acids can enter the tricarboxylic acid cycle where they are eliminated from the body as water and carbon dioxide. Glycolic acid can also be removed via the renal system.[44]

PLGA structures can be cast using several methods. PLGA particles (microspheres, microcapsules, nanocapsules) can be created using sonication and porous scaffolds can be made using porogen particles and electrospinning.[45] Particles can be used as drug carriers to deliver drugs to tissue where drugs are released by diffusing through the particles or by erosion mechanisms. The particles themselves are easily removed from the body by phagocytic leukocytes.[44] Thin films of PLGA can be made using solvent casting which involves dissolving PLGA crystals in an organic solvent and evaporating the solvent to leave behind a thin layer of PLGA that conforms to the structure of the mold.[44,46] This allows the creation of large PLGA structures that can be used as a reservoir for long term drug delivery.[44]

PLGA degradation rate and drug release profiles can be controlled by varying the concentration of lactic acid and glycolic acid.[47] The hydrophobicity and amorphous structure of PLGA contributes to the degradation rate. Hydrophobicity is attributed to the methyl groups in polylactic acid so increasing polylactic acid in PLGA will decrease degradation. PLGA crystallinity decreases when more polyglycolic acid is co-polymerized with polylactic acid.[44] As such, an increasing lactic acid to glycolic acid ratio decreases the degradation rate.

Drug release from PLGA reservoirs is dependent on drug hydrophilicity. Release kinetics of hydrophilic drugs are driven by passive diffusion and follow a biphasic model

where there is an initial burst release and a delayed release. The burst release is associated with drugs on the surface of the material immediately diffusing into the medium and the second release is when the outer layers degrade and release entrapped drugs.[44] Release kinetics of hydrophobic drugs is driven by passive diffusion and tends to follow a multiphasic model where drug release occurs when entrapped drugs are released.[48]

PLGA microparticles can elicit a low inflammatory response where they are easily phagocytosed by macrophages and lymphocytes. However, large PLGA structures can exacerbate the inflammatory response and cause chronic inflammation and/or fibrosis.[42] The exact mechanism and pathway of how PLGA triggers the inflammatory response has not yet been elucidated, but PLGA has been shown to activate the NF-κB pathway and upregulate proinflammatory cytokine secretion.[49] Stankevich *et al.* reported that monocytes cultured on polylactic acid films released a significant amount of TNF-α and CCL18 after 6 days of incubation.[50] PLGA can also induce macrophage phenotype change. Bartneck *et al*. demonstrated that macrophages differentiate into M1 phenotype and produced proinflammatory cytokines. M1 macrophages upregulated proinflammatory cytokines IL-1β and TNF-α and proangiogenic chemokine IL-8.[42] Similar to the macrophage response, fibroblasts were shown to express high levels of IL-1β after 24 hours of incubation on PLGA membranes.[51] Zhu and colleagues have reported that PLGA is able to activate and cause dendritic cells to produce IL-12 and TNF-α and promote T lymphocyte proliferation with a Type 1 (Th1) response.[52] Overall, PLGA induces an M1 macrophage phenotype that promotes inflammation and activates T cells.

1.4 POLYDIMETHYLSILOXANE

Polydimethylsiloxane (PDMS) is a transparent silicon-based organic polymer that is known, in general, for its inertness, nontoxicity and nonflammability. These properties make PDMS a popular material for pacemaker encapsulates, catheters, and contact lenses.[53] PDMS is also gas permeable, easy to fabricate, and has low manufacturing costs which makes it an ideal material to make complex microdevices for high throughput and sensitive applications, such as DNA sequencing, extracorporeal membrane oxygenators[19] and biosensors.[53]

Although PDMS is nontoxic, it is very susceptible to fouling. PDMS has a highly hydrophobic surface which causes nonspecific proteins and hydrophobic analytes to readily adsorb and cells and bacteria to adhere to the surface.[53] Fouling can trigger the immune response through PRR activation. Proteins adsorbed onto the surface can undergo conformational changes[14] and appear like a PAMP and adherent cells and bacteria contain PAMPs that are detected by PRRs on leukocytes.

Nonspecific protein adsorption on biomaterials initiates biological events that often lead to biomaterial complications and/or failure. Adsorbed proteins can cause chronic inflammation and fibrosis, which decreases sensitivity of diagnostic and immunological assays, and modifies therapeutic properties of biomaterials such as release profiles of drug carriers.[53] Fouling has been shown to prevent proper wound healing and enhance monocyte and macrophage activation.[5] In breast implants, PDMS implants can become loose and generate micromechanical forces that induce myofibroblast activity.[1,3] Thick fibrous encapsulation around silicone breast implants and persistent myofibroblast contractions cause implant deformation and chest pain in patients.

To attenuate fouling, there has been some research in surface modification techniques to make the surface less hydrophobic.[8] Some of these techniques include oxygen plasma and ozone or UV light treatment which decrease hydrophobicity by physically bonding molecules to the surface.[53] Molecules, such as PEG, can be covalently bond material to the surface.[53] PEG chains provide steric repulsion and increase hydrophilicity because of the highly methylated backbone.[14,53] However, fouling can only be delayed because anti-fouling coatings are easily destroyed by temperature and micromechanical forces and/or the coating comes off due to weak adsorption affinity to substrate.[53]

1.5 CAPSAICIN

Capsaicin is one of two capsaicinoids responsible for the pungent aroma in pepper fruits.[54,55] Polar solvents, such as chloroform, acetone, and ethyl acetate are used to extract capsaicin from chili peppers and capsaicin content can be measured at 228-280 nm wavelength using chromatography.[54,55] Capsaicin content is often measured to determine the pungency, or "spiciness", of peppers. Spiciness is measured using the Scoville heat units (SHU) scale where food can be categorized as non-pungent (0-700 SHU), mildly pungent (700-3000 SHU), moderately pungent (3000-25000 SHU) and highly pungent (25,000-70,000 SHU).[54] Pure capsaicin has a spicy level of 15-16 million SHU while more commonly consumed food, such as Sriracha sauce and green bell peppers are 2,500 SHU and 0 SHU, respectively.[54]

Capsaicin has pharmaceutical properties that can be taken advantage of. The chemical is most famous for its use in pepper sprays. Eyes and mouths that come in

contact with capsaicin undergo neurogenic inflammation resulting in pain.[54] Most interesting is the recent development in using capsaicin to treat autoimmune disease related pain and inflammation, bladder inflammation and cancer progression.[54,55] Capsaicin has been shown to induce M1 macrophages to express M2 markers in a dosage dependent manner.[56] LPS stimulated peritoneal macrophages upregulated arginase-1 after being treated with capsaicin for 24 hours.[57] Injections of capsaicin have been shown to reduce T-cell activity and leukocyte infiltration in rats with joint arthritis.[58]

1.6 PROSTAGLANDIN E_2

Prostaglandin E_2 (PGE2) is a prostanoid that has a wide range of effects. In prolonged pregnancy, PGE2 is used to soften the cervix and induce labour.[59] Elevated levels of PGE2 in the brain has been associated with neuroinflammation[60] and upregulated gastric-acid section[61] and PGE2 has shown to mediate the inflammatory response[62] by upregulating IL-10 secretion from macrophages.[63]

PGE2 is produced by human mesenchymal stem cells, stromal cells, macrophages and fibroblasts through activation of the cyclooxygenase (COX) pathway.[64] COX activation initiates two enzymes, COX-1 and COX-2, to catalyze arachidonic acid into prostaglandins. Non-steroidal anti-inflammatory drugs (NSAIDs) can block both COX-1 and COX-2 or selectively block COX-2 to reduce inflmamation.[65] COX-2 selective NSAIDs have been demonstrated to stop PGE2 secretion from macrophages to decrease pulmonary inflammation.[66]

Recent studies have shown that PGE2 can successfully modulate fibroblast activity to reduce fibrosis. In pulmonary pathology, PGE2 inhibited fibrogenesis in lung

allografts.[67] In TGF-β1 differentiated myofibroblasts, PGE2 reversed α-SMA activity and suppressed collagen production. PGE2 suppressed α-SMA activity in a dosage dependent manner and upregulated epithelial marker E-cadherin from EMT derived epithelial cells.[68,69] PGE2 also suppressed type I and type III collagen mRNA in TGF-β1 stimulated fibroblasts.[70,71]

1.7 POLYDOPAMINE

There has been recent interest in doing polydopamine (PDA) surface modification because of its simple chemistry. Surface modification techniques have become a popular method to prevent, or reduce, biomaterial interactions with tissue. There are many techniques but it is desirable to have a versatile method to modify biomaterials in a single step reaction using water as a solvent.[72] PDA surface modification is done using a facile self-assembly method where dopamine is polymerized through oxidation and covalently bound to the substrate.[73] During the reaction, pH-induced oxidation causes PDA to undergo a colour change and form a black-brown precipitate.[72–74]

PDA surface modification resulted in a homogenous nanolayer, except when the reaction is done on a conductive material, such as metals and carbons.[72] The layer is stable in water, but degrades in highly basic solutions,[72] and the thickness is dependent on concentration, incubation time, acidity, and temperature.[19,72] A thicker layer of PDA can be made by increasing the initial concentration, temperature and incubation time.[72] Proteins can be attached to PDA through secondary functionalization of thiol and amine groups in proteins and the quinone groups in PDA.[72] PDA has also shown to have no effect on surface energy where surface energy of PDA modified polymers were similar to

unmodified substrates.[72] This suggests that surface energy is dependent on the substrate material and composition.[72] Nevertheless, PDA itself can increase hydrophilicity and surface energy of metals[75] because of it is composed of many OH^- and NH_2^- groups.[74]

As previously mentioned, PDA can be used to attach macromolecules to reduce an immune response. Heparin has been bound to PDA modified PDMS devices, to reduce thrombus formation,[19] and to stainless steel implants to prevent platelet acuumulation.[75] PDA can also bind nanoparticles to surfaces such as silver nanoparticles to reduce biofouling from microalgae in wastewater treatment systems[76] and copper nanoparticles to create PTFE coatings with more wear resistance.[77]

The modification itself can have desirable effects. PDA surface modification has been used to increase surface roughness[74] of PMMA implants to have stronger adhesion with subcutaneous tissue.[78] PDA has been shown to have anti-inflammatory effects where keratocytes cultured on PDA modified surfaces secreted less proinflammatory IL-6 cytokine.[78] PDA can also act as an antioxidant because of the cation groups and free radicals on the modified surface that can function as an antioxidant.[72]

1.8 REFERENCES

1. Williams, D. F. On the mechanisms of biocompatibility. *Biomaterials* **29,** 2941–2953 (2008).

2. Williams, D. F. On the nature of biomaterials. *Biomaterials* **30,** 5897–5909 (2009).

3. Anderson, J. M. & McNally, A. K. Biocompatibility of implants: lymphocyte/macrophage interactions. *Semin. Immunopathol.* **33,** 221–233 (2011).

4. Anderson, J. M., Rodriguez, A. & Chang, D. T. Foreign body reaction to biomaterials. *Semin. Immunol.* **20,** 86–100 (2008).

5. Bonfield, T. L., Colton, E. & Anderson, J. M. Fibroblast stimulation by monocytes cultured on protein adsorbed biomedical polymers. I. Biomer and polydimethylsiloxane. *J. Biomed. Mater. Res.* **25,** 165–75 (1991).

6. Lee, J. M. & Kim, Y. J. Foreign Body Granulomas after the Use of Dermal Fillers: Pathophysiology, Clinical Appearance, Histologic Features, and Treatment. *Arch. Plast. Surg.* **42,** 232 (2015).

7. Anderson, J. M., Rodriguez, A. & Chang, D. T. Foreign body reaction to biomaterials. *Semin. Immunol.* **20,** 86–100 (2008).

8. Courtney, J. M., Lamba, N. M. K., Sundaram, S. & Forbes, C. D. Biomaterials for blood-contacting applications. *Biomaterials* **15,** 737–744 (1994).

9. Wojciechowski, P., Ten Hove, P. & Brash, J. . Phenomenology and mechanism of the transient adsorption of fibrinogen from plasma (Vroman effect). *J. Colloid Interface Sci.* **111,** 455–465 (1986).

10. Jung, S. Y. *et al.* The Vroman Effect: A Molecular Level Description of Fibrinogen Displacement. *J. Am. Chem. Soc.* **125,** 12782–12786 (2003).

11. Liu, L., Ratner, B. D., Sage, E. H. & Jiang, S. Endothelial Cell Migration on Surface-Density Gradients of Fibronectin, VEGF, or Both Proteins. *Langmuir* **23,** 11168–11173 (2007).

12. Hu, W. J., Eaton, J. W., Ugarova, T. P. & Tang, L. Molecular basis of biomaterial-mediated foreign body reactions. *Blood* **98,** 1231–8 (2001).

13. Tang, L., Wu, Y. & Timmons, R. B. Fibrinogen adsorption and host tissue responses to plasma functionalized surfaces. *J. Biomed. Mater. Res.* **42,** 156–163 (1998).

14. Roach, P., Farrar, D. & Perry, C. C. Interpretation of Protein Adsorption: Surface-Induced Conformational Changes. *J. Am. Chem. Soc.* **127,** 8168–8173 (2005).

15. Mosesson, M. W. Fibrinogen and fibrin structure and functions. *J. Thromb. Haemost.* **3,** 1894–1904 (2005).

16. Reinhart, W. H. Fibrinogen--marker or mediator of vascular disease? *Vasc. Med.* **8,** 211–216 (2003).

17. Oliveira, M. I. *et al.* Adsorbed Fibrinogen stimulates TLR-4 on monocytes and induces BMP-2 expression. *Acta Biomater.* (2016). doi:10.1016/j.actbio.2016.11.034

18. Kottke-Marchant, K., Anderson, J. M., Umemura, Y. & Marchant, R. E. Effect of albumin coating on the in vitro blood compatibility of Dacron arterial prostheses. *Biomaterials* **10,** 147–55 (1989).

19. Leung, J. M. *et al.* Surface modification of poly(dimethylsiloxane) with a covalent antithrombin–heparin complex for the prevention of thrombosis: use of polydopamine as bonding agent. *J. Mater. Chem. B* **3,** 6032–6036 (2015).

20. Bridges, A. W. & García, A. J. Anti-inflammatory polymeric coatings for implantable biomaterials and devices. *J. Diabetes Sci. Technol.* **2,** 984–94 (2008).

21. Onoprienko, L. V. Molecular mechanisms of regulation of the macrophage activity. *Russ. J. Bioorganic Chem.* **37,** 387–399 (2011).

22. Mogensen, T. H. Pathogen Recognition and Inflammatory Signaling in Innate Immune Defenses. *Clin. Microbiol. Rev.* **22,** 240–273 (2009).

23. Martinez, F. O. & Gordon, S. The M1 and M2 paradigm of macrophage activation: time for reassessment. *F1000Prime Rep.* **6,** 13 (2014).

24. Nikolic-Paterson, D. J., Wang, S. & Lan, H. Y. Macrophages promote renal fibrosis through direct and indirect mechanisms. *Kidney Int. Suppl.* **4,** 34–38 (2014).

25. Pilling, D. & Gomer, R. H. in *Stem Cell Mobilization* (eds. Kolonin, M. G. & Simmons, P. J.) **904,** 191–206 (Humana Press, 2012).

26. Mantovani, A. *et al.* The chemokine system in diverse forms of macrophage activation and polarization. *Trends Immunol.* **25,** 677–686 (2004).

27. Kennedy, A., Fearon, U., Veale, D. J. & Godson, C. Macrophages in synovial inflammation. *Front. Immunol.* **2,** 1–9 (2011).

28. Corporation, H. P. Understanding the Mysterious M2 Macrophage through Activation Markers and Effector Mechanisms. **2015,** 16–18 (2015).

29. Jablonski, K. A. *et al.* Novel markers to delineate murine M1 and M2 macrophages. *PLoS One* **10,** 5–11 (2015).

30. Mosser, D. M. & Zhang, X. Interleukin-10: new perspectives on an old cytokine. *Immunol. Rev.* **226,** 205–218 (2008).

31. Huang, X.-L. *et al.* Role of anti-inflammatory cytokines IL-4 and IL-13 in systemic sclerosis. *Inflamm. Res.* **64,** 151–9 (2015).

32. Yu, C.-C., Chien, C.-T. & Chang, T.-C. M2 macrophage polarization modulates epithelial-mesenchymal transition in cisplatin-induced tubulointerstitial fibrosis. *BioMedicine* **6,** 5 (2016).

33. Italiani, P. & Boraschi, D. From monocytes to M1/M2 macrophages: Phenotypical vs. functional differentiation. *Front. Immunol.* **5,** 1–22 (2014).

34. Kurowska-Stolarska, M. *et al.* IL-33 amplifies the polarization of alternatively activated macrophages that contribute to airway inflammation. *J. Immunol.* **183,** 6469–77 (2009).

35. Sica, A., Porta, C., Riboldi, E. & Locati, M. Convergent pathways of macrophage polarization: The role of B cells. *Eur. J. Immunol.* **40,** 2131–2133 (2010).

36. Colin, S., Chinetti-Gbaguidi, G. & Staels, B. Macrophage phenotypes in atherosclerosis. *Immunol. Rev.* **262,** 153–166 (2014).

37. Helm, O., Held-Feindt, J., Schafer, H. & Sebens, S. M1 and M2: there is no 'good' and 'bad'-How macrophages promote malignancy-associated features in tumorigenesis. *Oncoimmunology* **3,** e946818 (2014).

38. Brown, B. N. *et al.* Macrophage phenotype as a predictor of constructive remodeling following the implantation of biologically derived surgical mesh materials. *Acta Biomater.* **8,** 978–987 (2012).

39. Hinz, B. *et al.* Recent developments in myofibroblast biology: Paradigms for connective tissue remodeling. *Am. J. Pathol.* **180,** 1340–1355 (2012).

40. Hinz, B. *et al.* The Myofibroblast. *Am. J. Pathol.* **170,** 1807–1816 (2007).

41. Linehan, E. & Fitzgerald, D. C. Ageing and the immune system: focus on macrophages. *Eur. J. Microbiol. Immunol. (Bp).* **5,** 14–24 (2015).

42. Bartneck, M. *et al.* Inducing healing-like human primary macrophage phenotypes

by 3D hydrogel coated nanofibres. *Biomaterials* **33,** 4136–4146 (2012).

43. Lee, H. S. *et al.* Antimicrobial and biodegradable PLGA medical sutures with natural grapefruit seed extracts. *Mater. Lett.* **95,** 40–43 (2013).

44. Makadia, H. K. & Siegel, S. J. Poly Lactic-co-Glycolic Acid (PLGA) as Biodegradable Controlled Drug Delivery Carrier. *Polymers (Basel).* **3,** 1377–1397 (2011).

45. Corrigan, O. I. & Li, X. Quantifying drug release from PLGA nanoparticulates. *Eur. J. Pharm. Sci.* **37,** 477–485 (2009).

46. Jain, R. a. The manufacturing techniques of various drug loaded biodegradable poly(lactide-co-glycolide) (PLGA) devices. *Biomaterials* **21,** 2475–2490 (2000).

47. Nair, L. S. & Laurencin, C. T. Biodegradable polymers as biomaterials. *Prog. Polym. Sci.* **32,** 762–798 (2007).

48. Xiong, X. Y., Tam, K. C. & Gan, L. H. Release kinetics of hydrophobic and hydrophilic model drugs from pluronic F127/poly(lactic acid) nanoparticles. *J. Control. Release* **103,** 73–82 (2005).

49. Bartneck, M. *et al.* Inducing healing-like human primary macrophage phenotypes by 3D hydrogel coated nanofibres. *Biomaterials* **33,** 4136–4146 (2012).

50. Stankevich, K. S. *et al.* Surface modification of biomaterials based on high-molecular polylactic acid and their effect on inflammatory reactions of primary human monocyte-derived macrophages: Perspective for personalized therapy. *Mater. Sci. Eng. C* **51,** 117–126 (2015).

51. Iwasaki, Y., Sawada, S., Ishihara, K., Khang, G. & Lee, H. B. Reduction of surface-induced inflammatory reaction on PLGA/MPC polymer blend. *Biomaterials* **23,** 3897–3903 (2002).

52. Zhu, H. *et al.* Mesenchymal stem cells attenuated PLGA-induced inflammatory responses by inhibiting host DC maturation and function. *Biomaterials* **53,** 688–698 (2015).

53. Zhang, H. & Chiao, M. Anti-fouling Coatings of Poly(dimethylsiloxane) Devices for Biological and Biomedical Applications. *J. Med. Biol. Eng.* **35,** 143–155 (2015).

54. Othman, Z. A. Al, Ahmed, Y. B. H., Habila, M. A. & Ghafar, A. A. Determination of Capsaicin and Dihydrocapsaicin in Capsicum Fruit Samples using High Performance Liquid Chromatography. *Molecules* **16,** 8919–8929 (2011).

55. Juangsamoot, J., Ruangviriyachai, C., Techawongstien, S. & Chanthai, S. Determination of capsaicin and dihydrocapsaicin in some hot chilli varieties by RP-HPLC-PDA after magnetic stirring extraction and clean up with C 18 cartridge. *Int. Food Res. J.* **19,** 1217–1226 (2012).

56. Park, J.-Y. *et al.* Capsaicin inhibits the production of tumor necrosis factor alpha by LPS-stimulated murine macrophages, RAW 264.7: a PPARgamma ligand-like action as a novel mechanism. *FEBS Lett.* **572,** 266–70 (2004).

57. Kim, C.-S. *et al.* Capsaicin exhibits anti-inflammatory property by inhibiting IkB-a degradation in LPS-stimulated peritoneal macrophages. *Cell. Signal.* **15,** 299–306 (2003).

58. Hood, V. C., Cruwys, S. C., Urban, L. & Kidd, B. L. The neurogenic contribution to synovial leucocyte infiltration and other outcome measures in a guinea pig model of arthritis. *Neurosci. Lett.* **299,** 201–204 (2001).

59. Sobande, A. A., Al-Bar, H. M. & Archibong, E. I. A comparison of spontaneous labor with induced vaginal tablets prostaglandin E2 in grand multiparae. *Saudi Med. J.* **22,** 698–701 (2001).

60. Dadsetan, S. *et al.* Reducing Peripheral Inflammation with Infliximab Reduces Neuroinflammation and Improves Cognition in Rats with Hepatic Encephalopathy. *Front. Mol. Neurosci.* **9,** 1–16 (2016).

61. Saperas, E., Kauffman, G. & Taché, Y. Role of central prostaglandin E2 in the regulation of gastric acid secretion in the rat. *Eur. J. Pharmacol.* **209,** 1–7 (1991).

62. Wilson, W. J. *et al.* Immune Modulation as an Effective Adjunct Post-exposure Therapeutic for B. pseudomallei. *PLoS Negl. Trop. Dis.* **10,** e0005065 (2016).

63. MacKenzie, K. F. *et al.* PGE(2) induces macrophage IL-10 production and a regulatory-like phenotype via a protein kinase A-SIK-CRTC3 pathway. *J. Immunol.* **190,** 565–77 (2013).

64. Ylöstalo, J. H., Bartosh, T. J., Coble, K. & Prockop, D. J. Human mesenchymal stem/stromal cells cultured as spheroids are self-activated to produce prostaglandin E2 that directs stimulated macrophages into an anti-inflammatory phenotype. *Stem Cells* **30,** 2283–2296 (2012).

65. Antoniou, K., Malamas, M. & Drosos, A. a. Clinical pharmacology of celecoxib, a COX-2 selective inhibitor. *Expert Opin. Pharmacother.* **8,** 1719–1732 (2007).

66. Shinohara, T. *et al.* Persistent inactivation of macrophage cyclooxygenase-2 in mycobacterial pulmonary inflammation. *Am. J. Respir. Cell Mol. Biol.* **41,** 146–154

(2009).

67. Walker, N. M. *et al.* Prostaglandin E 2 as an inhibitory modulator of fibrogenesis in human lung allografts. *Am. J. Respir. Crit. Care Med.* **185,** 77–84 (2012).

68. Garrison, G. *et al.* Reversal of myofibroblast differentiation by prostaglandin E(2). *Am. J. Respir. Cell Mol. Biol.* **48,** 550–8 (2013).

69. Gerarduzzi, C., He, Q., Zhai, B., Antoniou, J. & Di Battista, J. A. Prostaglandin E2-Dependent Phosphorylation of RAS Inhibition 1 (RIN1) at Ser 291 and 292 Inhibits Transforming Growth Factor-β-Induced RAS Activation Pathway in Human Synovial Fibroblasts: Role in Cell Migration. *J. Cell. Physiol.* **232,** 202–215 (2017).

70. Huang, S., Wettlaufer, S. H., Hogaboam, C., Aronoff, D. M. & Peters-Golden, M. Prostaglandin E2 inhibits collagen expression and proliferation in patient-derived normal lung fibroblasts via E prostanoid 2 receptor and cAMP signaling. *AJP Lung Cell. Mol. Physiol.* **292,** L405–L413 (2006).

71. Zahner, G. *et al.* The effect of prostaglandin E2 on mRNA expression and secretion of collagens I, III, and IV and fibronectin in cultured rat mesangial cells. *J. Am. Soc. Nephrol.* **4,** 1778–85 (1994).

72. Ball, V. Physicochemical perspective on 'polydopamine' and 'poly(catecholamine)' films for their applications in biomaterial coatings (Review). *Biointerphases* **9,** 30801 (2014).

73. Liebscher, J. *et al.* Structure of Polydopamine: A Never-Ending Story? *Langmuir* **29,** 10539–10548 (2013).

74. Wu, C. *et al.* Mussel-inspired bioceramics with self-assembled Ca-P/polydopamine composite nanolayer: Preparation, formation mechanism, improved cellular bioactivity and osteogenic differentiation of bone marrow stromal cells. *Acta Biomater.* **10,** 428–438 (2014).

75. Luo, R. *et al.* In Vitro Investigation of Enhanced Hemocompatibility and Endothelial Cell Proliferation Associated with Quinone-Rich Polydopamine Coating. *ACS Appl. Mater. Interfaces* **5,** 1704–1714 (2013).

76. Ren, J., Han, P., Wei, H. & Jia, L. Fouling-resistant behavior of silver nanoparticle-modified surfaces against the bioadhesion of microalgae. *ACS Appl. Mater. Interfaces* **6,** 3829–3838 (2014).

77. Beckford, S., Mathurin, L., Chen, J., Fleming, R. A. & Zou, M. The effects of polydopamine coated Cu nanoparticles on the tribological properties of

polydopamine/PTFE coatings. *Tribol. Int.* **103,** 87–94 (2016).

78. Jeong, K. J. *et al.* Polydopamine coatings enhance biointegration of a model polymeric implant. *Soft Matter* **7,** 8305 (2011).

CHAPTER 2: CAPSAICIN REDUCES PLGA-INDUCED FIBROSIS BY PROMOTING M2 MACROPHAGES AND SUPPRESSING OVERALL INFLAMMATORY RESPONSE

Authors: Tich H. Truong and Kim S. Jones

Publication: To be submitted in 2017-2018

2.1 ABSTRACT

Capsaicin reduced poly(lactic-co-glycolic) acid (PLGA)-induced fibrosis by promoting IL-10 secretion and suppressing alpha-smooth muscle actin (α-SMA) expression. The lifetime and efficacy of tissue engineering scaffolds are determined by the foreign body response. In this study, we investigated the *in vitro and in vivo* effects of capsaicin to reduce biomaterial-induced fibrosis. RAW 264.7 cells cultured on PLGA films with capsaicin responded with significant upregulation in M2 markers arginase-1 and IL-10 and downregulation of M1 markers iNOS and IL-12, demonstrating potential of capsaicin to reduce PLGA-induced inflammation. Subsequent animal studies were conducted where PLGA and capsaicin-embedded implants were fabricated and implanted in C57BL/6 mice for 2 and 14 days. We found that explanted capsaicin-embedded PLGA implants had 40% less collagen than PLGA-only implants. Capsaicin caused a 35% increase in IL-10 which played a key role in suppressing fibrosis. Macrophage phenotype markers in peritoneal cells and adherent cells were unaffected by capsaicin, however capsaicin suppressed myofibroblast marker α-SMA in adherent cells by day 14. Overall, our results revealed that capsaicin reduced biomaterial-induced fibrosis and demonstrates that capsaicin has

potential to extend the lifetime of a tissue engineering scaffold when used in long-term drug release applications from hydrophobic biomaterials.

Keywords
capsaicin, fibrosis, macrophage phenotype, poly(lactic-co-glycolic) acid, myofibroblast

2.2 INTRODUCTION

Capsaicin is a pungent capsinoid that has been used as a therapeutic to treat chronic inflammatory diseases, such as rheumatoid arthritis.[1] We found that capsaicin released from biomaterials reduces the normal fibrotic response. Biomaterials have been used as monitoring devices, such as glucose sensors to prevent hyperglycemia,[2] therapeutic applications, such as targeted drug delivery systems,[3] and for regenerative medicine, such as tissue engineering scaffolds.[4] However, these devices are susceptible to the foreign body response which reduces the efficacy of the device and eventually causes the device to fail. We used capsaicin released from PLGA in an attempt to mitigate fibrotic responses elicited by the biomaterial.

The foreign body response to biomaterials is often detrimental to the efficacy of the device. Fibrous encapsulation of continuous glucose monitoring sensors decreases the sensitivity of the signal and reduces the longevity of the device.[5] There is extensive research in designing coatings to hide the biomaterial from the immune system but detection of the foreign material is inevitable.[6–8] An alternative method is to reduce the influence from pro-inflammatory and pro-fibrotic cell types, such as macrophages and myofibroblasts, by promoting alternative phenotypes or preventing differentiation, respectively. The idea is to interfere with the foreign body response at the early stages such that fibrous encapsulation is delayed and/or reduced.

Macrophages are the key mediators of the inflammatory response. Macrophages migrate to the implant and phagocytose or degrade the implant. Failure to digest the implant results in granuloma formation and the release of toxic radicals, inflammatory

cytokines and inflammatory lipid mediators in an attempt to degrade the material.[9] However, inflammatory agents exacerbate the response and promote fibrosis. Macrophages can express two phenotypes, the M1, or "classically activated", phenotype and the M2, or "alternatively activated", phenotype. M1 macrophages are identified by their high expression of inducible nitric oxide synthase (iNOS) and high production of interleukin-12 (IL-12) and IL-23.[9] The phenotype can be polarized with lipopolysaccharide (LPS) and interferon gamma (IFNγ) and its activity can be downregulated, or controlled, by transforming growth factor beta-1 (TGF-β1) and IL-10 stimulation.[9]

M2 phenotype macrophages are involved in mediating wound healing and angiogenesis. These cells express arginase-1 mRNA, produce IL-10 and IL-23, and can be differentiated from monocytes by IL-4 and IL-10 stimulation.[9] M2 macrophages can control extracellular material deposition by producing arginase-1, for collagen production, and TGF-β1 to regulate the M1 phenotype.[9] It has been shown that macrophage phenotype plays a critical role in fibrotic response to biomaterials where early transition to an M2 phenotype can lead to resolved wound healing,[10] but unregulated M2 macrophage functionality can lead to peritoneal dialysis failure.[11]

Myofibroblasts are crucial for wound healing and remodeling. Their ability to produce collagen and contract provides the necessary characteristics to close wounds. Although the origin of these cells is uncertain, it has been elucidated that prolonged stimulation from excessive TGF-β1 will induce the myofibroblast phenotype and cause severe fibrosis. These cells can be derived from many cell types including local residing

mesenchymal cells, epithelium and endothelium cells and bone marrow derived fibrocytes.[12] Myofibroblasts are characterized by their high expression of alpha smooth muscle actin (α-SMA) and low expression of cadherin-1 (E-cadherin).[13,14]

Recently there has been development in using flavonoids, such as capsaicin, to suppress inflammation. Capsaicin has shown to have anti-inflammatory properties and to promote macrophage phenotype transition from M1 to M2.[15] This pungent active ingredient in chili peppers reduces the severity of autoinflammatory disease such as arthritis, osteoarthritis, and rheumatoid arthritis.[1,16,17] To our knowledge, there has never been an investigation on the effects of this plant extract on biomaterial-induced inflammation and fibrosis.

Brown *et al.* speculated that an early M2 phenotype promotes good wound healing.[10] As such, we were interested in using capsaicin to promote early M2 phenotype transition and reduce biomaterial induced inflammation and fibrosis. We hypothesized that capsaicin would downregulate the inflammatory and fibrotic response by promoting the M2 phenotype and by preventing myofibroblast differentiation, respectively. To test this hypothesis, we used poly(lactic-co-glycolic) acid (PLGA) as the biomaterial-induced inflammation and fibrosis model because it has been demonstrated to cause an *in vitro* M1 response[18] and an *in vivo* fibrotic response.[19] We tested *in vitro* macrophage phenotype response by culturing RAW 264.7 cells on PLGA films and we looked at *in vivo* peritoneal cell expression by implanted capsaicin-embedded PLGA implants into C57BL/6 mice. Our results showed that capsaicin caused an upregulation in M2 markers both *in vitro* and *in vitro*. More importantly, histological analysis revealed that capsaicin-

embedded implants had significantly less collagen deposition around the disc than PLGA control implants.

2.3 MATERIALS & METHODS

Casting PLGA-lined Petri dishes

PLGA-lined Petri dishes were made using solvent casting. Poly(lactic-co-glycolic) acid (PLGA, 75:25) (Sigma-Aldrich, Milwaukee) was dissolved in ethyl acetate (Sigma-Aldrich, Oakville) to make a 0.01 g/mL solution. One milliliter of the solution was added to autoclaved 60 mm glass Petri dishes and placed in a sterile vacuum chamber for 24 hours with gentle rocking. The dishes were removed aseptically from the vacuum chamber and stored in a biosafety cabinet before use. The average thickness of the films was 0.1729 mm, had no openings when viewed under bright field microscopy **(Figure A.1)** and a 24 hour sterility assay revealed no contamination growth. Capsaicin-embedded PLGA films were cast by blending 0.18 μmol of capsaicin (Sigma Aldrich, Milwaukee) in the PLGA/ethyl acetate solution prior to casting.

Cell culture

Murine macrophage-like cells (RAW 264.7) (ATCC TIB-71) were cultured in Dulbecco's Modified Eagle Medium (DMEM) (Thermo Fisher Scientific, Burlington) supplemented with 10% fetal bovine serum (FBS) (Thermo Fisher Scientific, Burlington) and 100 U/mL penicillin-streptomycin (Thermo Fisher Scientific, Burlington). Cells were maintained in a 37°C and 5% CO_2 environment and subcultured at 80-90% confluency using phosphate buffered saline (PBS) (Mg^{--}, Ca^{--}, pH 7.4) and a cell scraper.

Cellular response to PLGA films

RAW 264.7 cells were seeded at a population of 1×10^6 cells on three different PLGA-lined Petri dishes conditions for 24 hours. The three conditions were pure PLGA films, PLGA films with 60 μM of capsaicin in the medium, and PLGA films blended with 0.18 μmol of capsaicin. Capsaicin was suspended in DMSO before adding to the medium where the volume of DMSO used was less than 1% of the medium. The medium was collected for IL-10 and IL-12 quantification and the cells were lysed to extract total RNA for relative quantification using qPCR.

Casting capsaicin-embedded PLGA discs

PLGA implants were made using solvent casting in autoclaved silicone molds (McMaster-Carr) with 3/8" wells **(Figure A.2)**. Using a solution of 0.011 g of PLGA and 1 mL of ethyl acetate, 90 μL were added to each well 12 times with 5 minutes of vacuuming between each addition. Discs were vacuumed for an additional hour before being removed aseptically and stored in a sterile environment at 4°C **(Figure A.3)**.

Capsaicin-embedded PLGA discs were made using the previously mentioned method but with 100 μg of capsaicin dissolved in the PLGA mixture. Implants had a 71% (w/w) loading efficiency and the discs stored in sterile Petri dishes at 4°C before use.

Animals and implantation procedure

Canadian Council on Animal (CCAC) guidelines for the care and use of laboratory animals were followed throughout the study. All animal experimental protocols were approved by the Animal Research Ethics Board at McMaster University under the Animal Utilization Protocol 15-01-02.

C57BL/6, 6-8 week old, male mice were purchased from Charles River (Montréal, QC) and housed in the Central Animal Facility at McMaster University for one week to acclimatize to the facility.

Mice were anesthetized with isoflurane and given a subcutaneous injection of buprenorphine (0.03 mg/mL) before undergoing surgery. PLGA discs were implanted into the peritoneal cavity and placed in the right lower abdominal quadrant and away from the omentum. The muscle wall was closed using degradable 4-0 Vicryl suture (Ethicon) before the mice were taken off isoflurane and placed in a recovery cage. Mice were housed individually for 2 or 14 days before they were sacrificed. No additional analgesics or anti-inflammatory drugs were provided to the mice for the duration of the study.

Animal sample collection and isolation

Prior to sacrificing the mice, a 2 mL peritoneal lavage was done using 0.9% saline. Lavages were collected in DNase/RNase free microcentrifuge tubes and immediately placed on ice before they were centrifuged at 1000 × g for five minutes at 4°C. The supernatant was collected for IL-10, IL-12 and IL-23 ELISA assay and the pellet was lysed using 1 mL of TRIzol.

Adherent cell RNA was extracted by placing explanted PLGA discs directly in 1 mL of TRIzol (Thermo Fisher Scientific, Burlington). The solution was immediately vortexed at high speeds for 30 seconds and left to incubate at room temperature for 1 hour before total RNA was extracted by following the manufacturer's protocol.

Capsaicin release from PLGA implants

Capsaicin-embedded PLGA discs were incubated at 37°C with 20 mL of PBS (Mg^{++}, Ca^{++}, pH 7.4) for two weeks. One milliliter samples were collected and replaced with fresh PBS at various time intervals. Samples were filtered using 0.22 µm PVDF hydrophobic syringe filters (EMD Millipore) and stored at 4°C before being measured at 237 nm using HPLC. Degassed and 0.2 µm filtered ddH_2O and HPLC grade methanol (Sigma-Aldrich, Oakville) were used as the mobile phases for HPLC. Samples were fed through a Luna C18 column (Acclaim, USA) using a gradient of 70% to 100% methanol over a period of 13 minutes. Capsaicin concentration was quantified using a standard curve generated from a serial dilution of capsaicin in HPLC grade methanol (0.1 µg/mL-7 µg/mL) with R^2=0.99.

RNA isolation and quantitative PCR

RNA was isolated from cells using TRIzol (Thermo Fisher Scientific, Burlington) and by following the manufacturer's protocol. Nanodrop was used to ensure RNA 260 nm/280 nm ratio was above 1.8. Total RNA was diluted to 50 ng/µL and converted to cDNA using the High-Capacity cDNA Reverse Transcription Kit with RNase inhibitor (Thermo Fisher Scientific, Burlington), as outlined in the manufacturer's protocol. cDNA samples were quantified using SYBR Green (Thermo Fisher Scientific, Burlington), 500 ng of cDNA and 200 nM of forward and reverse primers **(Table A.1)**. Genes of interest were measured using the one-step process on the Mx3000 qPCR system and semi-quantified using the $2^{-\Delta Ct}$ method described by Livak and Schmittgen.[20]

ELISA

IL-10, IL-12 and IL-23 cytokine concentrations in supernatant were quantified using ELISA kits (eBioscience, USA) and by following the manufacturer's protocol. Standard curves were fitted using a four parameter logistics curve with R^2=0.99.

Histology

Explanted PLGA discs were immediately fixed in 10% formalin for 48 hours. Samples were sent to the McMaster Immunology Research Center histology lab for processing where the samples were dehydrated through ascending grades of alcohol and xylene and impregnated with paraffin wax. Paraffin-embedded sections were stained with picrosirius red (PSR) (Sigma-Aldrich, Oakville) and hematoxylin and eosin (H&E) (Sigma-Aldrich, Oakville).

Imaging

Bright field micrographs were imaged using a Zeiss Axiovert 200M inverted microscope and Axiovision software (ver. 4.8.2.0). Polarized micrographs were imaged using an Olympus BX41 inverted microscope with an analyzer and polarizer set at 100% degree of polarization.

Collagen thickness quantification

Collagen thickness was quantified in a single blinded study. Collagen thickness was measured using a lab developed ImageJ macro[21] where measurements were made perpendicularly from the edge of the disc to the outer edge of collagen. Measurements were taken at five pixel intervals along the perimeter of the disc after which the measurements were averaged.

Statistics

The data were assumed to be normally distributed and presented as mean ± standard error of the mean (SEM). R was used for statistical analysis between treatments. Multiple comparisons between treatments and genes of interest where compared using a two-way ANOVA with Welch-like corrections for non-homogeneity and a *post hoc* Tukey's HSD if significance was detected. A value of $p<0.05$ was considered statistically significant and only select comparisons are shown in figures.

2.4 RESULTS AND DISCUSSION

Capsaicin upregulates arginase-1 in PLGA-induced macrophages

RAW 264.7 cells were cultured in three different conditions for 24 hours: PLGA film, PLGA film with 60 µM of capsaicin in the medium, and PLGA film blended with 60 µM of capsaicin. The cells were lysed and total RNA was extracted for quantification.

Capsaicin in the medium did not have a significant effect on M1 marker iNOS and M2 marker arginase-1 expression **(Figure 2.1)**. Compared to the PLGA control, suspended capsaicin decreased iNOS mRNA levels by 17% and increased arginase-1 levels by 50%, but not significantly. Suspended capsaicin also affected the difference between iNOS and arginase-1, however, capsaicin embedded in PLGA had a significant effect on macrophage genetic markers. Embedded capsaicin downregulated iNOS by almost 90% and upregulated arginase-1 levels by 70%. It also caused a statistically significant difference between iNOS and arginase-1 where arginase-1 was expressed fives times more than iNOS. These results showed that capsaicin altered macrophage phenotype change from M1 and M2, but embedded capsaicin was surprisingly more effective than capsaicin in suspension.

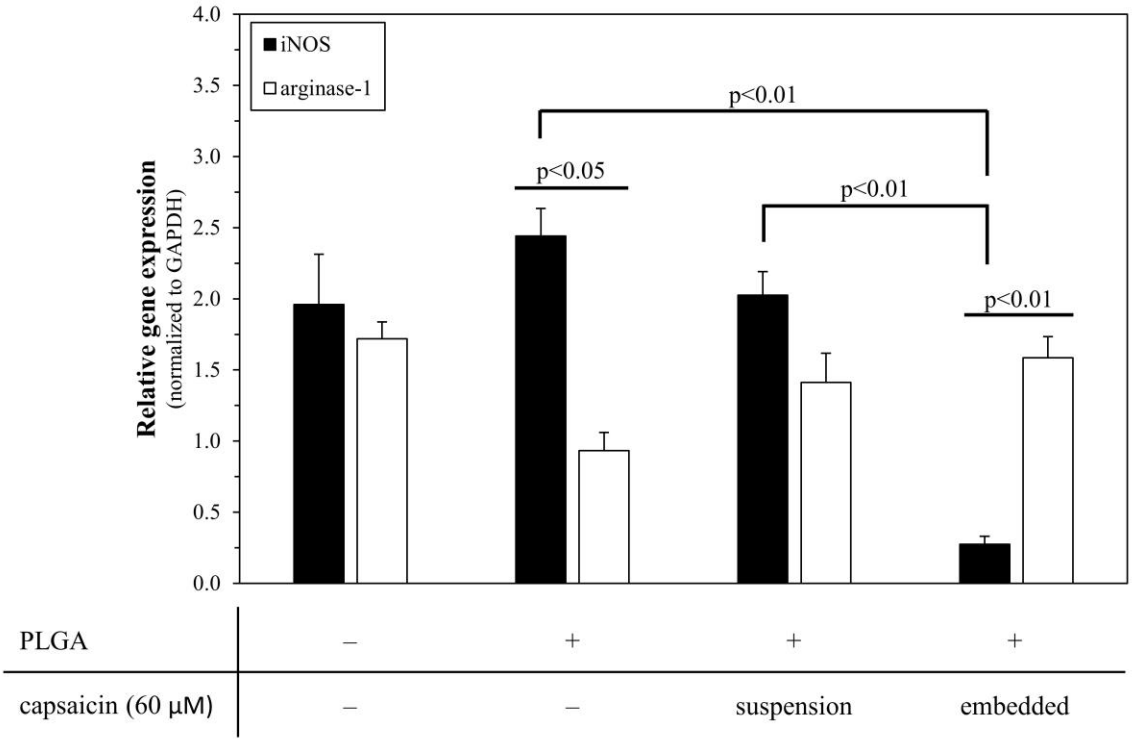

Figure 2.1. RAW 264.7 cells cultured on PLGA films with capsaicin suspended in the medium, or embedded in the film, for 24 hours. Capsaicin downregulated iNOS mRNA and upregulated arginase-1 mRNA. Embedded capsaicin was more effective at promoting the M2 phenotype than when in suspension. Values were normalized to GAPDH and expressed as mean ± SEM for five independent experiments.

The difference in gene expression between suspended and embedded capsaicin was due to the capsaicin concentration the cells were exposed to. There was a higher concentration of capsaicin on the surface of embedded film because capsaicin has very low solubility in water.[22] The hydrophobic capsaicin is less likely to diffuse from the hydrophobic PLGA carrier and into the hydrophilic medium. This conclusion is supported by Sahana *et al.*, who found that the cumulative release of hydrophobic estradiol from PLGA nanoparticles remained low within the first few days[23] and the majority of the drug remained in the carrier.

We have also seen that increasing concentrations of capsaicin in the medium suppressed iNOS and upregulated arginase-1 in IFNγ and LPS-stimulated macrophages

(Figure S2.1). Kim *et al.* have also demonstrated the anti-inflammatory effects of capsaicin where iNOS mRNA decreased with increasing capsaicin dosages, however this was only for LPS-stimulated macrophages.[24] IFNγ enhances activation of the NF-κB inflammation pathway[25,26] to produce a polarized M1 macrophage phenotype that is more difficult to alter than just LPS stimulation. For capsaicin to be able to revert the IFNγ and LPS-induced M1 phenotype, suggests that capsaicin is highly effective at altering phenotype regardless of the stimulating factors.

PLGA is a suitable biomaterial-inducing M1 phenotype model because it has similar effects to the LPS and IFNγ M1 macrophage model. Macrophages cultured on PLGA films respond with an M1 phenotype have an enhanced inflammatory response with upregulation of tumor necrosis factor-α (TNF-α) and production of reactive oxygen species (ROS).[27] We have seen that there is a positive correlation between PLGA exposure time and M1 phenotype polarization. There was a significance difference between iNOS and arginase-1 expression after 24 and 72 hours of incubation where iNOS was expressed two times more than arginase-1 after 24 hours and three times more than arginase-1 after 72 hours **(Figure S2.2).**

The decrease in gene expression was not associated with dying or apoptotic cells. There was no significant difference in viability between untreated cells and cells cultured on PLGA and cells stimulated with a maximum of 120 μM of capsaicin **(Figure S2.3)**. In fact, previous studies have also shown that capsaicin has no cytotoxic effects at dosages up to 200 μM.[16,24,28]

Capsaicin in suspension upregulates IL-10 production

RAW 264.7 cells were cultured on PLGA films with capsaicin in the medium for 24 hours. The supernatant was collected and M1 marker IL-12 and M2 marker IL-10 were quantified using ELISA.

Capsaicin caused a two-fold higher increase in IL-10 than cells cultured on PLGA **(Figure 2.2)**. Capsaicin-treated cells secreted significantly more IL-10 than IL-12, which supports the previous mRNA results where capsaicin promoted the M2 phenotype in PLGA-stimulated cells. Interestingly, IL-12 concentrations were similar to untreated PLGA-induced cells.

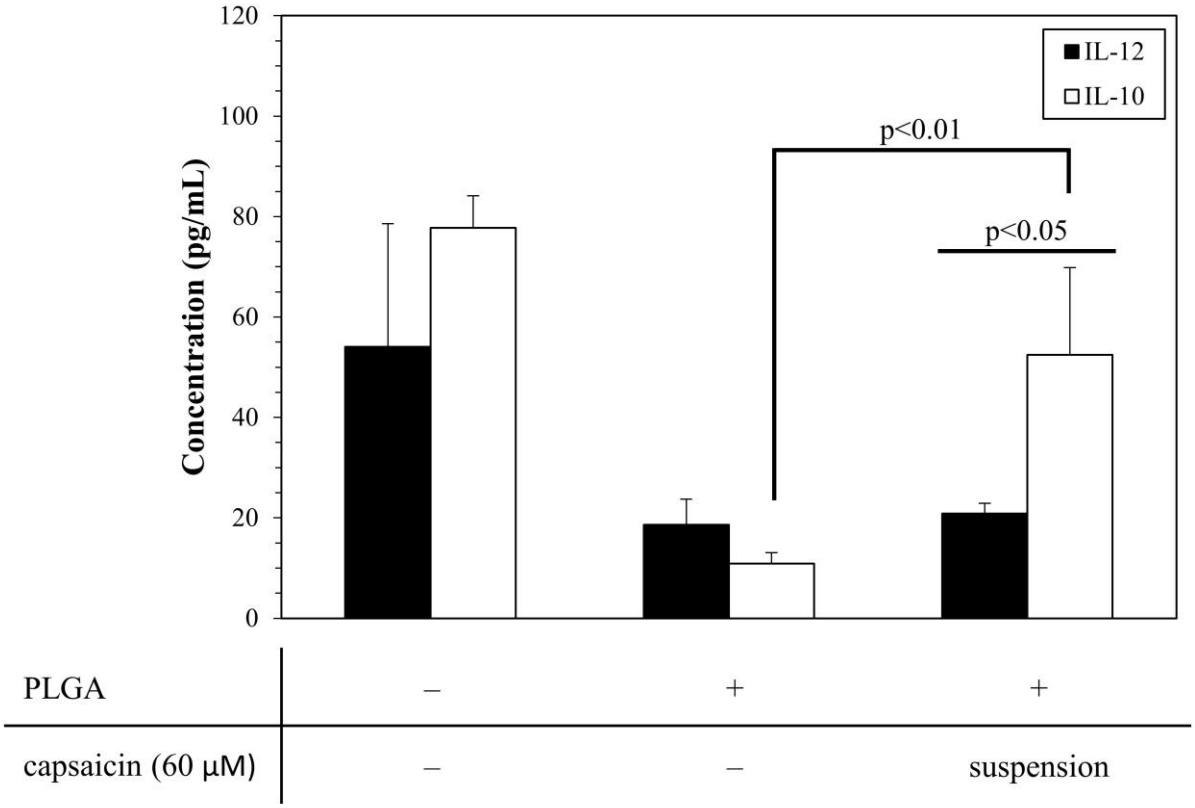

Figure 2.2. RAW 264.7 cells cultured on PLGA films with, and without, capsaicin for 24 hours. The medium was collected and IL-12 and IL-10 concentrations were quantified. Capsaicin caused significantly more IL-10 secretion than cells cultured on PLGA films. Each value represents mean ± SEM for three independent experiments.

Nitric oxide (NO) has been shown to inhibit IL-12 production by inhibiting the nuclear transcription factor-kappaB (NF-κB) pathway[26] but we showed that capsaicin in suspension upregulated iNOS mRNA levels. This suggests that there is an alternative pathway that is activating NF-κB. IL-12 might have a larger inhibitory effect on IL-10 than NO. The two-fold difference in IL-10 concentrations might be sufficient to decrease IL-12 production as Aste-Amezaga *et al.* demonstrated that IL-12 suppressed IL-10 production from LPS-stimulated cells.[29]

From genetic and cytokine analyses, we demonstrated that capsaicin had anti-inflammatory effects on PLGA-stimulated RAW 264.7 cells and upregulated M2 markers. Macrophages that interacted with capsaicin on the film and in the medium expressed high levels of the M2 markers arginase-1 and IL-10 and low M1 markers iNOS and IL-12. We used a unicellular model that might not be predictive of *in vivo* results, but these findings show that capsaicin is a promising anti-inflammatory compound, when blended with a polymer carrier, and we were interested in investigating its effects in an animal model.

Capsaicin reduces collagen from PLGA-induced fibrosis

PLGA and capsaicin-embedded PLGA discs were implanted intraperitoneally in C57BL/6 mice for 2 and 14 days to study the fibrotic response.[30] The discs were explanted and stained with PSR and H&E for collagen and cellularity analysis.

Using polarized light microscopy, PSR stained sections showed no birefringent areas around the discs on day 2 **(Figure 2.3a)**. This was expected as foreign body giant cell formation and fibrous encapsulation does not initiate until 5-7 days post-implantation.[8] By day 14, there were large birefringent regions around both types of

implants where PLGA discs appeared to have a thicker layer of collagen than capsaicin-embedded PLGA implants. Upon quantification, capsaicin-embedded PLGA implants had significantly less collagen than PLGA only discs **(Figure 2.3b)**. On average, capsaicin reduced collagen thickness by 40% which is a profound result that demonstrates that capsaicin has *in vivo* anti-fibrotic effects on PLGA-induced fibrosis.

H&E micrographs showed presence of cell recruitment and adhesion 2 days after implantation, with significantly more cells on day 14 **(Figure S2.4)**. PLGA implants on day 14 had a thicker layer of cells than capsaicin-embedded PLGA implants which suggests that capsaicin might have reduced cell recruitment and stimulated decreased collagen deposition.

Cell recruitment and stimulation might have been reduced through inhibiting

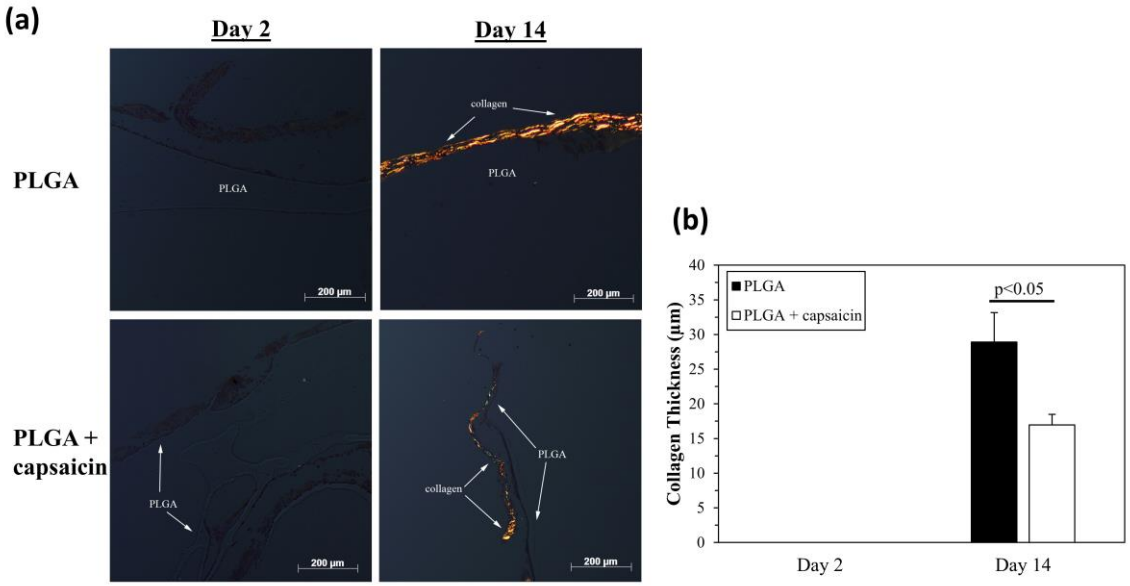

Figure 2.3. (a) Representative polarized micrographs of PSR stained PLGA and capsaicin-embedded PLGA discs explanted from mice after 2 and 14 days of incubation. No collagen was present until day 14 where PLGA implants had more birefringent regions than capsaicin-embedded implants. (b) Birefringent regions were quantified and revealed no detectable collagen on day 2 but significantly more collagen on PLGA implants than capsaicin-embedded implants. Each value represents mean ± SEM for three independent experiments.

nociceptor innervation and NO release. In a rat wound model, capsaicin-treated rats showed less pain sensation and poorer wound healing.[31] Smith *et al.* observed capsaicin-treated rats having 30-40% reduced wound healing and increased presence of α-smooth muscle actin (α-SMA). This was also seen in a rabbit wound model where wounds with surgically excised nerves exhibited poor wound healing and decreased macrophage presence than controls.[32] It is clear that capsaicin's analgesic effects are inhibiting cellular activity resulting in poor wound healing but it is uncertain what cell type capsaicin is affecting.

Capsaicin upregulates M2 cytokine but not M2 genetic markers from peritoneal cells

To understand how cells were responding to the implants, we looked at macrophage markers iNOS and arginase-1 mRNA of cells in the peritoneal cavity where there is a high population of macrophages[33] capable of expressing M1 and M2 phenotypes *ex vivo.*[24]

After 2 days of implantation, neither the sham mice nor the mice with implants showed any significant difference in iNOS mRNA **(Figure 2.4a)**. However, mice with PLGA implants showed increased levels of iNOS which suggests that PLGA is inducing the M1 phenotype. In addition, implants with capsaicin caused cells to express less iNOS than PLGA controls on day 2 and 14 which suggests that capsaicin inhibited iNOS.

Both types of implants caused significant suppression in arginase by day 14 **(Figure 2.4b)** which indicates that capsaicin upregulated arginase-1 activity in peritoneal cells. However, without identifying and quantifying the cells we cannot definitively say that capsaicin is promoting macrophages to have an early M2 phenotype which resulted

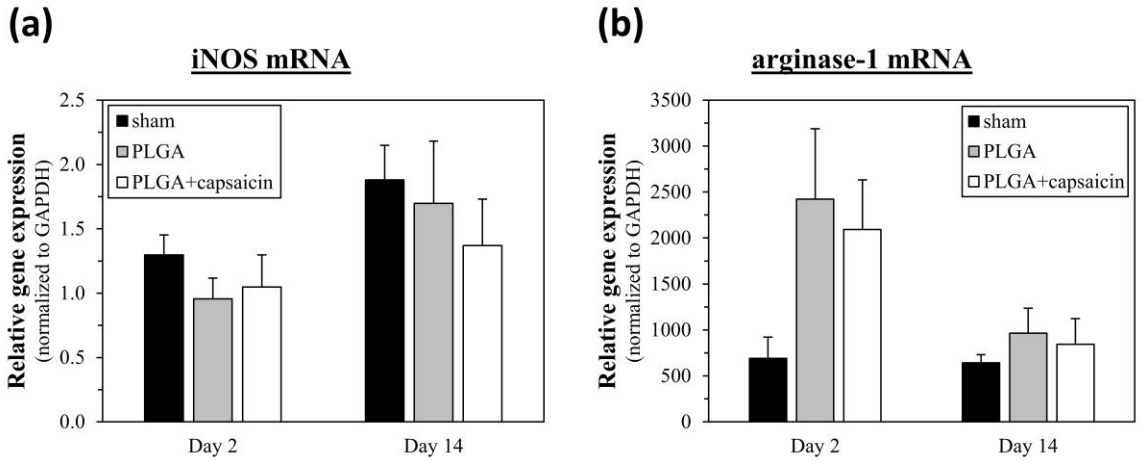

Figure 2.4. (a) iNOS and (b) arginase-1 gene expressions from peritoneal cells. Cells were collected from mice with PLGA and capsaicin-embedded PLGA discs incubated for 2 and 14 days. iNOS mRNA levels did not change after day 14, however cells exposed to implants expressed less arginase-1 on day 14. Each value was normalized to GAPDH and expressed as mean ± SEM for three independent experiments.

in a decrease in iNOS on day 14. Nevertheless, we decided to look at macrophage cytokine markers in the lavage to see if it agrees with our mRNA data.

Supernatant from lavages were collected and M1 cytokine markers IL-12and IL-23 and M2 cytokine marker IL-10 were quantified using ELISA. IL-12 was not detectable in any of the lavages but there were measureable levels of IL-23 and IL-10 **(Figure 2.5)**. Capsaicin stimulated early IL-10 secretion which continued to increase by the end of the study. Although both implants upregulated IL-10 by day 14, capsaicin caused 35% more secretion than PLGA. IL-10 levels were also significantly more than IL-23 which suggests capsaicin increased M2 macrophage activity.

Capsaicin might be decreasing the fibrotic response by upregulating early IL-10 levels to suppress TNF-α mediated inflammation and fibrosis. Previous studies have demonstrated that IL-10 reduces TNF-α activity in LPS and IFNγ-activated macrophages.[34,35] In clinical studies, healthy patients express high levels of IL-10 in respiratory epithelial lining fluid than patients with cystic fibrosis[35] and there is a strong

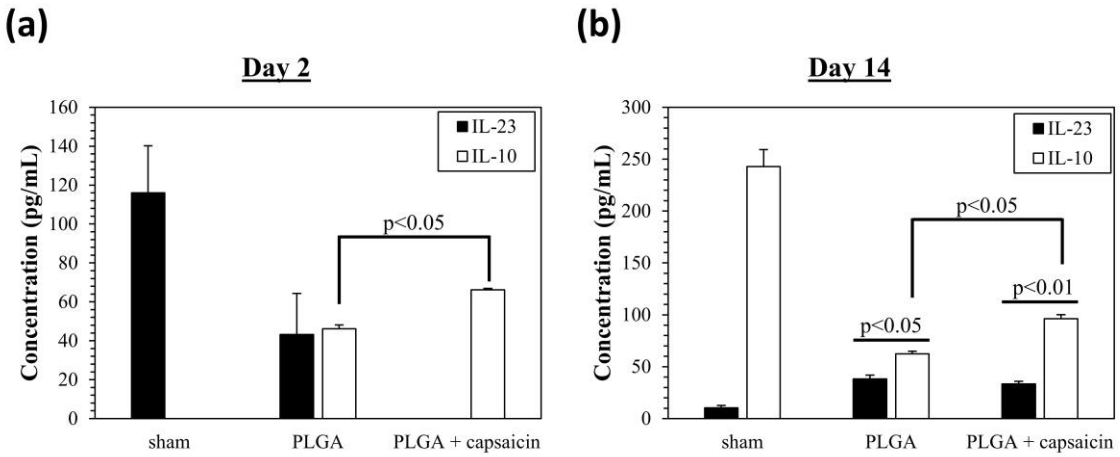

Figure 2.5. IL-23 and IL-10 concentrations in peritoneal lavages from mice implanted with PLGA and capsaicin-embedded PLGA discs. (a) Capsaicin caused a significant increase in IL-10 on day 2 and on (b) day 14. Undetectable levels of IL-10 and IL-23 in sham mice and mice with capsaicin-embedded PLGA disc, respectively, on day 2 and no IL-12 was detected in any samples. Each value represents mean ± SEM for three independent experiments.

positive correlation between TNF-α and IL-23. Slavov *et al.* discovered that healthy patients have lower levels of both TNF-α and IL-23 when compared with patients who have silicosis.[36] This coincides with our results where we saw significantly more IL-23 than IL-10 on day 14 when capsaicin was used.

From our results, it was clear that the implants and treatments have no significant effect on peritoneal cells. However, capsaicin is causing an abundance of early and late IL-10 secretion. Because we did not identify cell types in the peritoneal lavages, we cannot be certain that any of the peritoneal cells are responsible for producing the cytokines, however we hypothesize that cells on the implants are involved. To investigate this hypothesis, we extracted adherent cells and analysed macrophage and myofibroblast mRNA levels in the cells.

Capsaicin suppresses collagen-1 expression from adhered cells

A second set of experiments were done where implants were placed in lysing reagent to extract RNA for quantification. In addition to the iNOS and arginase-1

macrophage markers, we looked at markers that are associated with fibrotic cells such as cadherin-1 (E-cadherin), an epithelial cell marker, alpha smooth muscle actin (α-SMA), a myofibroblast marker, and collagen-1.

Capsaicin had no significant effects on iNOS, arginase-1, α-SMA, E-cadherin and collagen-1 on day 2 and 14 **(Figure 2.6)**. All genes of interest, except for arginase-1, showed a decreased expression on day 14. Interestingly, capsaicin almost caused a significant increase (p=0.06) in arginase-1 expression from day 2 to day 14.

Although there was no difference in gene expression between adhered cells on PLGA and capsaicin-embedded PLGA implants, this information gave insight into the overall expression of the cells on the discs. Capsaicin appeared to be downregulating

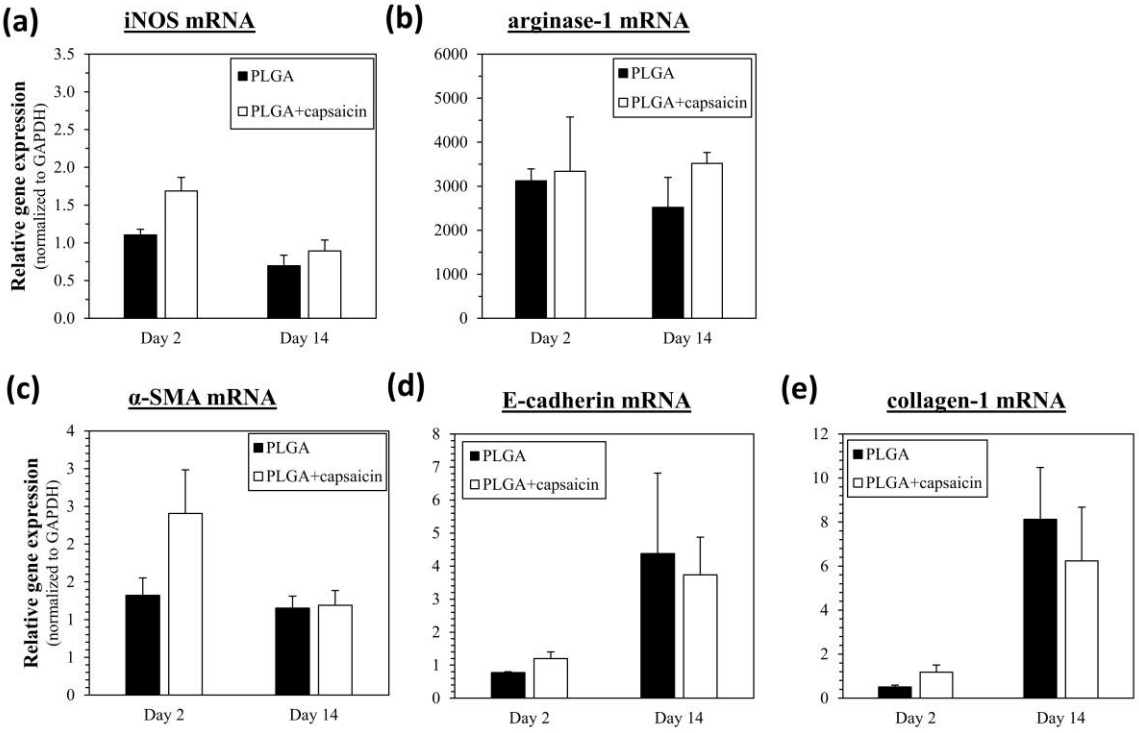

Figure 2.6. (a) iNOS, (b) arginase-1, (c) α-SMA, (d) E-cadherin and (e) collagen-1 gene expression from adherent cells on PLGA and capsaicin-embedded PLGA discs. Capsaicin upregulated arginase-1 while downregulating iNOS. Values were normalized to GAPDH and expressed as mean ± SEM for three independent experiments

iNOS and upregulating arginase-1 gene expression by day 14, but this trend was similar with PLGA implants. There were similar mRNA trends between PLGA and capsaicin-embedded PLGA implants except for α-SMA where capsaicin increased early α-SMA which decreased by day 14. Overall, capsaicin did not appear to promote early M2 phenotype in adherent cells to decrease the fibrotic response, as demonstrated by Brown *et al.*[10] In fact, adherent cells expressed similar levels of iNOS and arginase-1 as peritoneal cells. It is likely that capsaicin activated other anti-inflammatory mediators that amplified the phenotype transition.

IL-10 secretion is regulating macrophage and myofibroblast activity to reduce fibrosis. As previously mentioned, we saw high concentrations of IL-10 the peritoneal lavage. Boehler *et al.* have shown that IL-10 is capable of suppressing LPS and IFNγ stimulated macrophages by suppressing TNF-α expression[37] through activation of STAT3, which is thought to be the anti-inflammatory transcriptional regulator.[38,39] Hung *et al.* also showed that IL-10 is able to reduce liver thioacetamide-induced liver fibrogenesis where mice treated with IL-10 human plasmids had significant reduction in TNF-α, TGF-β1 and collagen-1 while attenuated α-SMA activation.[40]

Our results showed that capsaicin upregulated epithelial marker E-cadherin and downregulated myofibroblast marker α-SMA. This was confounding because macrophages with an M2 phenotype have been demonstrated to produce TGF-β1,[41] which promotes myofibroblast differentiation through epithelial-mesenchymal transition. As such, it was expected to see increased presence of myofibroblast markers when the upregulation of M2 arginase-1 marker.

Capsaicin might have both a multicellular effect on macrophages, fibroblasts and myofibroblasts to promote anti-fibrotic mediators such as prostaglandin E-2 (PGE-2). As previously mentioned, capsaicin's analgesics effects inhibit pain mediators that are essential for proper macrophage function and myofibroblast control. Widgerow and Kalaria reviewed that sensory nerve innervation is needed to stimulate macrophage activity and promote proper wound healing.[42] Nociceptor innervation stimulation causes macrophages to produce nitric oxide, which can lead to an abundance of inflammatory mediators to be released, such as prostaglandin E-2 (PGE2), to suppress α-SMA.[43] Our results showed that both adhered and peritoneal cells expressed iNOS levels, which indicate NO was being produced.

However, additional experiments are required to elucidate how capsaicin affected the cells and which genes played an important role in mediating fibrosis. As previously mentioned, one such experiment is to identify and quantify cell types in the peritoneal lavage and on the disc need to be quantified to determine the main gene that is being expressed.

Capsaicin is predicted to last until the implant fully degrades

To predict if capsaicin was present on day 14, *in vitro* release kinetics of capsaicin-embedded PLGA implants was determined by incubating the discs in PBS and measuring capsaicin concentration in the medium using HPLC.

Capsaicin followed first order release kinetics from the implant and only 20% of the loaded drug was release by day 14 **(Figure 2.7a)**. On day 14, we extracted all of the remaining capsaicin from the implant and collected approximately 63 μg **(Figure 2.7b)**. This slow release kinetics has been previously demonstrated in a similar system where a

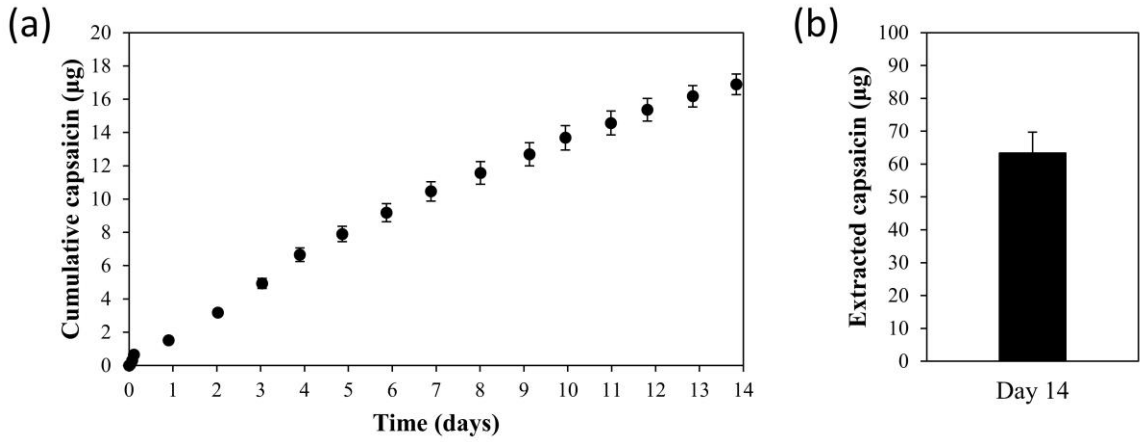

Figure 2.7. Cumulative release kinetics of capsaicin from capsaicin-embedded PLGA discs. Capsaicin was embedded in 0.01 g of PLGA and incubated in PBS for 14 days. (a) Capsaicin followed first order release kinetics during the 14 days of incubation. (b) By day 14, there was 63 µg of capsaicin remaining in the disc. Each value represents mean ± SEM for three independent experiments.

hydrophobic drug was released from poly(lactic acid) modified nanoparticles.[44] The slow release kinetics is attributed to the capsaicin's extremely low solubility and PLGA's degradation being driven by solubility-controlled bulk erosion process.[45,46]

We expect capsaicin to be present until the PLGA is fully degraded which can take at minimum six months.[46] If capsaicin-embedded PLGA discs were implanted beyond 14 days, we expect capsaicin to not cause chronic inflammation in mice because there was no upregulation in white blood cells (WBC) in whole blood on day 14 **(Figure S2.5)**. This shows that capsaicin is a promising compound for long term use beyond 14 days.

In summary, we demonstrated that capsaicin promoted the M2 phenotype from PLGA-induced macrophages *in vitro* and PLGA-induced peritoneal cells *in vivo*. Capsaicin reduced collagen thickness by 40% around PLGA discs implanted in mice after 14 days of incubation in the peritoneal cavity. The decreased fibrotic response is evidently driven by the increased IL-10 production while peritoneal cells and adherent

cells showed no genetic responses to capsaicin. Capsaicin was released from PLGA at a slow rate and approximately 80% of capsaicin remained in PLGA by day 14. This demonstrates that capsaicin is a promising drug for long term anti-inflammatory and anti-fibrotic applications to extend the lifetime of the biomaterial. Further work is needed to determine the cell types in the peritoneum and on the implants to determine the cells and pathways that are responsible for mediating fibrosis.

2.5 ACKNOWLEDGMENTS

The authors would like to acknowledge that this work was supported by the Natural Sciences and Engineering Research Council. We thank Emma Buller, Ugonwa Echendu and Anthony Saraco for their assistance with animal studies and blinded collagen thickness and blood smear quantification studies.

2.6 DISCLOSURE STATEMENT

The authors declare that there were no conflicts of interests regarding the publication of this paper.

2.7 REFERENCES

1. Joe, B. & Lokesh, B. R. Prophylactic and therapeutic effects of n-3 polyunsaturated fatty acids, capsaicin, and curcumin on adjuvant induced arthritis in rats. *J. Nutr. Biochem.* **8,** 397–407 (1997).

2. Vallejo-Heligon, S. G., Brown, N. L., Reichert, W. M. & Klitzman, B. Porous, Dexamethasone-loaded polyurethane coatings extend performance window of implantable glucose sensors in vivo. *Acta Biomater.* **30,** 106–115 (2016).

3. Pichavant, L. *et al.* pH-controlled delivery of gentamicin sulfate from orthopedic devices preventing nosocomial infections. *J. Control. Release* **162,** 373–381 (2012).

4. Wu, Z. *et al.* Decellularized scaffolds containing hyaluronic acid and EGF for promoting the recovery of skin wounds. *J. Mater. Sci. Mater. Med.* **26,** 59 (2015).

5. Avula, M. *et al.* Local release of masitinib alters in vivo implantable continuous glucose sensor performance. *Biosens. Bioelectron.* **77,** 149–156 (2016).

6. Hu, W. J., Eaton, J. W., Ugarova, T. P. & Tang, L. Molecular basis of biomaterial-mediated foreign body reactions. *Blood* **98,** 1231–8 (2001).

7. Courtney, J. M., Lamba, N. M. K., Sundaram, S. & Forbes, C. D. Biomaterials for blood-contacting applications. *Biomaterials* **15,** 737–744 (1994).

8. Anderson, J. M., Rodriguez, A. & Chang, D. T. Foreign body reaction to biomaterials. *Semin. Immunol.* **20,** 86–100 (2008).

9. Mosser, D. M. The many faces of macrophage activation. *J. Leukoc. Biol.* **73,** 209–212 (2003).

10. Brown, B. N. *et al.* Macrophage phenotype as a predictor of constructive remodeling following the implantation of biologically derived surgical mesh materials. *Acta Biomater.* **8,** 978–987 (2012).

11. Bellon, T. *et al.* Alternative activation of macrophages in human peritoneum: implications for peritoneal fibrosis. *Nephrol. Dial. Transplant.* **26,** 2995–3005 (2011).

12. Hinz, B. *et al.* The Myofibroblast. *Am. J. Pathol.* **170,** 1807–1816 (2007).

13. Hinz, B. *et al.* Recent developments in myofibroblast biology: Paradigms for connective tissue remodeling. *Am. J. Pathol.* **180,** 1340–1355 (2012).

14. Bonde, A.-K., Tischler, V., Kumar, S., Soltermann, A. & Schwendener, R. A.

Intratumoral macrophages contribute to epithelial-mesenchymal transition in solid tumors. *BMC Cancer* **12,** 35 (2012).

15. Raychaudhuri, A., Colombo, C., Pastor, G., Wong, M. & Jeng, A. Y. Effect of capsaicin on carrageenan-induced inflammation in rat pleurisy and exudate substance P level. **34,** 9–11 (1991).

16. Bitencourt, S. *et al.* Capsaicin induces de-differentiation of activated hepatic stellate cell. *Biochem. Cell Biol.* **90,** 683–90 (2012).

17. Chen, X. W., Serag, E. S., Sneed, K. B. & Zhou, S. F. Herbal bioactivation, molecular targets and the toxicity relevance. *Chem. Biol. Interact.* **192,** 161–176 (2011).

18. Bartneck, M. *et al.* Inducing healing-like human primary macrophage phenotypes by 3D hydrogel coated nanofibres. *Biomaterials* **33,** 4136–4146 (2012).

19. Feng, W. *et al.* Anti-inflammation and anti-fibrosis with PEGylated, apigenin loaded PLGA nanoparticles in chronic pancreatitis disease. *RSC Adv.* **5,** 83628–83635 (2015).

20. Livak, K. J. & Schmittgen, T. D. Analysis of relative gene expression data using real-time quantitative PCR and the 2^(-ΔΔCT) method. *Methods* **25,** 402–408 (2001).

21. Truong, T. ImageJ-perpendicularThicknessTool. (2016). doi:10.5281/zenodo.50157

22. De Lourdes Reyes-Escogido, M., Gonzalez-Mondragon, E. G. & Vazquez-Tzompantzi, E. Chemical and pharmacological aspects of capsaicin. *Molecules* **16,** 1253–1270 (2011).

23. Taylor, M. J., Tanna, S. & Sahota, T. In vivo study of a polymeric glucose-sensitive insulin delivery system using a rat model. *J. Pharm. Sci.* **99,** 4215–4227 (2010).

24. Kim, C.-S. *et al.* Capsaicin exhibits anti-inflammatory property by inhibiting IkB-a degradation in LPS-stimulated peritoneal macrophages. *Cell. Signal.* **15,** 299–306 (2003).

25. Held, T. K. *et al.* Gamma Interferon Augments Macrophage Activation by Lipopolysaccharide by Two Distinct Mechanisms , at the Signal Transduction Level and via an Autocrine Mechanism Involving Tumor Necrosis Factor Alpha and Interleukin-1 Gamma Interferon Augments Macrophage. *Infect. Immnuity* **67,** 206–212 (1999).

26. Xiong, H. *et al.* Inhibition of interleukin-12 p40 transcription and NF-kappaB activation by nitric oxide in murine macrophages and dendritic cells. *J. Biol. Chem.* **279,** 10776–83 (2004).

27. Kim, S. *et al.* Reduced inflammatory responses to poly(lactic-co-glycolic acid) by the incorporation of hydroxybenzyl alcohol releasing polyoxalate. *Macromol. Res.* **19,** 1242–1249 (2011).

28. Kim, Y. & Lee, J. Anti-Inflammatory Activity of Capsaicin and Dihydrocapsaicin through Heme Oxygenase-1 Induction in Raw264.7 Macrophages. *J. Food Biochem.* **38,** n/a-n/a (2014).

29. Aste-Amezaga, M., Ma, X., Sartori, A. & Trinchieri, G. Molecular mechanisms of the induction of IL-12 and its inhibition by IL-10. *J. Immunol.* **160,** 5936–44 (1998).

30. Kolb, M. *et al.* Differences in the Fibrogenic Response after Transfer of Active Transforming Growth Factor- β 1 Gene to Lungs of 'Fibrosis-prone' and 'Fibrosis-resistant' Mouse Strains. *Am. J. Respir. Cell Mol. Biol.* **27,** 141–150 (2002).

31. Smith, P. G. & Liu, M. Impaired cutaneous wound healing after sensory denervation in developing rats: Effects on cell proliferation and apoptosis. *Cell Tissue Res.* **307,** 281–291 (2002).

32. Yagmur, C., Guneren, E., Kefeli, M. & Ogawa, R. The effect of surgical denervation on prevention of excessive dermal scarring: A study on rabbit ear hypertrophic scar model. *J. Plast. Reconstr. Aesthetic Surg.* **64,** 1359–1365 (2011).

33. Wang, J. *et al.* A review of rodent models of peritoneal dialysis and its complications. *Int. Urol. Nephrol.* **47,** 209–215 (2015).

34. Park-Min, K. H., Antoniv, T. T. & Ivashkiv, L. B. Regulation of macrophage phenotype by long-term exposure to IL-10. *Immunobiology* **210,** 77–86 (2005).

35. Bonfield, T. L. *et al.* Normal bronchial epithelial cells constitutively produce the anti-inflammatory cytokine interleukin-10, which is downregulated in cystic fibrosis. *Am. J. Respir. Cell Mol. Biol.* **13,** 257–261 (1995).

36. Slavov, E., Miteva, L., Prakova, G., Gidikova, P. & Stanilova, S. Correlation between TNF-alpha and IL-12p40-containing cytokines in silicosis. *Toxicol. Ind. Health* **26,** 479–86 (2010).

37. Boehler, R. M. *et al.* Lentivirus delivery of IL-10 to promote and sustain

macrophage polarization towards an anti-inflammatory phenotype. *Biotechnol. Bioeng.* **111,** 1210–1221 (2014).

38. Lang, R. Tuning of macrophage responses by Stat3-inducing cytokines: Molecular mechanisms and consequences in infection. *Immunobiology* **210,** 63–76 (2005).

39. Krishnamurthy, P. *et al.* IL-10 inhibits inflammation and attenuates left ventricular remodeling after myocardial infarction via activation of STAT3 and suppression of HuR. *Circ. Res.* **104,** 9–18 (2009).

40. Hung, K. S. *et al.* Interleukin-10 gene therapy reverses thioacetamide-induced liver fibrosis in mice. *Biochem. Biophys. Res. Commun.* **336,** 324–331 (2005).

41. Gong, D. *et al.* TGFb signalling plays a critical role in promoting alternative macrophage activation. (2012).

42. Widgerow, A. D. & Kalaria, S. Pain mediators and wound healing - Establishing the connection. *Burns* **38,** 951–959 (2012).

43. Garrison, G. *et al.* Reversal of myofibroblast differentiation by prostaglandin E(2). *Am. J. Respir. Cell Mol. Biol.* **48,** 550–8 (2013).

44. Xiong, X. Y., Tam, K. C. & Gan, L. H. Release kinetics of hydrophobic and hydrophilic model drugs from pluronic F127/poly(lactic acid) nanoparticles. *J. Control. Release* **103,** 73–82 (2005).

45. Körber, M. PLGA erosion: Solubility- or diffusion-controlled? *Pharm. Res.* **27,** 2414–2420 (2010).

46. Makadia, H. & Siegel, S. Poly lactic-co-glycolic acid (PLGA) as biodegradable controlled drug delivery carrier. *Polymers (Basel).* **3,** 1377–1397 (2011).

47. Truong, T. ImageJ-bloodSmearCount. (2016). doi:10.5281/zenodo.153873

S2: CHAPTER 2 – SUPPLEMENTARY INFORMATION

S2.1 MATERIALS & METHODS

Cytotoxicity of capsaicin and PLGA

RAW 264.7 cells were subcultured in 35 mm 6-well plates with DMEM (10% FBS, 1% penicillin/streptomycin) at a population of 1×10^6 cells. Cells were given 1 hour to adhere to the plates before treatments were applied. For dosage response cytotoxicity, cells were incubated with 30 μM, 60 μM and 120 μM capsaicin/DMSO mixture for 24 hours before being resuspended and stained with trypan blue. The volume of DMSO used was less than the total volume of media in each well. For PLGA cytotoxicity, cells were cultured on PLGA-lined Petri dishes for 24 hours before being resuspended and stained with trypan blue.

Capsaicin dosage response to LPS and IFNγ-induced macrophages

RAW 264.7 cells were seeded at a population of 1×10^6 cells into 35 mm 6-well plates with 3 mL of DMEM (10% FBS, 100 U/mL penicillin/streptomycin). Subcultured cells were given 1 hour to adhere to the dish before adding 10 ng/mL of lipopolysaccharide (LPS) (Sigma-Aldrich) and 100 U/mL of interferon-gamma (IFNγ) (eBioscience). Capsaicin, suspended in DMSO, was also added simultaneously with LPS and IFNγ at a concentration of 30 μM, 60 μM or 120 μM. The volume of DMSO used was less than 1% of the total volume of medium. Cells were incubated with LPS, IFNγ and capsaicin for 24 hours before total RNA was extracted from the cells.

Time response of cells cultured on PLGA films

RAW 264.7 cells were cultured in PLGA-lined dishes at a population of 3×10^6 for 6, 12, 24 and 72 hours before they were lysed and RNA was extracted.

Blood collection and quantification

Blood samples were collected, via heart puncture, into EDTA tubes and stored on ice before being used to make blood smears. Blood smears were stained using Giemsa-Wright stain (Sigma-Aldrich) and following the manufacturer's protocol. Smears were then imaged using brightfield microscopy and quantified in a single blinded study using a lab developed ImageJ macro.[47]

S2.2 FIGURES

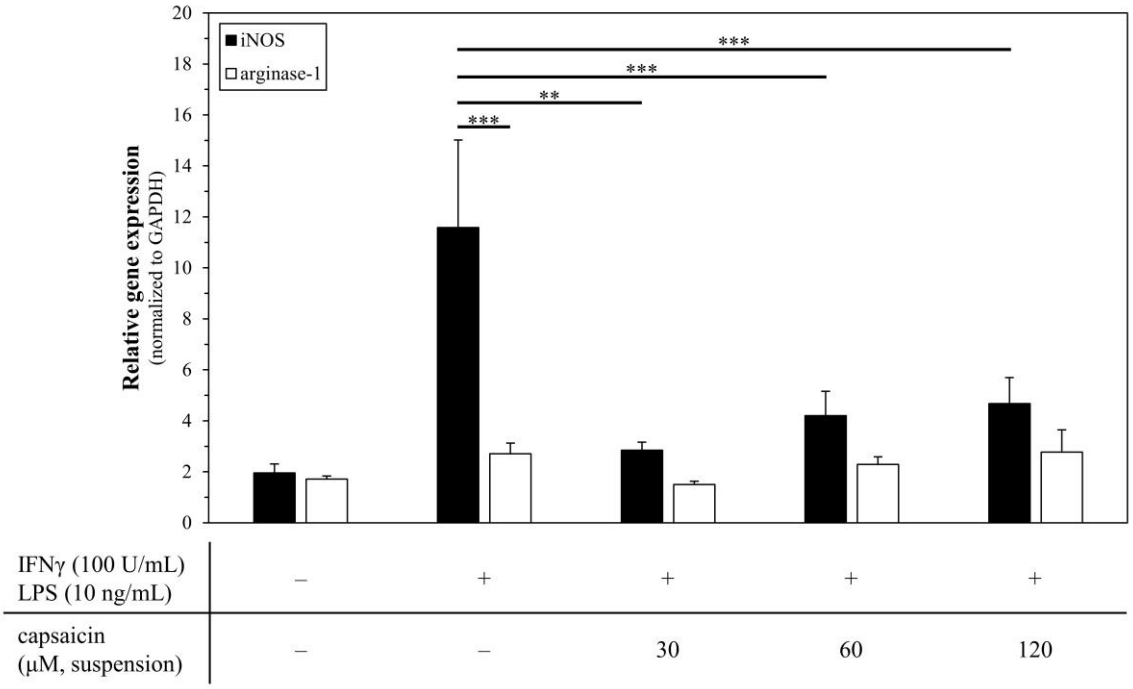

Figure S2.1. Relative gene expression of iNOS and arginase-1 from RAW 264.7 cells stimulated with M1 inducing agents, IFNγ and LPS, and three capsaicin concentrations in suspension for 24 hours. Capsaicin upregulated arginase-1 expression in a dose dependant manner while significantly suppressing iNOS mRNA levels. Values were normalized to GAPDH and expressed as mean ± SEM for five independent experiments. ** indicates $p<1\times10^{-2}$ and *** indicates $p<1\times10^{-3}$.

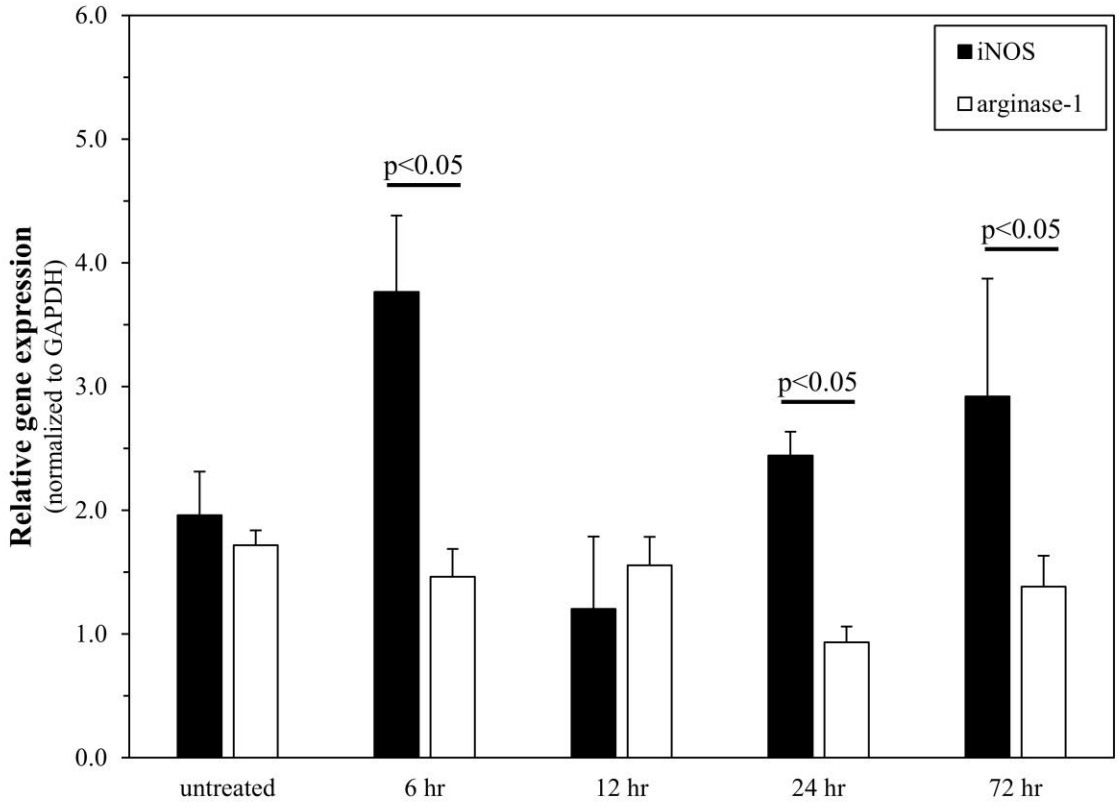

Figure S2.2. RAW 264.7 cells cultured on PLGA films for 6, 12, 24 and 72 hours. PLGA increased iNOS expression after 24 and 48 hours of incubation. Values were normalized to GAPDH and expressed as mean ± SEM for five independent experiments.

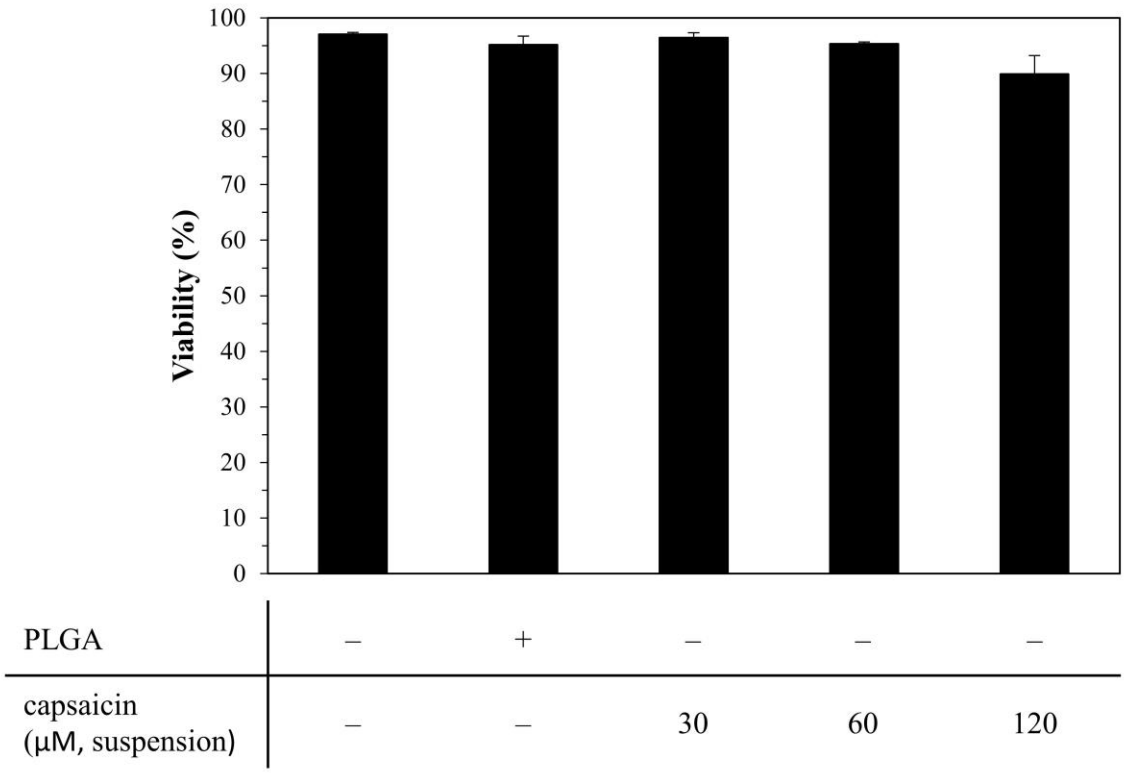

Figure S2.3. Cytotoxicity assay of RAW 264.7 incubated with PLGA, 30 μM, 60 μM and 120 μM of capsaicin for 24 hours. All treatments had no significant effect on viability compared to untreated cells. Each value represents mean ± standard error for three independent experiments.

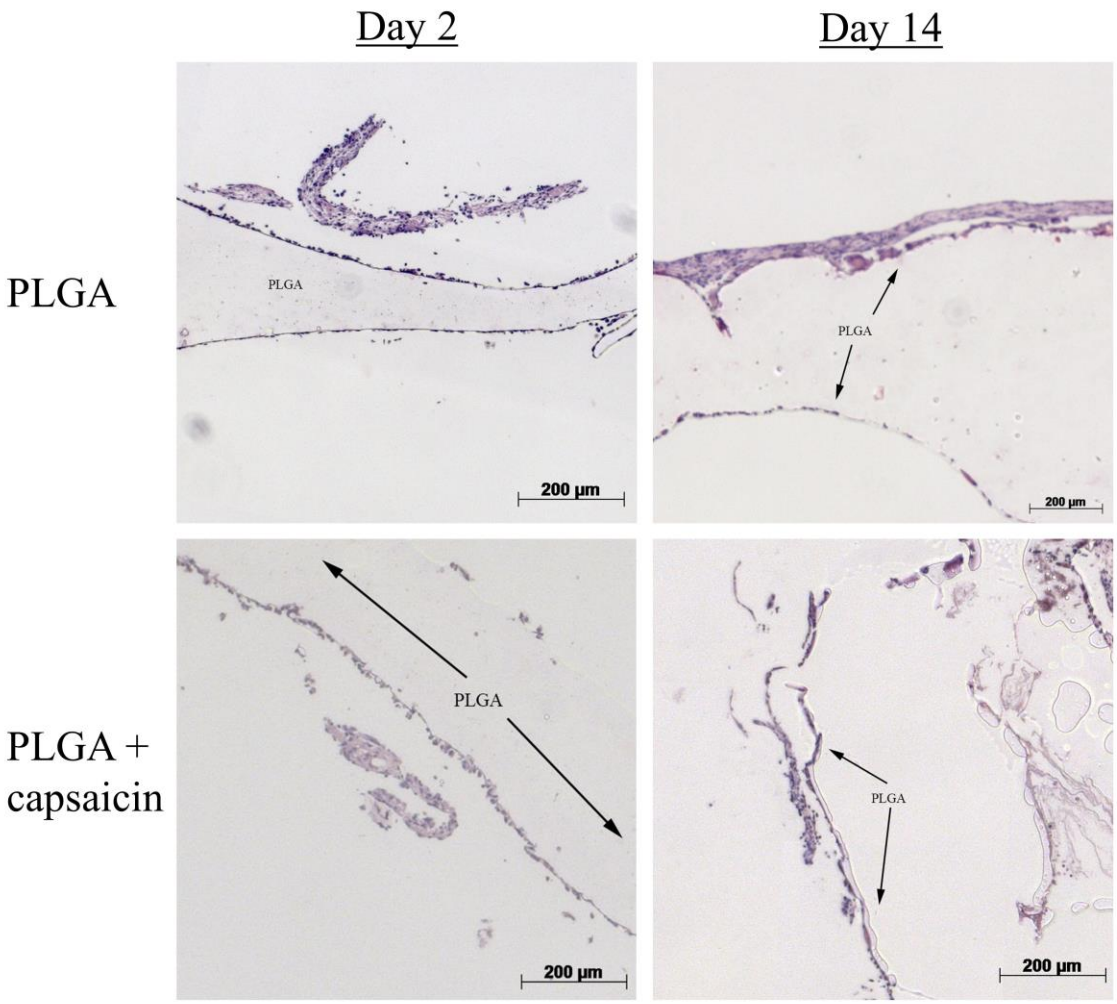

Figure S2.4. Representative micrographs of H&E stained PLGA implants explanted from C57BL/6 mice after 2 and 14 days of incubation in the peritoneal cavity. Arrows indicate the length and/or width of the implant.

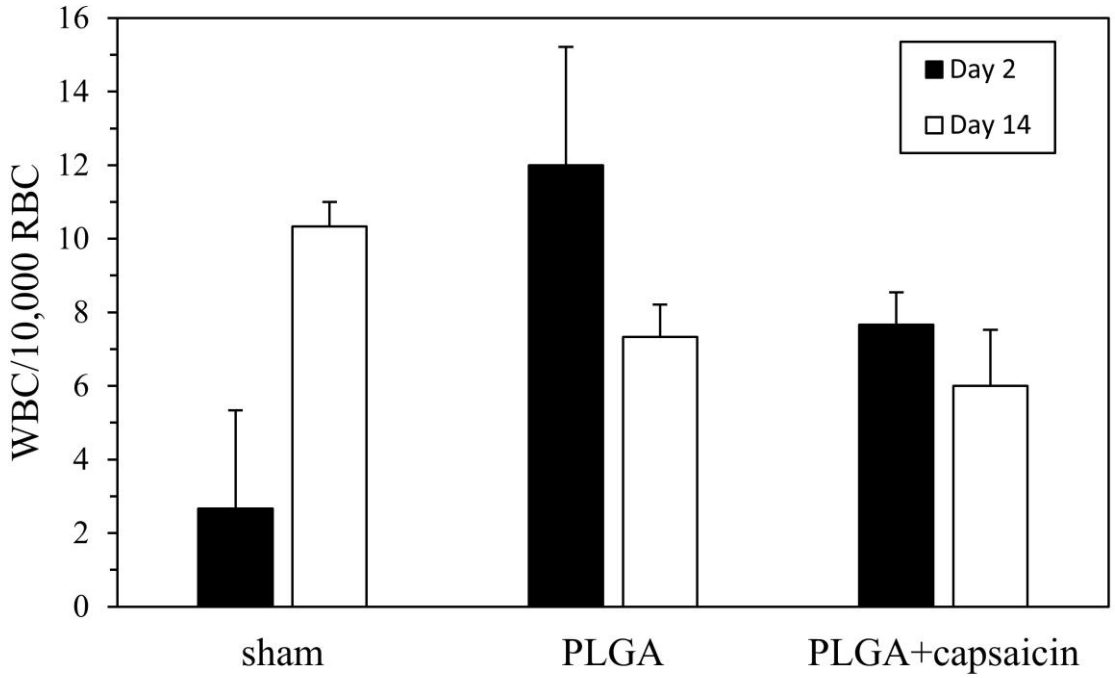

Figure S2.5. White blood cell (WBC) count from whole blood extracted from mice. Both types of implants had no significant effects on circulating white blood cells. WBC counts were scaled up to 10,000 red blood cells (RBCs) and expressed as mean ± SEM for three independent experiment.

CHAPTER 3: PROSTAGLANDIN E_2 SUPPRESSES SCAR TISSUE IN PLGA-INDUCED FIBROSIS: IMPLICATIONS FOR BIOMATERIAL IMPLANTATION

Authors: Tich H. Truong, Kimia Sorouri, Manreet Padwal, Peter Margetts, Kim S. Jones

Publication: To be submitted in 2017-2018

3.1 ABSTRACT

Prostaglandin E_2 (PGE2) attenuated poly(lactic-co-glycolic) acid (PLGA)-induced fibrosis by promoting early M2 macrophage activity to mediate late myofibroblast activity. When biomaterials are implanted as part of a tissue engineered construct, an immune response, resulting in fibrosis and subsequent scar formation around the biomaterial, can interfere with the intended function. The fibrotic tissue is formed through myofibroblast activity where collagen is produced in an uncontrollable fashion. In this study, we investigated the effects of PGE2 on biomaterial-induced fibrosis using an *in vitro* transforming growth factor β1 (TGF-β1) and PLGA model and an *in vivo* PLGA-induced fibrosis model. Myofibroblast and macrophage markers were identified using immunoblotting assays and quantitative PCR. PGE2 was able to reverse *in vitro* myofibroblast differentiation by suppressing α-smooth muscle actin (α-SMA) and promoting E-cadherin protein secretion by 10-fold. Implanted PGE2-embedded PLGA discs had 55% less collagen after 14 days of implantation and 40% less collagen after 42 days. Our results indicated that PGE2 attenuated scar tissue formation by stimulating peritoneal cells to express M2 macrophage markers and producing early IL-10 to suppress pro-inflammatory macrophage and myofibroblast activity. The M2 phenotype remained

present on day 42 and continued to promote controlled wound healing by fibroblasts and myofibroblasts on the implant. Our results indicate that PGE2 is a promising long term anti-fibrotic compound capable of increasing the efficacy of implantable tissue engineered constructs by regulating proper wound healing.

Keywords
myofibroblast, macrophage, PLGA, fibrosis, inflammation

3.2 INTRODUCTION

Prostaglandin E_2 (PGE2) alters the phenotypes of macrophages and myofibroblasts[1,2] which makes it an appealing tool to reduce biomaterial-induced fibrosis. A fibrotic response to biomaterials will compromise their function in applications including tissue engineering,[3,4] drug delivery[5] and implanted biosensors[6]. Here, we used the structured biomaterial itself to release an anti-fibrotic substance.

The host response to polymers, known as the foreign body response, can be subdivided into multiple stages. One stage that greatly impedes biomaterial function is scar tissue formation, or fibrosis.[7] Fibrosis results from a cascade of immunological reactions that can be detrimental during pathological fibrosis.[8] The primary identifying characteristic of fibrosis is the excess accumulation of extracellular matrix components, such as collagen, and alpha-smooth muscle actin (α-SMA) expressing cells. This results in tissue remodelling that generates scar tissue which significantly hinders the structural integrity, function and lifespan of biomaterial implants.[9,10]

The build-up of scar tissue results from a chronic inflammatory response[11] caused by an array of stimuli including chemical insults, tissue injury and macrophage response.[8] Biomaterials act as a stimulus that inevitably induces a fibrotic response due to its nonautologous nature. Moreover, the process of implanting the biomaterial construct creates tissue injury and recruits macrophages to the site and exacerbates the fibrotic response. Macrophages can display phenotypes that can regulate the inflammatory response through activation of tumor necrosis factor-alpha (TNF-α). The M1, or "classically activated", phenotype secretes proinflammatory mediators that upregulate

inflammation[12] and the M2, or "alternative", phenotype has been shown to reduce fibrosis and promote wound healing.[13] M1 macrophages can be identified by high expression of inducible nitric oxide (iNOS) and secretion of IL-12 and IL-23 whileM2 macrophages can be identified by high expression of arginase-1 and secretion of IL-10.[12]

Myofibroblasts play a critical role in the extent of fibrosis. These cells are associated with extracellular matrix protein production, such as collagen, and fibrous encapsulation of biomaterials.[14] Approximately 27% of cells in a fibrous capsule are composed of myofibroblasts.[15] Myofibroblasts are derived from a multitude of cells, including epithelial cells.[8] Epithelial cells and myofibroblasts can be differentiated from each other by their upregulation of E-cadherin and α-SMA, respectively.

Suppressing epithelial and fibroblast cells has been shown to reduce fibrosis while promoting good wound healing.[16] PGE2 has been shown to have anti-fibrotic capabilities and has been used successfully as an anti-fibrotic agent in pulmonary pathological fibrosis[17] and as an inhibitory modulator of fibrogenesis in human lung allografts.[18] PGE2 has also been shown to reduce collagen proliferation from lung fibroblasts.[19]

The aim of this study was to reduce poly(lactic-co-glycolic acid) (PLGA)-induced fibrosis by suppressing myofibroblast differentiation using PGE2. We hypothesized that PGE2 reverses myofibroblast differentiation to mitigate fibrosis. To test this hypothesis, we demonstrated the anti-fibrotic capabilities of PGE2 using an *in vitro* transforming growth factor beta-1 (TGF-β1) model and an *in vivo* fibrosis model. Our results revealed that PGE2 significantly reduced α-SMA *in vitro* and reduced scar tissue formation around PLGA implants after 42 days of incubation in mice.

3.3 MATERIALS & METHODS

PLGA film coating

A solution of 75:25 PLGA (Sigma-Aldrich, Oakville) in ethyl acetate was prepared at a concentration of 0.01 g/mL. To coat the sterile 60 mm glass Petri dishes with PLGA, 1 mL of the solution was added to each dish and the dishes were placed in a sterile vacuum chamber for 6 hours. PLGA coated dishes were incubated for an additional 5 days at 37°C before being stored at 4°C. The film was 0.1729 mm thick with no apparent openings or contamination **(Figure A.1)**.

Cell culture

Human kidney epithelial cells (HK-2) (ATCC CRL-2190) were cultured in a 50:50 ratio of Dulbecco's Modified Essential Medium (DMEM) and Ham's F12 medium (ThermoFisher Scientific, Burlington), supplemented with 10% (v/v) fetal bovine serum (FBS) (ThermoFisher Scientific, Burlington) and 100 U/mL penicillin-streptomycin (ThermoFisher Scientific, Burlington). Cells were seeded at a population of 8×10^5 in 120 mm tissue culture treated Petri dishes (TCPS) and maintained in a 5% CO_2 environment at 37°C.

Inducing myofibroblast differentiation and PGE2 treatment

Cells were seeded at a population of 1.5×10^5 cells in 60 mm Petri dishes and treated with 2 ng/mL of TGF-β1 (B&D Systems, USA). In select experiments, cells were cultured on 60 mm glass petri dishes coated with PLGA and treated with TGF-β1 and/or 500 nM of PGE2 (Cayman Chemicals, USA).

Immunoblotting Assay

Total protein was collected using standard lysis buffer (available in Supplementary Information) supplemented with 2 μL/mL aprotinin, 2 μL/mL leupeptin,

and 1 mM phenylmethylsulfonyl fluoride. Lysate was separated through a 10% SDS-PAGE gel by electrophoresis and transferred to a polyvinylidene fluoride (PVDF) membrane by electroblotting. Membranes were probed for E-cadherin using 1:1000 monoclonal mouse anti-human E-Cadherin primary antibody in 5% milk-TBST (BD Biosciences #610181, USA) and β-actin (Sigma-Aldrich, Missouri) was used as a loading marker. HRP conjugated secondary antibodies (BIO-RAD #1706516, USA) was used at a concentration of 1:5000 and developed with chemiluminescent HRP substrate (Millipore Corporation, Massachusetts). Protein bands were imaged using the ChemiDoc MP System and Image Lab software (ver. 2.0) and densitometry was quantified using ImageJ.

Immunofluorescence staining

Cells were cultured for 24 hours on cover slips in six well plates before being fixed in 4% formaldehyde in PBS (Mg^{++}, Ca^{++}, pH 7.4) for 5 minutes at room temperature and permeabilized with 1% Triton X-100 (Sigma-Aldrich, Switzerland), supplemented with 1% sodium citrate in ddH_2O, for 5 minutes at room temperature. Cells were then saturated with 3% bovine serum albumin (ThermoFisher Scientific, Burlington), supplemented with 0.1% Triton X-100, for 30 minutes at room temperature. Primary antibodies for monoclonal mouse anti-human α-SMA antibody (1:150) (Dako, Burlington) with a Texas Red goat anti-mouse IgG secondary antibody (1:100) (ThermoFisher, Burlington) were prepared in 1% BSA and 0.1% Tween 20 in PBS. Coverslips were mounted using Vectashield mounting medium with DAPI (Vector Laboratories, USA).

Casting PGE2-embedded PLGA discs

PLGA and PGE2-embedded PLGA implants were created in a sterile environment using solvent casting and custom made autoclaved silicone molds with 3/8" wells **(Figure A.2)**. A 90 μL mixture of 0.011 g of 75:25 PLGA per 1 mL of ethyl acetate (Sigma-Aldrich) was added 12 times to the wells with 5 minutes of vacuuming between each interval. Implants were vacuumed for an additional hour, removed aseptically and stored at 4°C in a sterile Petri dish before use **(Figure A.3)**.

PGE2-embedded PLGA discs were made using the aforementioned method but with 100 μg of PGE2 (Cayman Chemicals, USA) dissolved in the PLGA/ethyl acetate solution. Discs had a 5.0% (w/w) loading efficiency and were stored in a sterile Petri dish at 4°C before use.

Animals

CCAC guidelines for the care and use of laboratory animals were observed throughout the study. All animal experimental protocols were approved by the Animal Research Ethics Board at McMaster University under the Animal Utilization Protocol #15-01-02. C57BL/7, 6-8 week old, male mice were purchased from Charles River (Montréal, QC) and housed in the Central Animal Facility at McMaster University for one week before undergoing surgery.

Mice were given buprenorphine (0.03 mg/mL) and were anesthetized with isoflurane. PLGA discs were implanted into the peritoneal cavity and placed in the right lower abdominal quadrant. The muscle wall was sutured using 4-0 Vicryl degradable suture (Ethicon) and the epidermis was closed using stainless steel wound clips. Mice were housed individually for 2, 14 or 42 days before they were sacrificed by

exsanguination. No analgesics or anti-inflammatory drugs were provided to the mice for the duration of the study.

Cumulative PGE2 release kinetics from PLGA implant

PGE2-embedded PLGA discs were incubated in 20 mL of PBS (Mg^{++}, Ca^{++}, pH 7.4) at 37°C. One milliliter samples were removed, for analysis, and replaced with fresh PBS. PGE2 concentrations in samples were quantified using ELISA (Cayman Chemicals, USA) and a standard curve with R^2=0.99.

Collagen thickness quantification

In a single-blinded study, collagen thickness in polarized PSR stained micrographs was quantified using a lab developed ImageJ macro.[20] The thickness was determined by averaging perpendicular measurements from the edge of the implant to the edge of the birefringent region at 5 pixel intervals along the implant.

Quantitative PCR

Total RNA was extracted using TRIzol reagent (ThermoFisher Scientific, Burlington) and by following the manufacturer's protocol. Only RNA samples with 260 nm/280 nm ratio greater than 1.8 were converted to cDNA for quantification. Total RNA was diluted to 50 ng/µL and then converted to cDNA using the High-Capacity cDNA Reverse Transcription Kit with RNase inhibitor (ThermoFisher Scientific, Burlington) and by following the manufacturer's protocol. cDNA samples were quantified using 500 ng of cDNA, 200 nM of forward primer and 200 nM of reverse primer. Primer sequences are available in **Table A.1**.

Human E-cadherin was assayed using ABI Prism 7500 Sequence Detector and Taqman probe and were normalized to 18s rRNA using the standard curve method.

Mouse genes of interest were assayed using Mx3000 qPCR System and SYBR Green probe and normalized to GAPDH. All samples were semi-quantified using the $2^{-\Delta Ct}$ method as described by Livak and Schmittgen.[21]

ELISA

Cytokine concentrations in peritoneal lavages were quantified using IL-10, IL-12 and IL-23 ELISA kits (eBioscience, USA) and by following the manufacturer's protocol. Standard curves were fitted to a four parameter logistics curve with R^2=0.99.

Histology

PLGA implants were fixed in 10% formalin for 48 hours before being sent to the McMaster Immunology Research Center (MIRC) histology lab for processing. Samples were dehydrated through ascending grades of alcohol and xylene and impregnated with paraffin wax before being stained with picrosirius red (PSR) (Sigma-Aldrich, Oakville) and hematoxylin and eosin (H&E) (Sigma-Aldrich, Oakville).

Imaging

An AxioCam ICc3 microscope and AxioVision software (ver. 4.8.2.0) was used for immunofluorescence microscopy. A Zeiss Axiovert 200M microscope and was used for bright-field microscopy and an Olympus BX41 inverted microscope with an analyzer and polarizer set to 100% degree of polarization was used for polarized microscopy.

Statistics

The data were presented as mean ± standard error of the mean (SEM) and assumed to be normally distributed. R was used to analyze data sets using two-way ANOVA with Welch-like corrections for non-homogeneity, when necessary, and *post hoc* Tukey's HSD. *P* values less than 0.05 were defined as statistically significant and only select statistical comparisons were shown in figures.

3.4 RESULTS AND DISCUSSION

PGE2 reverses PLGA and TGF-β1-induced myofibroblast differentiation

HK-2 cells were plated on PLGA-coated Petri dishes and stimulated with TGF-β1 for 24 hours. Our findings indicated that PGE2 treatment reversed the resulting myofibroblast differentiation. PGE2 treated cells, cultured in the presence of PLGA and TGF-β1, produced 10 times more E-cadherin protein than PLGA and TGF-β1-stimulated cells **(Figure 3.1)**. At the mRNA level, PGE2 significantly upregulated E-cadherin mRNA by nearly 2-fold **(Figure 3.2)** and immunofluorescence staining for α-SMA showed that PGE2 and TGF-β1 treated cells had no apparent morphological changes or α-SMA expression **(Figure 3.3)**. In fact, PGE2-treated cells had similar morphology and α-SMA expression as untreated cells cultured on TCPS.

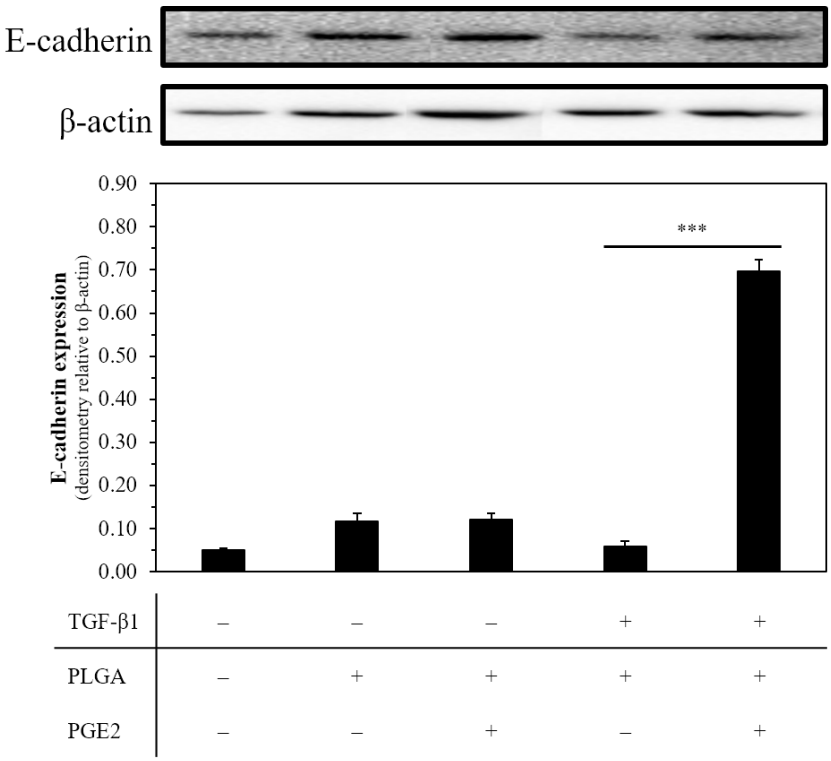

Figure 3.1. HK-2 cells plated on PLGA coated Petri dishes. Cells were treated with PGE2 at 500 nM and 2 ng/mL of TGF-β1. PGE2 significantly upregulated E-cadherin in TGF-β1 and PLGA-stimulated cells. Values were normalized to β-actin loading marker. Each value represents mean ± SEM for three independent experiments. *** represents $p<1\times10^{-3}$.

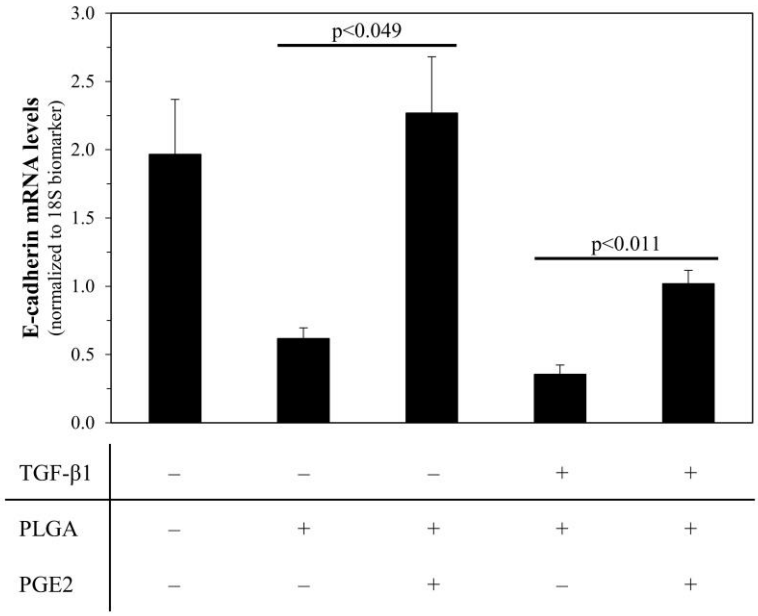

Figure 3.2. HK-2 cells plated on PLGA coated Petri dishes with, and without, TGF-β1 (2 ng/mL) and PGE2 (500 nM) for 24 hours. E-cadherin was upregulated when TGF-β1 stimulated cells were cultured on PLGA and treated with PGE2. Values were quantified using the standard curve method and normalized to the housekeeping gene 18s rRNA. Each value represents mean ± SEM for three independent experiments.

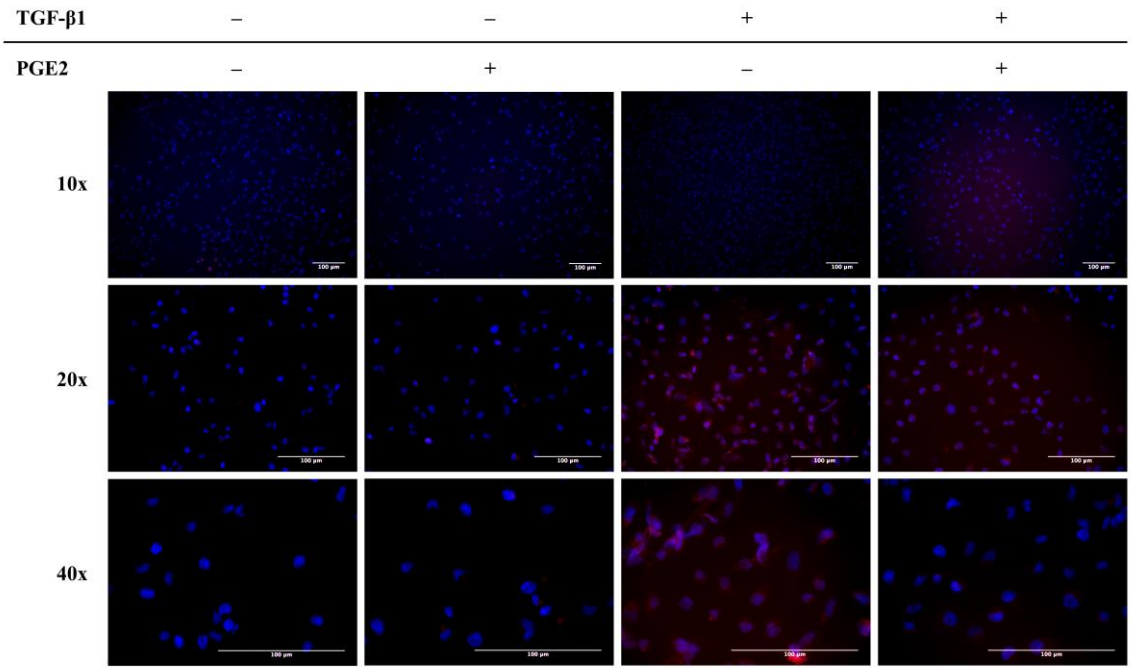

Figure 3.3. Representative micrographs show HK-2 cells (blue) stained for α-SMA (red). PGE2 treated cells had visibly less α-SMA expression compared to TGF-β1-induced cells. Cells were treated with PGE2 (500 nM) and TGF-β1 (2 ng/mL) for 24 hours in two independent experiments.

PLGA is a suitable myofibroblast inducing agent. At the mRNA level, untreated cells cultured on PLGA expressed four times less E-cadherin mRNA than PGE2-treated cells. This indicates that HK-2 cells have reduced, or lost, their ability to express the epithelial phenotype and are transitioning into myofibroblasts. PLGA triblock copolymer hydrogels have also shown to recruit proliferating cells to epidermal diabetic wound sites and accelerate reepithelialization.[22] Other polymers, such as collagen[23] and dextranomer/hyaluronic acid,[24] have been shown to cause a high degree of fibrosis and myofibroblast recruitment but the genetic response of the cells was never investigated.

The high expression of E-cadherin protein and mRNA and low expression of α-SMA indicate that PGE2 reverted PLGA and TGF-β1-induced myofibroblasts back to epithelial-like cells.[25,26] Previous studies have also shown inhibitory effects of PGE2 where increasing PGE2 concentrations decreased α-SMA protein in TGF-β1-stimulated lung fibroblasts. Concentrations as high as 500 nM have shown to significantly suppress α-SMA after five days of treatment with PGE2.[1] TGF-β1 has been used frequently as a myofibroblast-inducing model to study myofibroblast differentiation pathways[27]; however, to our knowledge, there has been no research in using PGE2 to treat polymer-induced myofibroblast differentiation. These promising results prompted us to see if PGE2 can reduce biomaterial-induced fibrosis in a mouse model.

PGE2 reduces collagen encapsulation

PLGA and PGE2-embedded PLGA discs were implanted intraperitoneally in C57BL/6 mice for 2, 14 and 42 days with no systemic inflammation occurring **(Figure S3.1)**. The discs were explanted and stained with H&E and PSR to look at cellularity and collagen thickness, respectively. H&E staining revealed cells adhered to the surface of the

material and there was no visible difference between PLGA and PGE2-embedded PLGA implants on day 2 and 14, but PLGA had significantly more surrounding tissue cells than PGE2-embedded implants on day 42 **(Figure S3.2)**.

Upon viewing PSR stained implants using polarized microscopy, there were significantly more birefringent regions of collagen around PLGA implants than PGE2-embedded PLGA implants **(Figure 3.4a)**. The thickness of the birefringent regions was quantified and we found that PGE2 significantly reduced collagen by 55% on day 14 and 40% on day 42 **(Figure 3.4b)**.

These results demonstrate that PGE2 is able to reduce scar tissue formation after a very long implantation period and it shows that PGE2 has potential to extend the efficacy of biomedical devices. For example, implantable biosensors often lose sensitivity because of fibrous encapsulation and there is research in releasing anti-fibrotic compounds to

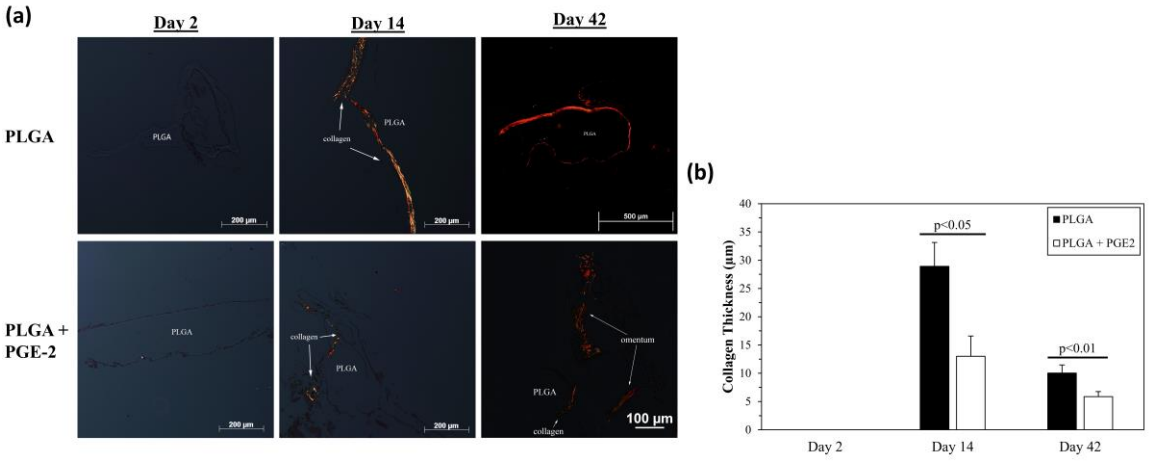

Figure 3.4. (a) Representative polarized micrographs of PSR stained implants explanted from C57BL/6 after 2, 14 and 42 days of incubation in the peritoneal cavity. PLGA implants on day 14 and 42 had the most birefringent collagen compared to any other implant. (b) Birefringent regions were quantified revealing a statistically significant difference in collagen thickness in PGE2-embedded implants compared to PLGA implants. There were no detectable birefringent regions around day 2 implants. Each value represents mean ± SEM for three independent experiments.

increase the efficacy of the device. Avula *et al.* investigated the anti-fibrotic effects of tyrosine kinase on biosensor encapsulation and found that it was ineffective and did not reduce fibrosis around continuous glucose monitoring sensors.[6] Our results showed that PGE2 is a promising compound to reduce collagen deposition but has diminishing effects by day 42. This suggests that PGE2 does not permanently stop fibrosis but delays collagen deposition. To investigate the cellular response that led to differences in collagen deposition, we looked at genetic markers in cells adhered on the implants and peritoneal cells.

PGE2 promotes early epithelial cell activity and late myofibroblast and M1 macrophage activity

PLGA discs were explanted and adherent cells were collected and lysed to extract RNA for analysis. We looked at collagen-1, epithelial cell marker E-cadherin, myofibroblast marker α-SMA, and macrophage markers iNOS and arginase-1. Compared to PLGA alone, PGE2 upregulated early response of all genes on day 2, but the effects diminished by day 14 and only α-SMA and M1 marker iNOS remained upregulated **(Figure 3.5)**. By day 42, PGE2 caused a decrease in M2 marker arginase-1 and an increase in iNOS, α-SMA, E-cadherin and collagen-1.

PGE2 upregulated macrophage activity on day 42 by inducing the M1 phenotype. Over the 42 days, arginase-1 levels were steadily declining but iNOS was significantly upregulated on day 42, indicating that there was an increased presence of inflammatory macrophages. In addition, adherent cells on PGE2-embedded PLGA discs had more iNOS activity and less arginase-1 activity than cells on PLGA control discs which suggests that PGE2 induced an M1 phenotype. This was an unexpected result because

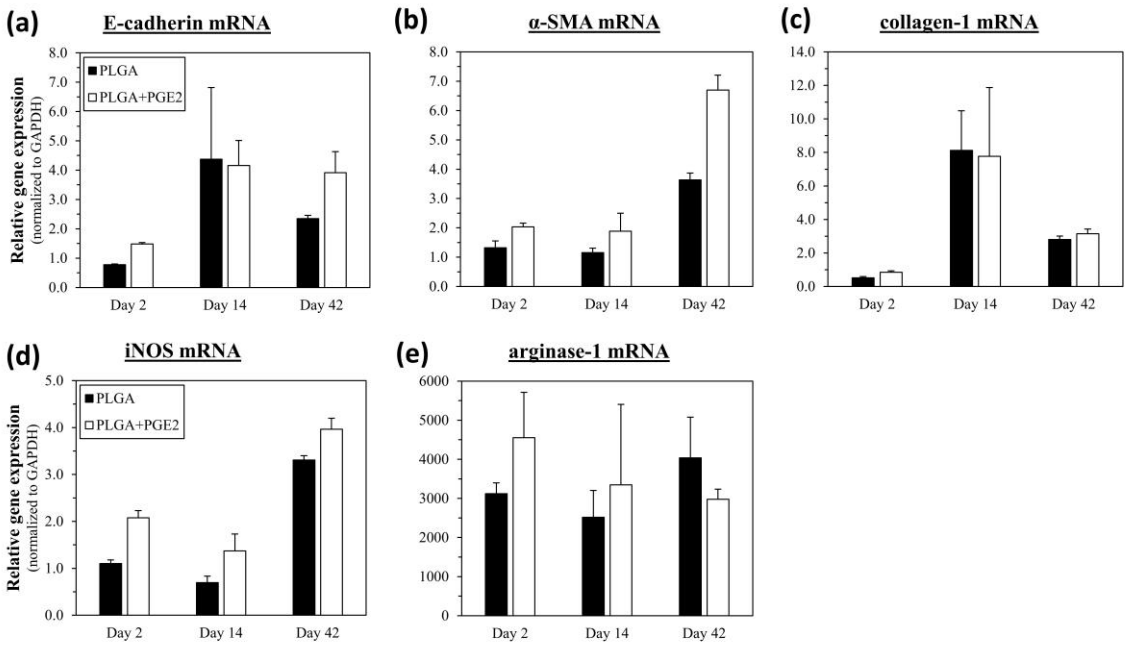

Figure 3.5. (a) E-cadherin, (b) α-SMA, (c) collagen-1, (d) iNOS and (e) arginase-1 mRNA response from cells adhered onto PLGA and PGE2-embedded PLGA discs explanted after 2, 14 and 42 days of incubation in mice. PGE2 caused an upregulation in α-SMA and iNOS by day 14 and the genes continued to increase by day 42. Values were normalized to GAPDH and presented as mean ± SEM for three independent experiments.

macrophage activity is expected to end 14 days after implantation[7,28] and prolonged macrophage activity often leads to chronic inflammation and fibrosis.[29] However, our results show that collagen remains decreased by day 42, which suggests M1 macrophages are either suppressing collagen production or have negligible effects on fibrosis during the late stage.

PGE2 delayed early myofibroblast activity but its effect was lost by day 42. Myofibroblast marker α-SMA expression in PGE2 treated adherent cells were similar to untreated control until day 42, where α-SMA increased by almost 4-folds and was expressed two times more than the control. Although adherent cells expressed more of the myofibroblast phenotype, they were not producing collagen which is evident by the

decrease in collagen-1 mRNA on day 42 and the decrease in collagen thickness. This indicates that PGE2 might have regulated early myofibroblast activity and decreased collagen secretion, where is has been shown that uncontrolled myofibroblast differentiation and activity often leads to uncontrolled fibrosis.[30]

However, the *in vivo* effects of PGE2 are different from *in vitro* results where adherent cells had both E-cadherin and α-SMA upregulated while *in vitro* experiments showed E-cadherin was upregulated and α-SMA was downregulated. We expected similar results because PGE2 has inhibitory effects on fibroblast migration,[31] but the high expression of both E-cadherin and α-SMA suggests that there is a greater percentage of fibroblasts and myofibroblasts attached to PGE2 implants. Without quantifying the cell types, we can only speculate which cell type is responsible for expressing fibroblast and myofibroblast markers and how they are related to reducing the collagen layer.

PGE2 upregulates early anti-inflammation markers from peritoneal cells

Peritoneal cells and supernatant were separated from peritoneal lavages to analyze M1 macrophage markers iNOS, IL-12 and IL-23 and M2 macrophage markers arginase-1 and IL-10. PGE2 had no effect on iNOS mRNA but upregulated early arginase-1 which continued to increase to day 42 **(Figure 3.6)**. There were undetectable levels of IL-10 in all supernatant samples but IL-23 production from day 2 to day 14 was significantly suppressed by PGE2 while IL-10 remained constant over the 14 days **(Figure 3.7)**.

Upregulation of arginase-1 and IL-10 suggests that PGE2 promoted early M2 macrophages which led to less collagen deposition. Early M2 macrophages have been shown to resolve scar tissue formation where Brown *et al.* demonstrated that early M2

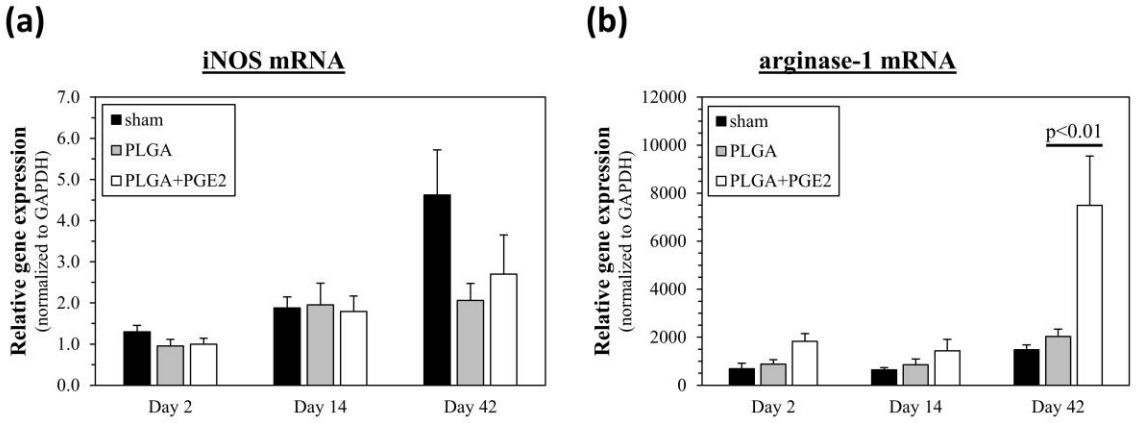

Figure 3.6. PLGA and PGE2-embedded PLGA implants were incubated in C57BL/6 mice for 2, 14 and 42 days. Peritoneal cells were collected by peritoneal lavages to determine (a) iNOS and (b) arginase-1 gene expression. PGE2 had no effect on iNOS but caused upregulation of arginase-1 on days 2 and 42. Values were normalized to GAPDH and are presented as mean ± SEM for three independent experiments.

macrophage activity resulted in better wound healing of various meshes implanted in rats.[32] PGE2 itself can promote the anti-inflammatory response by activating stromal cells to secrete more PGE2 to stimulate secretion of anti-inflammatory mediators from M2 macrophages.[33,34]

Interestingly there was a significant upregulation in arginase-1 by day 42 which

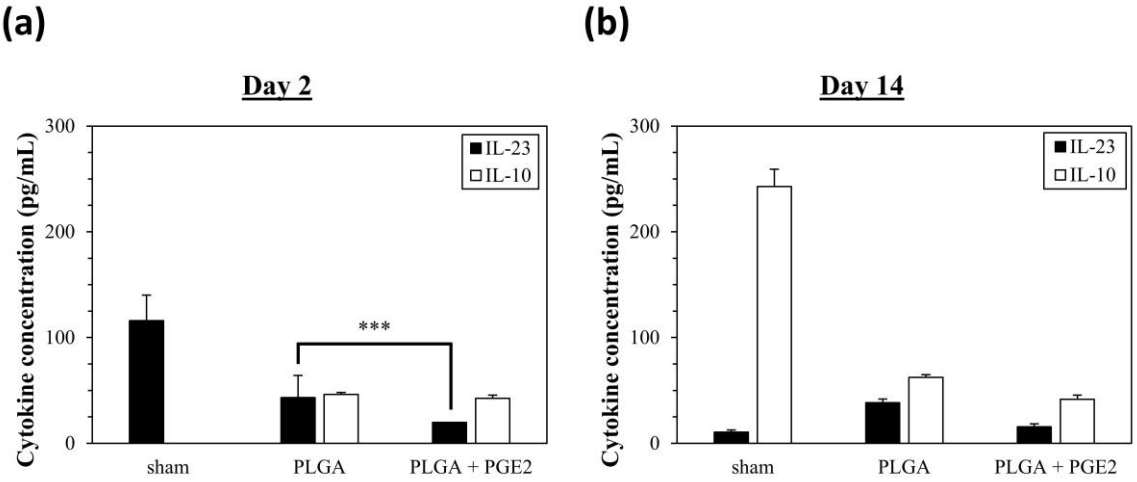

Figure 3.7. (a) IL-23 and (b) IL-10 concentrations in peritoneal lavage after 2 and 14 days of incubation with PLGA and PGE2-embedded PLGA implants. PGE2 caused early suppression if IL-10 but the effect was not retained by day 14. There were undetectable levels of IL-10 on day 2 and IL-12 in the lavages. Each values represents mean ± SEM for three independent experiments.

suggests that M2 macrophage activity continued into the later stages of fibrosis. Extended stimulation with PGE2 might have caused macrophages to upregulate arginase-1 expression. Although there was most likely no more PGE2 present on day 42,[35] arginase-1 expressing macrophages are capable of producing PGE2 through a positive feedback mechanism.[33] M2 macrophages in the microenvironment might be producing anti-inflammatory mediators that induce adhered cells to attenuate and resolve collagen encapsulation around PGE2-embedded implants.[32] However, without quantifying cell types, we can only speculate that peritoneal lavage cells are mainly composed of free floating monocytes and macrophages which are maintaining arginase-1 upregulation.

Suppression of T-cell induced inflammation might have contributed to reducing scar tissue formation. Suppression of early and late IL-23 suggests PGE2 mitigated a T-cell mediated immune response and TNF-α mediated inflammation and fibrosis. IL-23 has been shown to mediate T-cell activity in autoimmune diseases,[36,37] such as Crohn's disease[38] and arthritis,[39] and downregulation of T-cells has directly led to reduce collagen-induced arthritis.[40]

We were curious to see if PGE2 was still being released from PLGA on day 42 because our results showed that adherent cells upregulated iNOS and α-SMA expression on day 42 and peritoneal cells upregulated arginase-1 on day 42. If PGE2 was not present, it would indicate that an alternative mechanism was activating and upregulating cell activity.

Fibrosis remains reduced after all of PGE2 is released

PGE2 release kinetics were simulated in PBS over a period of 23 days. PGE2 followed first order release kinetics with a distinct burst release profile within the first 24

hours and a plateau over the next 22 days **(Figure 3.8)**. By 48 hours, 70% of the PGE2 was released from the implant and only 10% was predicted to be left by day 14 and less than 1% by day 42. PGE2 follows the classic first order release kinetics of hydrophilic molecules released from hydrophobic carriers. In similar release models, approximately 80% of all hydrophilic drugs are released from a hydrophobic carrier within the first 24 hours.[35]

The burst release of PGE2 creates a concentrated environment that would upregulate gene activity of cells on the implants. As we saw in the *in vitro* study, HK-2 cells cultured on PLGA upregulated E-cadherin when exposed to PGE2 and *in vivo* adherent cells on PGE2-embedded PLGA implants upregulated E-cadherin on day 2. Since most of the drug was released by day 14, the concentration is lower and the cells

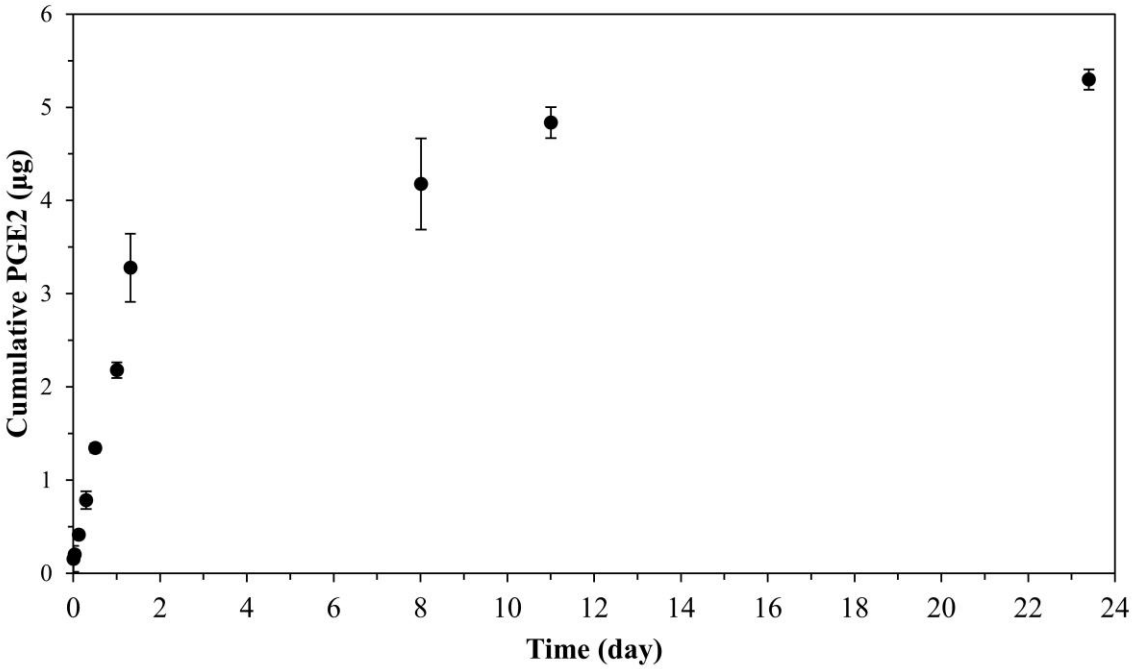

Figure 3.8. Cumulative release of PGE2 from PLGA disc. Implants were submerged in PBS (pH 7.4) for 23 days. Each value represents mean ± standard deviation for three independent experiments.

are less stimulated, which explains why most of the genes did not remain upregulated by day 14.

However, PGE2 treatment led to reduced collagen deposition on day 42, even when almost all of the drug was released. This indicates that either PGE2 delayed the fibrotic response and fibrosis will return or the short stimulation period was sufficient enough to activate a different pathway that resulted in reduced encapsulation. Either way, PGE2 shows promise as an effective drug to delay the fibrotic response.

In conclusion, we have demonstrated that PGE2 has potential as an anti-fibrotic compound for short term and long term applications. The extent of fibrosis is controlled by targeting cells in the microenvironment. During the early stages of the foreign body response, PGE2 promoted early anti-inflammatory IL-10 release which resulted in 55% less collagen deposited around PLGA implants. Early PGE2 stimulation promoted late M2 macrophage activity, in peritoneal cells, which led to wound healing and 40% less collagen than PLGA implants. Overall, PGE2 is a promising anti-fibrotic drug that promotes proper wound healing and delays the fibrotic response for drug release applications.

3.5 ACKNOWLEDGMENTS

The authors would like to acknowledge that this work was supported by the Natural Sciences and Engineering Research Council. We thank Emma Buller, Ugonwa Echendu, and Anthony Saraco for their assistance with animal studies and blinded collagen thickness and blood smear quantification studies.

3.6 DISCLOSURE STATEMENT

The authors declare that there were no conflict of interests regarding the publication of this paper.

3.7 REFERENCES

1. Garrison, G. *et al.* Reversal of myofibroblast differentiation by prostaglandin E(2). *Am. J. Respir. Cell Mol. Biol.* **48,** 550–8 (2013).

2. Kalinski, P. Regulation of immune responses by prostaglandin E2. *J. Immunol.* **188,** 21–8 (2012).

3. Jung, I. K., Lee, S. B., Kim, J. H. & Park, C. K. Foreign body reaction in glaucoma drainage implant surgery. *Investig. Ophthalmol. Vis. Sci.* **54,** 3957–3964 (2013).

4. Lam, M. T. & Wu, J. C. Biomaterial applications in cardiovascular tissue repair and regeneration. *Expert Rev. Cardiovasc. Ther.* **10,** 1039–1049 (2012).

5. Makadia, H. K. & Siegel, S. J. Poly Lactic-co-Glycolic Acid (PLGA) as Biodegradable Controlled Drug Delivery Carrier. *Polymers (Basel).* **3,** 1377–1397 (2011).

6. Avula, M. *et al.* Local release of masitinib alters in vivo implantable continuous glucose sensor performance. *Biosens. Bioelectron.* **77,** 149–156 (2016).

7. Anderson, J. M., Rodriguez, A. & Chang, D. T. Foreign body reaction to biomaterials. *Semin. Immunol.* **20,** 86–100 (2008).

8. Utsunomiya, H. *et al.* Extracellular matrix remodeling in oral submucous fibrosis: its stage specific modes revealed by immunohistochemistry and in situ hybridization. *J. oral Pathol. Med.* **34,** 498–507 (2005).

9. Xiao, W., Zhao, D.-X. & Xue, L.-Q. Rapid bilateral anterior capsule contraction following high myopic cataract surgeries: a case report. *Int. J. Ophthalmol.* **4,** 207–209 (2011).

10. Hwang, K., Sim, H. B., Huan, F. & Kim, D. J. Myofibroblasts and capsular tissue tension in breast capsular contracture. *Aesthetic Plast. Surg.* **34,** 716–721 (2010).

11. Sharkawy, A. A., Klitzman, B., Truskey, G. A. & Reichert, W. M. Engineering the tissue which encapsulates subcutaneous implants. II. Plasma-tissue exchange properties. *J. Biomed. Mater. Res.* **40,** 586–597 (1998).

12. Martinez, F. O. & Gordon, S. The M1 and M2 paradigm of macrophage activation: time for reassessment. *F1000Prime Rep.* **6,** 13 (2014).

13. Brown, B. N. *et al.* Macrophage phenotype as a predictor of constructive remodeling following the implantation of biologically derived surgical mesh

materials. *Acta Biomater.* **8,** 978–987 (2012).

14. Jenkins, R. H., Thomas, G. J., Williams, J. D. & Steadman, R. Myofibroblastic differentiation leads to hyaluronan accumulation through reduced hyaluronan turnover. *J. Biol. Chem.* **279,** 41453–41460 (2004).

15. Duffield, J. S. Cellular and molecular mechanisms in kidney fibrosis. *J. Clin. Invest.* **124,** 2299–2306 (2014).

16. Warsinske, H. C. *et al.* Computational modeling predicts simultaneous targeting of fibroblasts and epithelial cells is necessary for treatment of pulmonary fibrosis. *Front. Pharmacol.* **7,** (2016).

17. Mehal, W. Z., Iredale, J. & Friedman, S. L. Scraping fibrosis: Expressway to the core of fibrosis. *Nat. Med.* **17,** 552–553 (2011).

18. Walker, N. M. *et al.* Prostaglandin E 2 as an inhibitory modulator of fibrogenesis in human lung allografts. *Am. J. Respir. Crit. Care Med.* **185,** 77–84 (2012).

19. Huang, S., Wettlaufer, S. H., Hogaboam, C., Aronoff, D. M. & Peters-Golden, M. Prostaglandin E2 inhibits collagen expression and proliferation in patient-derived normal lung fibroblasts via E prostanoid 2 receptor and cAMP signaling. *AJP Lung Cell. Mol. Physiol.* **292,** L405–L413 (2006).

20. Truong, T. ImageJ-perpendicularThicknessTool. (2016). doi:10.5281/zenodo.50157

21. Livak, K. J. & Schmittgen, T. D. Analysis of relative gene expression data using real-time quantitative PCR and the 2^(-ΔΔCT) method. *Methods* **25,** 402–408 (2001).

22. Lee, P.-Y., Li, Z. & Huang, L. Thermosensitive hydrogel as a Tgf-beta1 gene delivery vehicle enhances diabetic wound healing. *Pharm. Res.* **20,** 1995–2000 (2003).

23. Jansen, R. G., van Kuppevelt, T. H., Daamen, W. F., Kuijpers-Jagtman, A. M. & Von den Hoff, J. W. Interferon-γ-loaded collagen scaffolds reduce myofibroblast numbers in rat palatal mucosa. *Eur. J. Orthod.* **33,** 1–8 (2011).

24. Arena, S. *et al.* Dextranomer/Hyaluronic Acid Copolymer Implant for Vesicoureteral Reflux: Role of Myofibroblast Differentiation. *J. Urol.* **181,** 2695–2701 (2009).

25. Phan, S. H. Biology of fibroblasts and myofibroblasts. *Proc. Am. Thorac. Soc.* **5,** 334–7 (2008).

26. Wan, J. *et al.* Role of Complement 3 in TNF-α-Induced Mesenchymal Transition of Renal Tubular Epithelial Cells In Vitro. *Mol. Biotechnol.* **54,** 92–100 (2013).

27. Evans, R. A., Tian, Y. C., Steadman, R. & Phillips, A. O. TGF-β1-mediated fibroblast-myofibroblast terminal differentiation - The role of Smad proteins. *Exp. Cell Res.* **282,** 90–100 (2003).

28. Williams, D. F. On the mechanisms of biocompatibility. *Biomaterials* **29,** 2941–2953 (2008).

29. Mortier, S., Faict, D., Schalkwijk, C. G., Lameire, N. H. & De Vriese, A. S. Long-term exposure to new peritoneal dialysis solutions: Effects on the peritoneal membrane. *Kidney Int.* **66,** 1257–1265 (2004).

30. Hinz, B. *et al.* The Myofibroblast. *Am. J. Pathol.* **170,** 1807–1816 (2007).

31. White, E. S. *et al.* Prostaglandin E2 inhibits fibroblast migration by E-prostanoid 2 receptor-mediated increase in PTEN activity. *Am. J. Respir. Cell Mol. Biol.* **32,** 135–141 (2005).

32. Brown, B. N. *et al.* Macrophage phenotype as a predictor of constructive remodeling following the implantation of biologically derived surgical mesh materials. *Acta Biomater.* **8,** 978–987 (2012).

33. Rodriguez, M. *et al.* Polarization of the innate immune response by prostaglandin E2: a puzzle of receptors and signals. *Mol Pharmacol* **85,** 187–197 (2014).

34. Ylöstalo, J. H., Bartosh, T. J., Coble, K. & Prockop, D. J. Human mesenchymal stem/stromal cells cultured as spheroids are self-activated to produce prostaglandin E2 that directs stimulated macrophages into an anti-inflammatory phenotype. *Stem Cells* **30,** 2283–2296 (2012).

35. Xiong, X. Y., Tam, K. C. & Gan, L. H. Release kinetics of hydrophobic and hydrophilic model drugs from pluronic F127/poly(lactic acid) nanoparticles. *J. Control. Release* **103,** 73–82 (2005).

36. Hirota, K., Martin, B. & Veldhoen, M. Development, regulation and functional capacities of Th17 cells. *Semin. Immunopathol.* **32,** 3–16 (2010).

37. Annunziato, F. *et al.* Phenotypic and functional features of human Th17 cells. *J. Exp. Med.* **204,** 1849–61 (2007).

38. Kobayashi, T. *et al.* IL23 differentially regulates the Th1/Th17 balance in ulcerative colitis and Crohn's disease. *Gut* **57,** 1682–1689 (2008).

39. Lubberts, E. Th17 cytokines and arthritis. *Semin. Immunopathol.* **32,** 43–53

(2010).

40. Tu, L. *et al.* The therapeutic effects of daphnetin in collagen-induced arthritis involve its regulation of Th17 cells. *Int. Immunopharmacol.* **13,** 417–423 (2012).

41. Truong, T. ImageJ-bloodSmearCount. (2016). doi:10.5281/zenodo.153873

S3: CHAPTER 3 – SUPPLEMENTARY INFORMATION

S3.1 MATERIALS & METHODS

Lysis Buffer

- 50mM Tris (pH 7.4)
- 150mM NaCl
- 5mM EDTA
- 1% Triton X-100
- 10% glycerol
- 1mM NaF
- 1mM β-glycerol phosphate
- 0.1mM Na_3VO_4
- H_2O

White blood cell quantification in blood smears

Whole blood was collected via cardiac puncture and made into blood smears using Giemsa-Wright stain (Sigma-Aldrich, Milwaukee) and by following the manufacturer's protocol. White blood cells (WBCs), from a portion of the blood smear, were quantified in a single blinded study using an in-lab developed ImageJ macro.[41] WBC counts were scaled up to 10,000 red blood cells.

S3.2 FIGURES

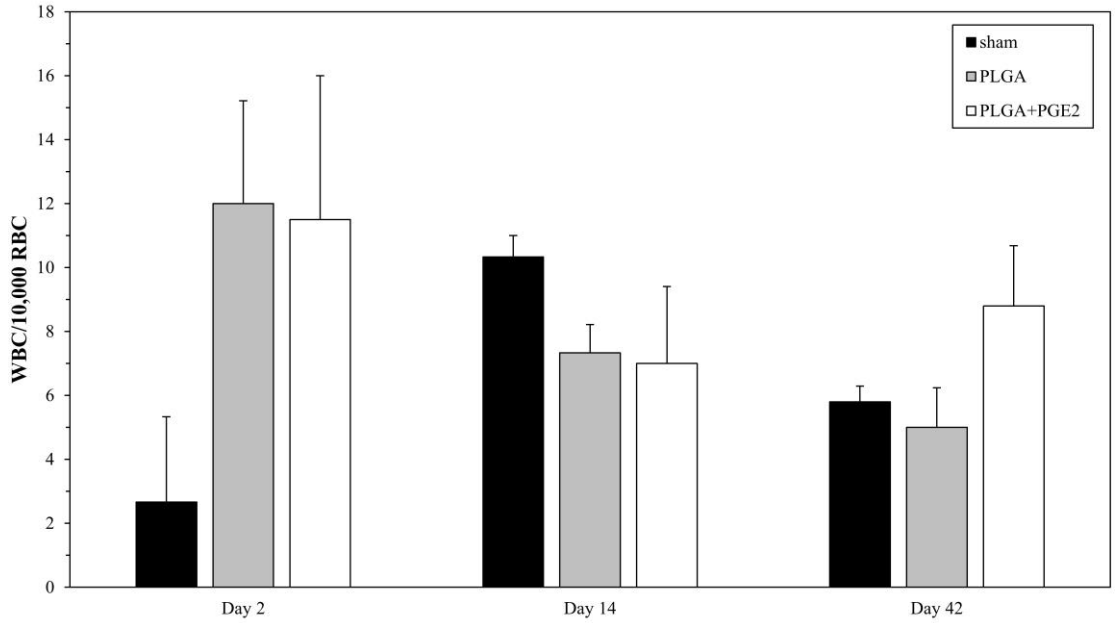

Figure S3.1. PLGA and PGE2-embedded PLGA implants showed a decrease in white blood cell count (WBC) per red blood cell (RBC) after 42 days of incubation. Each value represents mean ± SEM for five independent experiments.

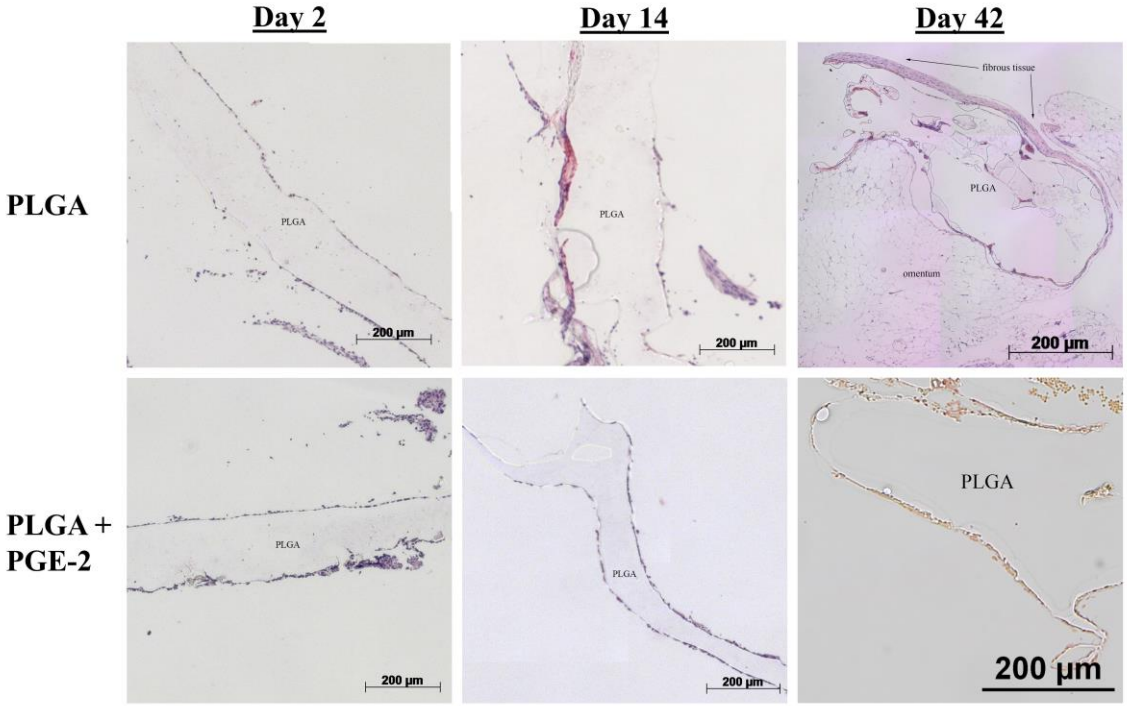

Figure S3.2. Representative micrographs of H&E stained PLGA and PGE2-embedded PLGA discs explanted after 2,14 and 42 days of incubation in C57BL/6 mice. A thin layer of cells is visible around all implants and day 42 PLGA implants have the thickest cellularity layer.

CHAPTER 4: POLYDOPAMINE SURFACE MODIFICATION REDUCES PDMS-INDUCED FIBROSIS

Authors: Tich H. Truong, Darren Sandejas, John L. Brash, Kim S. Jones

Publication: To be submitted in 2017-2018

4.1 ABSTRACT

Polydopamine (PDA) surface modification is an easy chemical reaction that provides the ability to immobilize peptides to substrates. In this study, PDA films coated on polydimethylsiloxane (PDMS) discs gave an unexpected result by reducing fibrosis *in vivo*. PDA modified PDMS (PDMS-PDA) discs were implanted into the peritoneum of C57BL/6 mice for 14 days and explanted for cellularity and collagen deposition analysis using fluorescence and polarized microscopy. PDA modification reduced cellularity by 50% and significantly decreased collagen thickness by 30%. Quantitative PCR was used to analyze mRNA from peritoneal and adherent cells. PDA stimulated adherent cells to produce high levels of fibroblast marker E-cadherin and low levels of collagen-1 while peritoneal cells responded with an M2 macrophage phenotype with upregulated arginase-1 and downregulated inducible nitric oxide synthase (iNOS). Although fibrosis was reduced, PDMS-PDA implants showed high adsorption of fibrinogen suggesting fibrinogen-induced acute inflammation did not play a critical role in late stage fibrosis. PDA surface modification is a low cost method that provides anti-fibrotic properties for implantable biomedical devices.

Keywords
polydimethylsiloxane, polydopamine, fibrosis, fibrinogen, macrophage

4.2 INTRODUCTION

Polydopamine (PDA) is a nature inspired polymer that is used to immobilize molecules to surfaces to obtain engineered responses.[1] We came upon an unexpected result where biomaterials surface modified with PDA reduced fibrosis to the same extent as PDA modified surfaces functionalized with an anti-fibrotic molecule. PDA has become a popular compound to bind macromolecules[2] and metal nanoparticles[3] to reduce fouling. Immediately after implantation, proteins non-specifically adsorb to the surface and trigger an immune response.[4] Continual accumulation of proteins exacerbates the response and promotes chronic inflammation and fibrosis, which are detrimental to the patient[5] and to the efficacy of the biomaterial. Here, we investigated macrophage and myofibroblast responses and fibrinogen adsorption to PDA modified biomaterials.

Cytokines, chemokines and nonspecifically-adsorbed proteins quickly accumulate onto the biomaterial and activate macrophage activity through pathogen associated molecular pattern (PAMP) and danger associated molecular pattern (DAMP) signalling.[4,6] Macrophages recruited to the site produce proinflammatory mediators that promote monocyte differentiation into the classically activated M1 macrophage phenotype. These macrophages produce additional proinflammatory mediators, including IL-12 and IL-23, which exacerbate the situation. M1 macrophages are identified by their high expression of inducible NOS (iNOS) and low expression of arginase-1 whereas their counterpart phenotype M2 macrophages have low iNOS and high arginase-1 expression and produce IL-10.[7]

Persistent macrophage activity promotes transforming growth factor beta-1 (TGF-β1) secretion from resident cells and thus myofibroblast differentiation. Epithelial cells produce TGF-β1 to stimulate myofibroblast differentiation through epithelial to mesenchymal transition (EMT).[8,9] EMT is described by the loss of epithelial cadherin (E-cadherin) expression and gain of alpha-smooth muscle actin (α-SMA). Myofibroblasts are fibroblast-like cells that express α-SMA which gives them contractile abilities. Unlike fibroblasts, myofibroblasts produce an excess amount collagen which causes severe fibrosis.[8,10,11]

Under physiological conditions, macrophage and myofibroblast activity is tightly regulated. However, repeated injury, such as insertion of peritoneal tubing, triggers the foreign body response and causes peritonitis.[12] Medical tubing is commonly made of polydimethylsiloxane (PDMS), due to its nonreactive chemical composition,[13] but PDMS is susceptible to protein fouling.[14] As such, the inflammatory response and presence of monocyte-derived macrophages is often initiated by nonspecific protein adsorption.[4]

There has been a recent interest in using polydopamine (PDA) as a "glue" to immobilize molecules to surfaces to extend the lifetime and efficacy of a biomaterial.[1] PDA has been used to immobilize antimicrobial peptides to urinal catheters to reduce biofilm formation[15] and immobilize cationic peptides to improve cytocompatibility.[16] PDA has also been used to bind heparin to PDMS gas exchange devices to reduce thrombus formation in a blood contacting environment.[17]

In this study, we investigated macrophage and myofibroblast response to PDMS and PDA surface modified PDMS (PDMS-PDA) material. In a pilot *in vivo* experiment

using an anti-fibrotic molecule bound to PDA modified PDMS discs, we made the unexpected discovery that PDMS-PDA controls had reduced surrounding cellularity to the same extent as the discs functionalized with the molecule. This prompted us to investigate the fibrotic response of PDMS-PDA and PDMS controls. We implanted PDMS and PDMS-PDA discs into the peritoneum of C57BL/6 mice for 14 days and analyzed collagen deposition using histology and macrophage and myofibroblast markers using qPCR. Our results revealed that the PDA modification significantly reduced cellularity thickness and collagen deposition by altering macrophages to display the alternative M2 phenotype and by reducing α-SMA expression in myofibroblasts.

4.3 MATERIALS & METHODS

Preparation of PDMS discs

Polydimethylsiloxane (PDMS) discs were cast in autoclaved stainless steel molds with 1 cm circle cut outs **(Figure A.4)**. Four milliliters of Sylgard 184 Silicone Elastomer Kit (Dow Corning) were added to each well and left on a vertical rocker for 48 hours at room temperature and in a sterile environment. PDMS discs had a diameter of 1 cm and thickness of 1.54 ± 0.33 mm. The discs were separated from the mold and autoclaved before undergoing surface modification or implantation. A 24 hour sterility test revealed no contamination growth.

Polydopamine surface modification

Polydopamine surface modified PDMS (PDMS-PDA) discs were made using a modified method from Wu *et al.*[1]. A 4 g/L solution of polydopamine (Sigma-Aldrich, Milwaukee) and Trizma (10 mM, pH 8.0) (Sigma-Aldrich, Milwaukee) was made and sterilized using a 0.2 μm syringe filter. Autoclaved discs were incubated in the

polydopamine-Trizma solution for 24 hours at room temperature. Modified discs were washed three times by incubating in fresh sterile phosphate buffered saline (PBS) (pH 7.4) at room temperature for two hours before they were stored in PBS at 4°C. A 24 hour sterility test revealed no contamination growth.

Animal

A single blinded study was conduced on 6-8 week old C57/BL6 mice (Charles River, Montreal, Quebec). All animal experimental protocols followed the Canadian Council on Animal Care guidelines and were approved by the Animal Research Ethics Board at McMaster University (15-01-02). Mice were housed in the Central Animal Facility, at McMaster University, for one week before undergoing surgery.

Isoflurane and buprenorphine were given to the mouse for the duration of the surgery. PDMS and PDMS-PDA discs were implanted intraperitoneally in the right lower abdominal quadrant. Mice were transferred to a heated recovery cage before being housed individually for 2 and 14 days before they were sacrificed. No analgesics or anti-inflammatory drugs were provided to the mice for the duration of the study and mice had no systemic inflammation **(Figure S4.1)**.

Immunofluorescence cellularity staining

Explanted discs were fixed in 37% formalin for 72 hours and placed in 30% sucrose/PBS solution for 24 hours. Samples were then embedded in OCT compound and cut into 20 μm sections. Cryostat sections were mounted on microscope slides and stained with DAPI (Thermo Fisher Scientific, Burlington) by following the manufacturer's protocol.

Collagen thickness quantification

Collagen thickness was measured in a single blinded study using a lab developed ImageJ macro.[18] Average thickness was defined as the average perpendicular distance from the edge of the disc to the outer edge of collagen measured at five pixel intervals along the perimeter of the disc.

Peritoneal and adherent cell collection

Prior to sacrificing the mice, a 2 mL peritoneal lavage was performed using 0.9% saline to collect free floating cells for analysis. Lavages were immediately centrifuged at 1000 × g for five minutes at 4°C after which the pellet was lysed using 1 mL of TRIzol (Thermo Fisher Scientific, Burlington).

PDMS and PDMS-PDA discs were explanted and placed directly in 1 mL of TRIzol. The solution was vortexed at high speeds for 30 seconds and incubated at room temperature for 1 hour before RNA extraction was done.

Preparation of PDMS and PDMS-PDA films

Three millilitres of the Sylgard 184 Silicone Elastomer Kit were added to autoclaved

60 mm glass Petri dishes and left to cure on a vertical rocker, in a biosafety cabinet, for 48 hours. PDMS-lined Petri dishes were then autoclaved and stored in a sterile environment at 4°C before use.

PDMS-PDA films were made by incubating 13.02 mL of sterile polydopamine-Trizma solution (4 mg/mL) on sterile PDMS-lined Petri dishes for 24 hours at room temperature. Films were washed three times by incubating in sterile PBS at room temperature for two hours before they were stored in a sterile environment at 4°C. All

procedures were done in a biosafety cabinet and a 24 hour sterility test revealed no contamination growth.

Cell culture

In vitro experiments were performed using the RAW 264.7 cell line (ATCC TIB-71). Cells were cultured in Dulbecco's Modified Eagle Medium (DMEM) (Thermo Fisher Scientific, Burlington) supplemented with 10% fetal bovine serum (FBS) (Thermo Fisher Scientific, Burlington) and 100 U/mL penicillin-streptomycin (Thermo Fisher Scientific, Burlington). Cells were seeded in tissue culture plates and subcultured at 80-90% confluency using PBS (pH 7.4, Mg^{--}, Ca^{--}) and a cell scraper. Cells were incubated at 37°C in a humidified atmosphere of 5% CO_2.

Culturing cells on PDMS and PDMS-PDA films

RAW 264.7 cells were cultured on sterile PDMS and PDMS-PDA films for 24 and 48 hours. Cells were seeded at a population of 1×10^6 cells in DMEM supplemented with 10% FBS and 1% penicillin/streptomycin. Analyses were performed 24 and 48 hours after treatment.

Radiolabelled fibrinogen adsorption

PDMS and PDMS-PDA discs were incubated in 200 μL of 0.1, 1 and 2 mg/mL concentrations of fibrinogen in a 96-well plate. Discs were incubated for three hours at room temperature before they were rinsed with PBS and radioactivity was measured.

Fibrinogen (Fg) solutions were prepared using 10% radiolabeled fibrinogen (90% unlabeled fibrinogen) in PBS (pH 7.4). Fibrinogen (Enzyme Research Laboratories, South Bend, IN) was radiolabeled with ^{125}Iodine ($Na^{125}I$) from the McMaster Nuclear

Reactor (Hamilton, ON). A solution of 10 mg of fibrinogen, 22.3 μL of iodine monochloride reagent, 5 μL of $Na^{125}I$ and 240 μL of glycine buffer was prepared. Unbound isotope was removed by column filtration using glass wool soaked with AG 1-X4 anion exchange resin (BioRad, Mississauga, ON). To determine the amount of unbound isotope, free iodine was tested. Radiolabeled protein solution was added to trichloroacetic (20% w/v in water) to precipitate the protein. Free iodine is expressed as the radioactivity of the supernatant divided by the radioactivity of the total protein solution and is <5%.

RNA extraction and quantitative PCR (qPCR)

Total RNA was extracted using TRIzol and by following the manufacturer's protocol. Only RNA samples with 260 nm/280 nm absorbance ratio greater than 1.8 were quantified. Total RNA (50 ng/μL) was converted to cDNA using the High-Capacity cDNA Reverse Transcription Kit with RNase inhibitor (Thermo Fisher Scientific, Burlington). cDNA samples were quantified using 500 ng of cDNA, 200 nM of forward primer and 200 nM of reverse primer. Primer sequences are available in **Table A.1**. Genes of interest were detected using the Mx3000 qPCR System and SYBR Green probe (Thermo Fisher Scientific, Burlington) and semi-quantified using the $2^{-\Delta Ct}$ method[19] and glyceraldehyde 3-phosphate dehydrogenase (GAPDH) as the housekeeping gene. All assays were completed by following the manufacturer's protocol.

Histology

PDMS and PDMS-PDA discs were explanted after 14 days and immediately fixed in 10% formalin for 48 hours. Discs were then mounted in molds using HistoGel (Thermo Fisher Scientific, Burlington) before being sent to the McMaster Immunology Research

Center Histology Lab for processing. Samples were dehydrated through ascending grades of alcohol and xylene and impregnated with paraffin wax before being stained with picrosirius red (PSR) (Sigma-Aldrich, Oakville).

Imaging

Immunofluorescence micrographs were taken using AxioCam ICc3 microscope and AxioVision (ver. 4.8.2.0). Bright-field micrographs were taken using Zeiss Axiovert 200M microscope and Axiovision software. Polarized micrographs were taken using Olympus BX41 inverted microscope with an analyzer and polarizer set at 100% degree of polarization. Multiple micrographs were taken and stitched together unedited using Adobe Photoshop.

Statistics

Data were presented as mean ± standard error of the mean (SEM). All data were assumed normally distributed and analyzed using R and two-way ANOVA with *post hoc* Tukey's Honestly Significant Difference. *P* values less than 0.05 were defined as statistically significant.

4.4 RESULTS AND DISCUSSION

PDA modification decreases cellularity and collagen deposition

Anti-fibrotic molecule-bound PDMS-PDA (PDMS-PDA+molecule), PDA surface modified PDMS (PDMS-PDA) and PDMS discs were explanted after 14 days of incubation in C57BL/6 mice. The discs were stained for cellularity and collagen using DAPI and PSR, respectively. Both surface modifications resulted in 50% less cellularity thickness than unmodified PDMS discs and cellularity also appeared to be less dense around the perimeter of modified implants **(Figure 4.1)**.

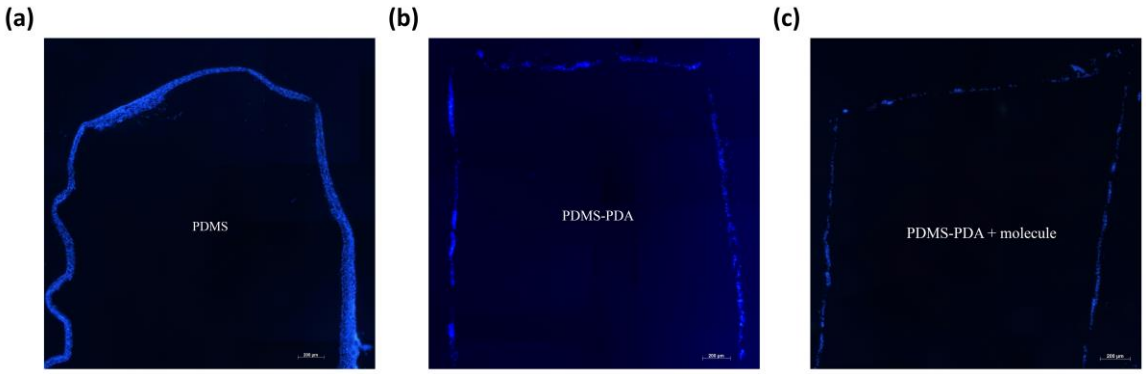

Figure 4.1. Fluorescence micrographs of DAPI stained cells on the perimeter of (a) PDMS, (b) PDMS-PDA and (c) PDMS-PDA + anti-fibrotic molecule discs. Cellularity around antifibrotic molecule bound PDA and PDA controls were similar and cellularity around PDMS-PDA discs was half the thickness of PDMS discs. Discs were incubated in the peritoneum of C57BL/6 mice for 14 days and micrographs are representative of three independent experiments.

Our pilot study yielded an unexpected and interesting result where surface modification with an anti-fibrotic compound had similar levels of cellularity as the PDMS-PDA control. We hypothesized that the PDA modification was sufficient to reduce fibrosis and tested this by conducting another set of *in vivo* experiments where collagen thickness was quantified.

Polarized PSR stained micrographs revealed less birefringent collagen around PDMS-PDA discs compared to PDMS discs **(Figure 4.2a)**. PDMS-PDA discs had scattered collagen development along the perimeter whereas collagen formed along the entire perimeter of the PDMS disc. We quantified collagen thickness and found that PDA modification significantly reduced collagen deposition by 30% **(Figure 4.2b)**.

PDA surface modification modulated cellularity to reduce collagen deposition. Fluorescent and PSR micrographs showed scattered cellularity and collagen development along the edges of PDMS-PDA implants. This suggests that PDA modification might have created

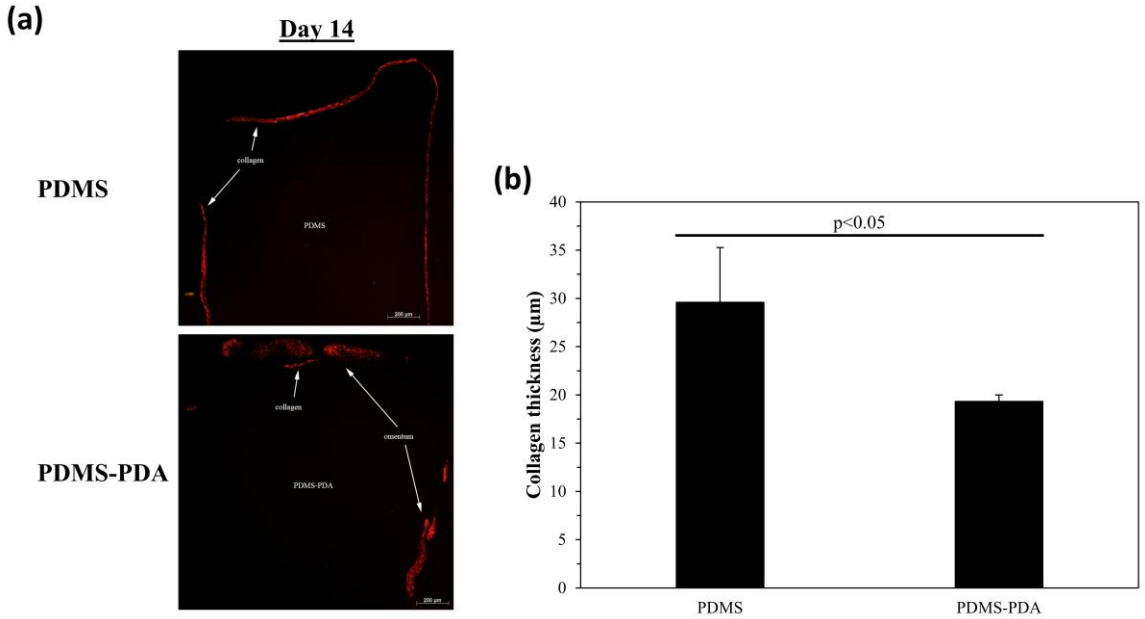

Figure 4.2. Representative polarized micrographs of PSR stained PDMS and PDMS-PDA discs 14 days post-implantation. Collagen was present around the entire perimeter of PDMS implants but was only found at small sections of PDMS-PDA implants. (b) Quantified birefringent regions revealed PDMS-PDA implants had 30% less collagen buildup than PDMS implants. Values shown represent mean ± SEM (n=5) and micrographs are representative of five independent experiments.

unfavourable sections for cell interactions because PDMS has been shown to cause severe fibrosis and cell activity. PDMS discs explanted after 30 days of in submammary pockets of rats were severely encapsulated[20] and PDMS-embedded cochlear implants gradually lost signal detection due to scar tissue development around the device.[21]

PDA promotes M2 peritoneal cells to mediate collagen-1 from adherent cells

PDA reduced myofibroblast cell activity in adherent cells by upregulating epithelial cell marker E-cadherin. Macrophage and myofibroblast markers were extracted from cells attached onto discs that were incubated for 2 and 14 days in mice. Adherent cells had upregulated E-cadherin and downregulated myofibroblast marker α-SMA which suggests a greater presence of epithelial cells than EMT differentiated myofibroblasts

(Figure 4.3). A similar response was seen in PDA surface modified titanium implants where PDA promoted epithelial cell attachment while reducing smooth muscle cell attachment.[22] In contrast, unmodified PDMS promotes myofibroblast activity by stimulating fibroblasts differentiation into myofibroblasts,[23] especially when PDMS is coupled with TGF-β1.[24] High activity of epithelial cells also explains the low collagen-1 mRNA on day 14 and scar tissue buildup from histological analysis. Upregulated type I collagen suggests downregulated myofibroblast activity because type I collagen promotes EMT-derived myofibroblasts whereas epithelial cell phenotype is regulated by type IV collagen.[25] Myofibroblasts have unregulated collagen-1 production that contributes to many fibrosis related diseases including peritoneal fibrosis and renal fibrosis.[11,26]

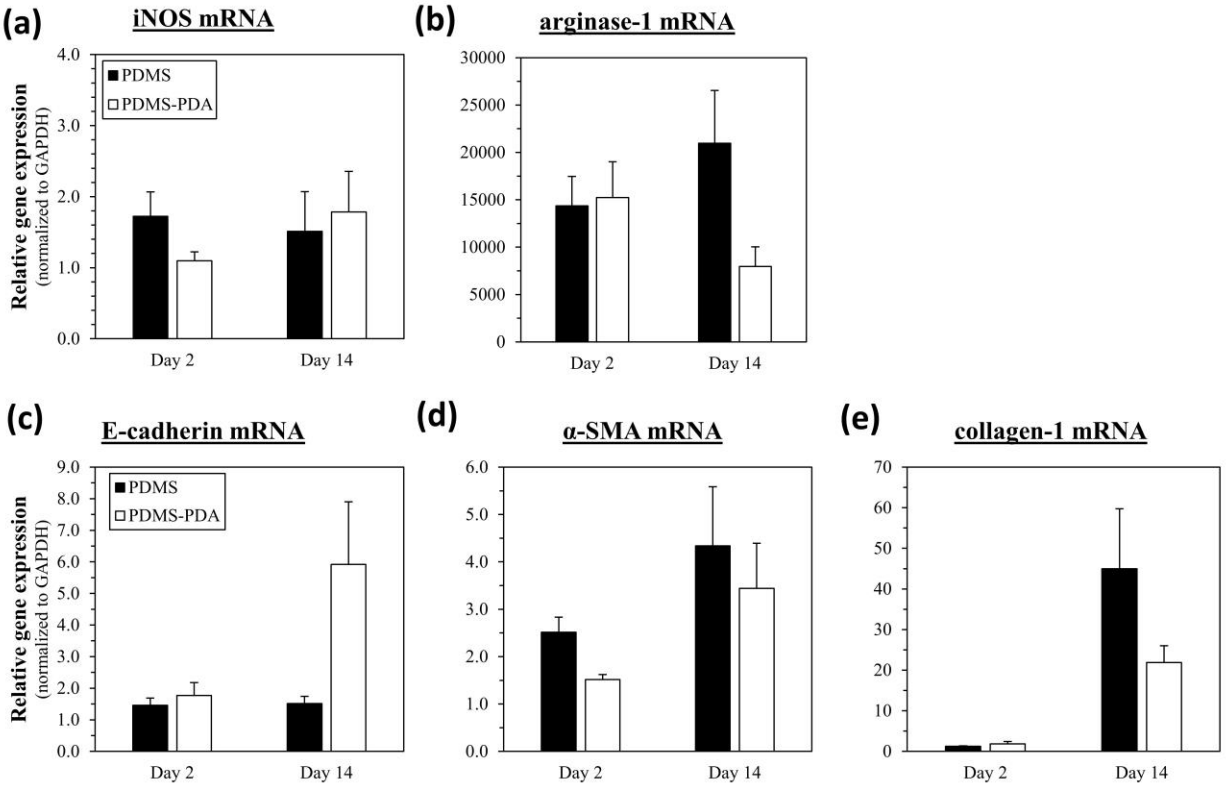

Figure 4.3. (a) iNOS, (b) arginase, (c) E-cadherin, (d) α-SMA and (e) collagen-1 gene expression from cells adhered on implants. After 14 days of implantation, PDMS-PDA upregulated E-cadherin and downregulated collagen-1. Values represent mean ± SEM for five independent experiments.

However, without quantifying adherent cell types we can only speculate that a major population of adherent cells are epithelial cells.

PDA caused peritoneal cells to display an M2 phenotype by upregulating M2 marker arginase-1 and M1 marker iNOS on day 14 **(Figure 4.4)**. Cells displaying the M2 phenotype might have affected adherent cells through cytokine stimulation. M2 macrophages can secrete IL-10 to inhibit tumor necrosis factor alpha (TNF-α)-mediated inflammation[27] to decrease inflammation encourage proper wound tissue repair.[28]

M2 macrophages can also stimulate prostaglandin E_2 (PGE2) production from fibroblasts and stromal cells to regulate myofibroblast differentiation and inflammation.[29,30] PGE2 has been shown to suppress α-SMA activity to reduce EMT-

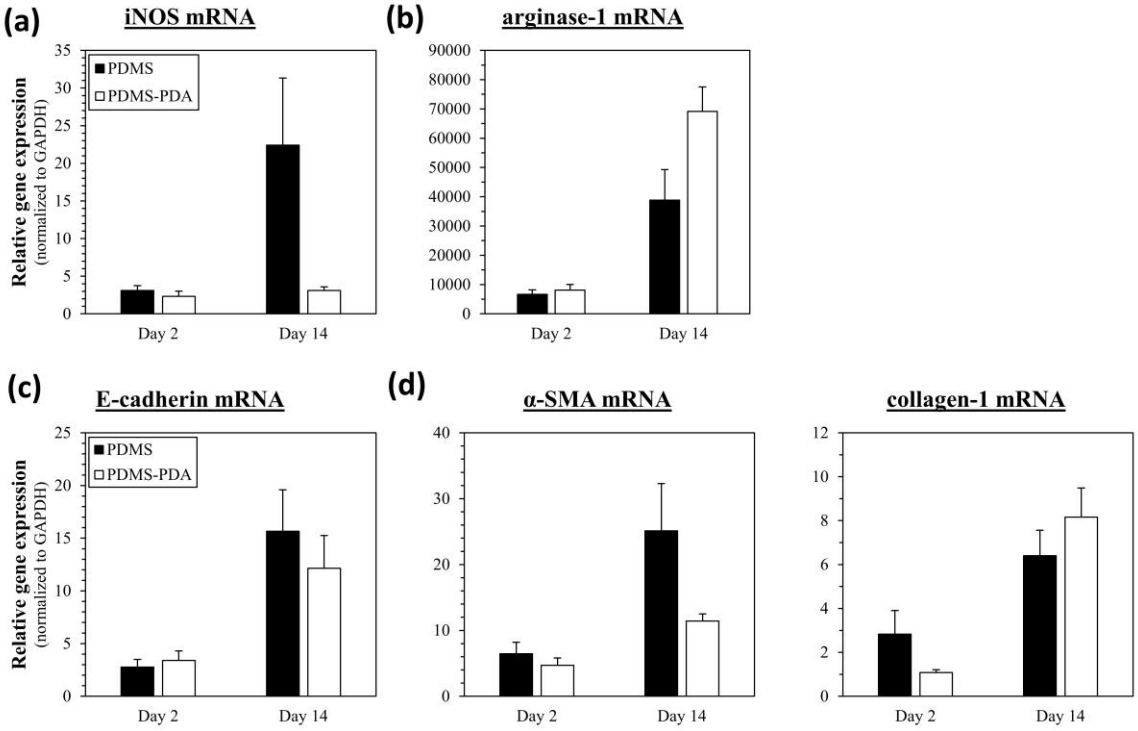

Figure 4.4. (a) iNOS, (b) arginase-1, (c) E-cadherin, (d) α-SMA and (e) collagen-1 Gene response from cells extracted from peritoneal lavages. PDA caused M2 phenotype response with high arginase-1 and low iNOS expression. Values represent mean ± SEM for five independent experiments.

derived myofibroblasts in a TGF-β1 model[31] and reduce inflammation by mitigating M1 phenotype polarization and promoting M2 macrophages to release anti-inflammation mediators.[30]

PDMS-PDA cultured RAW 264.7 responded with a neutral phenotype

To determine if PDA induces an M2 macrophage phenotype in adherent cells, RAW 264.7 cells were cultured on PDMS and PDMS-PDA films for 24 and 48 hours with no change in cell morphology **(Figure S4.2)**. By 48 hours, cells on PDMS films displayed an M2 phenotype with nearly a 2 fold increase in arginase-1 compared to modified surfaces while cells on PDMS-PDA films showed no phenotype polarization **(Figure 4.5)**. Cells cultured on PDMS-PDA had constant arginase-1 levels over the two days but iNOS slightly increased.

Decreasing *in vitro* and *in vivo* iNOS activity suggests that PDA induces an alternative mechanism to activate the nuclear factor-kappa B (NF-κB) proinflammatory signalling pathway. iNOS induces nitric oxide secretion to upregulate TNF-α activity and activates TNF-α.[32] However, our results showed that PDA downregulated both *in vitro* and *in vitro* iNOS mRNA expression. In addition, RAW 264.7 cells cultured on PDA-

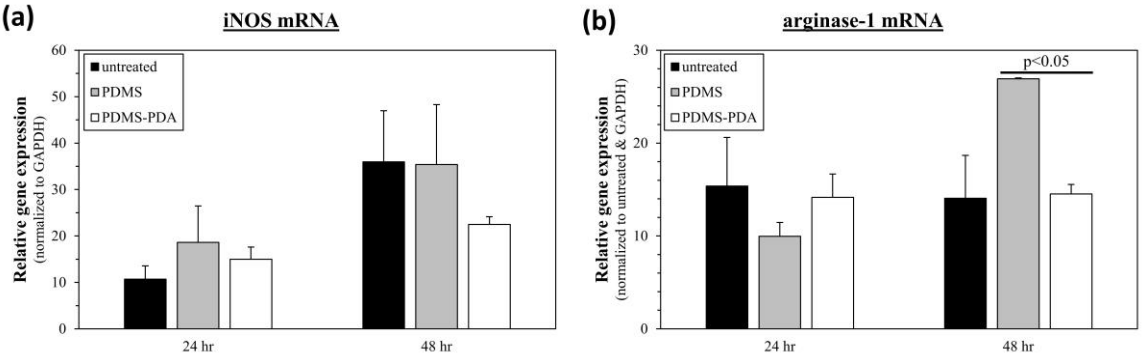

Figure 4.5. Gene response from RAW 264.7 cells cultured on PMDS and PDMS-PDA surfaces for 24 and 48 hours. Values represent mean ± SEM for three independent experiments.

modified titanium implants had no upregulated nitric oxide secretion[33] and downregulated TNF-α activity.[16,33] Endothelial cells also secreted less TNF-α but when cultured on PDA modified poly(lactic acid) meshes.[34]

However, NF-κB can also be activated by members of the IL-1 receptor families such as IL-1β. Yang *et al.* have shown that PDA modified surfaces can upregulate IL-1β secretion after 48 hours of culturing the cells on the material.[34] This suggests that cytokines might be upregulating NF-κB activation and requires further investigation.

Fibrinogen adsorbs to PDMS-PDA in a concentration dependent manner

In addition to the macrophage and myofibroblast response, the extent of fibrosis is also driven by nonspecific protein adsorption. PDA can be used as a "glue" to bind proteins and macromolecules to the surface of a material to prevent, or reduce, protein adsorption.[1] We investigated the adsorption rate of fibrinogen on PDMS and PDMS-PDA implants. Implants were incubated in increasing concentrations of radiolabelled fibrinogen for 3 hours and adsorbed fibrinogen concentrations were quantified.

Fibrinogen adsorbed onto PDMS and PDMS-PDA implants in a concentration dependent manner **(Figure 4.6)**. At low concentrations, PDA surface modification resulted in significantly more fibrinogen adsorption than unmodified discs. However, the difference in fibrinogen adsorption diminished at higher concentrations indicating that surface modification has no effect on fibrinogen adsorption in environments with high fibrinogen. Such environments include blood plasma and the peritoneal plasma where the concentration is 2-4 mg/mL[35] and 3 mg/mL,[36] respectively, in humans.

The fibrinogen adsorption rate is related to the rate of inflammation. Tang *et al.* showed that there is a positive correlation between fibrinogen adsorption and leukocyte

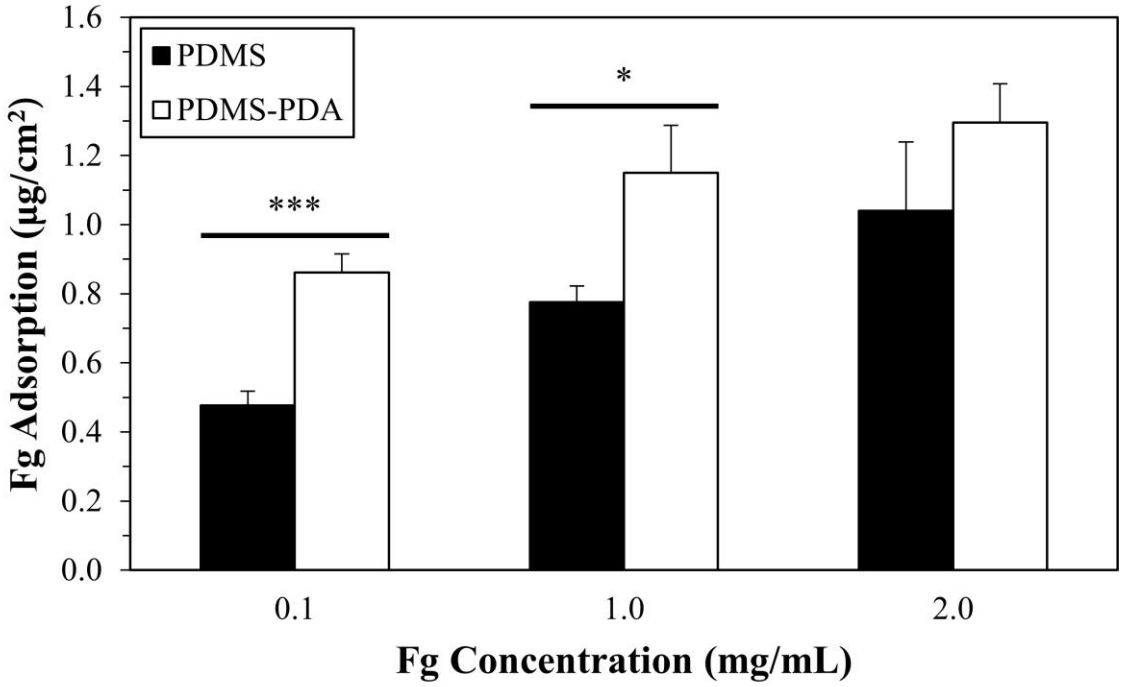

Figure 4.6. Adsorption of radiolabelled fibrinogen (Fg) to PDMS and PDMS-PDA implants after three hours of incubation. Fibrinogen adsorption to PDMS-PDA followed a concentration dependent manner. Values represent mean ± standard deviation for three independent experiments. * represents $p<0.05$ and *** represents $p<0.001$.

response. Materials implanted in the peritoneum of mice that had lower fibrinogen adsorption also had fewer adherent phagocytes.[37] Fibrinogen is recognized by the $\alpha_M\beta_2$ and $\alpha_X\beta_2$ receptors on leukocytes[38] and can activate several immune responses including cell migration and the complement system.[39] For example, fibrinogen coated nanomaterials have upregulated inflammatory responses compared to uncoated materials[40] where Bonfield *et al.* showed that fibrinogen coated PDMS increases macrophage activity. Macrophages stimulated with fibrinogen upregulated IL-1 and basic fibroblast growth factor (bFGF) production which activates NF-κB mediated inflammation and stimulates fibroblast activity, respectively.[41] This suggests that PDMS-PDA implants should cause early acute inflammation.

However, our results show that early acute inflammation resulted in a lower fibrotic response. Histological samples indicated that PDA caused less collagen deposition and cellularity. Fibrinogen might play a role in the early response, but PDA is stimulating other mechanisms that are mediating fibrosis in the late stage. Additional experiments are needed to elucidate this result. This can be done by determining the population of macrophages, fibroblasts and myofibroblasts in adherent cells on PDMS-PDA implants and by quantifying secretion levels of members of the IL-1 family.

PDA modification alters surface characteristics to resolve scar tissue formation. PDA surface modification can increase the substrate's wettability to reduce an inflammatory response. Hydrophobicity and contact angle decreases on a substrate because PDA contains many OH^- and NH_2^- groups.[1] As previously mentioned, RAW 264.7 cells cultured on PDA modified titanium substrates secreted less proinflammatory mediators.[16,33,42] In general, it is seen that hydrophilic substrates result in lower inflammatory responses because they promote cell adhesion and proliferation.[4,43] PDA modification also increases substrate surface roughness where surface roughness has been shown to promote cell adhesion and proliferation[42] but reduce cell spreading.[43]

In this study, we investigated the fibrotic response from PDA modified PDMS implants. PDA surface modification caused less collagen deposition and cellularity thickness by promoting adherent cells to respond in a antifibrotic manner where epithelial marker E-cadherin was upregulated and collagen-1 was downregulated. In addition, peritoneal cells displayed M2 markers with high arginase-1 and low iNOS. Fibrinogen was readily adsorbed onto PDMS-PDA to stimulate acute inflammation but early immune

response had no effect on scar tissue formation. Several drug release methods have been developed to extend the lifetime of implantable biomedical devices but releasing drugs can be expensive. PDA surface modification offers a low cost and easy method to reduce fibrosis.

4.5 ACKNOWLEDGMENTS

The authors would like to acknowledge that this work was supported by the Natural Sciences and Engineering Research Council. We thank Emma Buller and Ugonwa Echendu for their assistance with animal studies and blinded collagen thickness and blood smear quantification studies.

4.6 DISCLOSURE STATEMENT

The authors declare that there were no conflicts of interests regarding the publication of this paper.

4.7 REFERENCES

1. Wu, C. *et al.* Mussel-inspired bioceramics with self-assembled Ca-P/polydopamine composite nanolayer: Preparation, formation mechanism, improved cellular bioactivity and osteogenic differentiation of bone marrow stromal cells. *Acta Biomater.* **10,** 428–438 (2014).

2. Ball, V. Physicochemical perspective on 'polydopamine' and 'poly(catecholamine)' films for their applications in biomaterial coatings (Review). *Biointerphases* **9,** 30801 (2014).

3. Beckford, S., Mathurin, L., Chen, J., Fleming, R. A. & Zou, M. The effects of polydopamine coated Cu nanoparticles on the tribological properties of polydopamine/PTFE coatings. *Tribol. Int.* **103,** 87–94 (2016).

4. Anderson, J. M., Rodriguez, A. & Chang, D. T. Foreign body reaction to biomaterials. *Semin. Immunol.* **20,** 86–100 (2008).

5. Anderson, J. M. Chapter 4 Mechanisms of inflammation and infection with implanted devices. *Cardiovascular Pathology* **2,** 33–41 (1993).

6. Williams, D. F. On the mechanisms of biocompatibility. *Biomaterials* **29,** 2941–2953 (2008).

7. Martinez, F. O. & Gordon, S. The M1 and M2 paradigm of macrophage activation: time for reassessment. *F1000Prime Rep.* **6,** 13 (2014).

8. Kaneko, K., Hamada, C. & Tomino, Y. Peritoneal fibrosis intervention. *Perit. Dial. Int.* **27,** (2007).

9. Radisky, D. C., Kenny, P. a & Bissell, M. J. Fibrosis and cancer: do myofibroblasts come also from epithelial cells via EMT? *J. Cell. Biochem.* **101,** 830–9 (2007).

10. Hinz, B. *et al.* The Myofibroblast. *Am. J. Pathol.* **170,** 1807–1816 (2007).

11. Klingberg, F., Hinz, B. & White, E. S. The myofibroblast matrix: Implications for tissue repair andfibrosis. *J. Pathol.* **229,** 298–309 (2013).

12. Shen, J. *et al.* Tissue engineering bone using autologous progenitor cells in the peritoneum. *PLoS One* **9,** 1–7 (2014).

13. Khorasani, M. T. & Mirzadeh, H. In vitro blood compatibility of modified PDMS surfaces as superhydrophobic and superhydrophilic materials. *J. Appl. Polym. Sci.* **91,** 2042–2047 (2004).

14. Zhang, H. & Chiao, M. Anti-fouling Coatings of Poly(dimethylsiloxane) Devices for Biological and Biomedical Applications. *J. Med. Biol. Eng.* **35,** 143–155 (2015).

15. Lim, K. *et al.* Development of a catheter functionalized by a polydopamine peptide coating with antimicrobial and antibiofilm properties. *Acta Biomater.* **15,** 127–138 (2015).

16. Xu, D. *et al.* Surface functionalization of titanium substrates with cecropin B to improve their cytocompatibility and reduce inflammation responses. *Colloids Surfaces B Biointerfaces* **110,** 225–235 (2013).

17. Leung, J. M. *et al.* Surface modification of poly(dimethylsiloxane) with a covalent antithrombin–heparin complex for the prevention of thrombosis: use of polydopamine as bonding agent. *J. Mater. Chem. B* **3,** 6032–6036 (2015).

18. Truong, T. ImageJ-perpendicularThicknessTool. (2016). doi:10.5281/zenodo.50157

19. Livak, K. J. & Schmittgen, T. D. Analysis of relative gene expression data using real-time quantitative PCR and the 2^(-ΔΔCT) method. *Methods* **25,** 402–408 (2001).

20. Ng, K. K., Awad, N., Brook, M. a, Holloway, A. C. & Sheardown, H. Local delivery of nicotine does not mitigate fibrosis but may lead to angiogenesis. *J. Biomater. Appl.* **26,** 349–58 (2011).

21. Bohl, A. *et al.* Development of a specially tailored local drug delivery system for the prevention of fibrosis after insertion of cochlear implants into the inner ear. *J. Mater. Sci. Mater. Med.* **23,** 2151–2162 (2012).

22. Zhong, S. *et al.* Effects of polydopamine functionalized titanium dioxide nanotubes on endothelial cell and smooth muscle cell. *Colloids Surfaces B Biointerfaces* **116,** 553–560 (2014).

23. Deng, L. Substrate stiffness influences TGF-β1-induced differentiation of bronchial fibroblasts into myofibroblasts in airway remodeling. *Mol. Med. Rep.* **7,** 419–424 (2012).

24. Amoozgar, B., Fitzpatrick, S. & Sheardown, H. Effect of anti-TGF-β2 surface modification of polydimethylsiloxane on lens epithelial cell markers of posterior capsule opacification. *J. Bioact. Compat. Polym.* **28,** 637– 651 (2013).

25. Zeisberg, M. *et al.* Renal fibrosis: collagen composition and assembly regulates epithelial-mesenchymal transdifferentiation. *Am. J. Pathol.* **159,** 1313–21 (2001).

26. Wan, J. *et al.* Role of Complement 3 in TNF-α-Induced Mesenchymal Transition of Renal Tubular Epithelial Cells In Vitro. *Mol. Biotechnol.* **54,** 92–100 (2013).

27. Park-Min, K. H., Antoniv, T. T. & Ivashkiv, L. B. Regulation of macrophage phenotype by long-term exposure to IL-10. *Immunobiology* **210,** 77–86 (2005).

28. Brown, B. N. *et al.* Macrophage phenotype as a predictor of constructive remodeling following the implantation of biologically derived surgical mesh materials. *Acta Biomater.* **8,** 978–987 (2012).

29. Kalinski, P. Regulation of immune responses by prostaglandin E2. *J. Immunol.* **188,** 21–8 (2012).

30. Ylöstalo, J. H., Bartosh, T. J., Coble, K. & Prockop, D. J. Human mesenchymal stem/stromal cells cultured as spheroids are self-activated to produce prostaglandin E2 that directs stimulated macrophages into an anti-inflammatory phenotype. *Stem Cells* **30,** 2283–2296 (2012).

31. Garrison, G. *et al.* Reversal of Myofibroblast Differentiation by Prostaglandin E 2. *Am. J. Respir. Cell Mol. Biol.* **48,** 550–558 (2013).

32. Hall, D. T., Ma, J. F., Di Marco, S. & Gallouzi, I.-E. Inducible nitric oxide synthase (iNOS) in muscle wasting syndrome, sarcopenia, and cachexia. *Aging (Albany. NY).* **3,** 702–715 (2011).

33. Xie, D., Cai, K., Hu, Y. & Luo, Z. Surface engineering of titanium substrates with chitosan-atorvastatin conjugate for reduced inflammation responses and improved cytocompatibility. *J. Biomed. Mater. Res. - Part A* **101 A,** 2005–2014 (2013).

34. Yang, W. *et al.* Improving cytoactive of endothelial cell by introducing fibronectin to the surface of poly L-Lactic acid fiber mats via dopamine. *Mater. Sci. Eng. C* **69,** 373–379 (2016).

35. Tennent, G. a *et al.* Human plasma fibrinogen is synthesized in the liver Human plasma fibrinogen is synthesized in the liver Short title : **109,** 1971–1975 (2009).

36. Prinsen, B. H. C. M. T. *et al.* Increased albumin and fibrinogen synthesis rate in patients with chronic renal failure. *Kidney Int.* **64,** 1495–1504 (2003).

37. Tang, L., Wu, Y. & Timmons, R. B. Fibrinogen adsorption and host tissue responses to plasma functionalized surfaces. *J. Biomed. Mater. Res.* **42,** 156–163 (1998).

38. Ugarova, T. P. & Yakubenko, V. P. Recognition of fibrinogen by leukocyte integrins. *Ann. N. Y. Acad. Sci.* **936,** 368–85 (2001).

39. Forsyth, C. B., Solovjov, D. a, Ugarova, T. P. & Plow, E. F. Integrin alpha(M)beta(2)-mediated cell migration to fibrinogen and its recognition peptides. *J. Exp. Med.* **193,** 1123–1133 (2001).

40. Marucco, A., Gazzano, E., Ghigo, D., Enrico, E. & Fenoglio, I. Fibrinogen enhances the inflammatory response of alveolar macrophages to TiO2, SiO2 and carbon nanomaterials. *Nanotoxicology* **5390,** 1–9 (2014).

41. Bonfield, T. L., Colton, E. & Anderson, J. M. Fibroblast stimulation by monocytes cultured on protein adsorbed biomedical polymers. I. Biomer and polydimethylsiloxane. *J. Biomed. Mater. Res.* **25,** 165–75 (1991).

42. Hamlet, S., Alfarsi, M., George, R. & Ivanovski, S. The effect of hydrophilic titanium surface modification on macrophage inflammatory cytokine gene expression. *Clin. Oral Implants Res.* **23,** 584–590 (2012).

43. Dowling, D. P., Miller, I. S., Ardhaoui, M. & Gallagher, W. M. Effect of Surface Wettability and Topography on the Adhesion of Osteosarcoma Cells on Plasma-modified Polystyrene. *J. Biomater. Appl.* **26,** 327–347 (2011).

44. Truong, T. ImageJ-bloodSmearCount. (2016). doi:10.5281/zenodo.153873

S4: CHAPTER 4 – SUPPLEMENTARY INFORMATION

S4.1 MATERIALS & METHODS

White blood cell quantification in whole blood

Cardiac puncture was used to collect whole blood for blood smear quantification. Blood smears were made using Giemsa-Wright stain (Sigma-Aldrich, Milwaukee) and by following the manufacturer's protocol. In a single blinded study, white blood cells were quantified using an in-lab developed ImageJ macro.[44]

S4.2 FIGURES

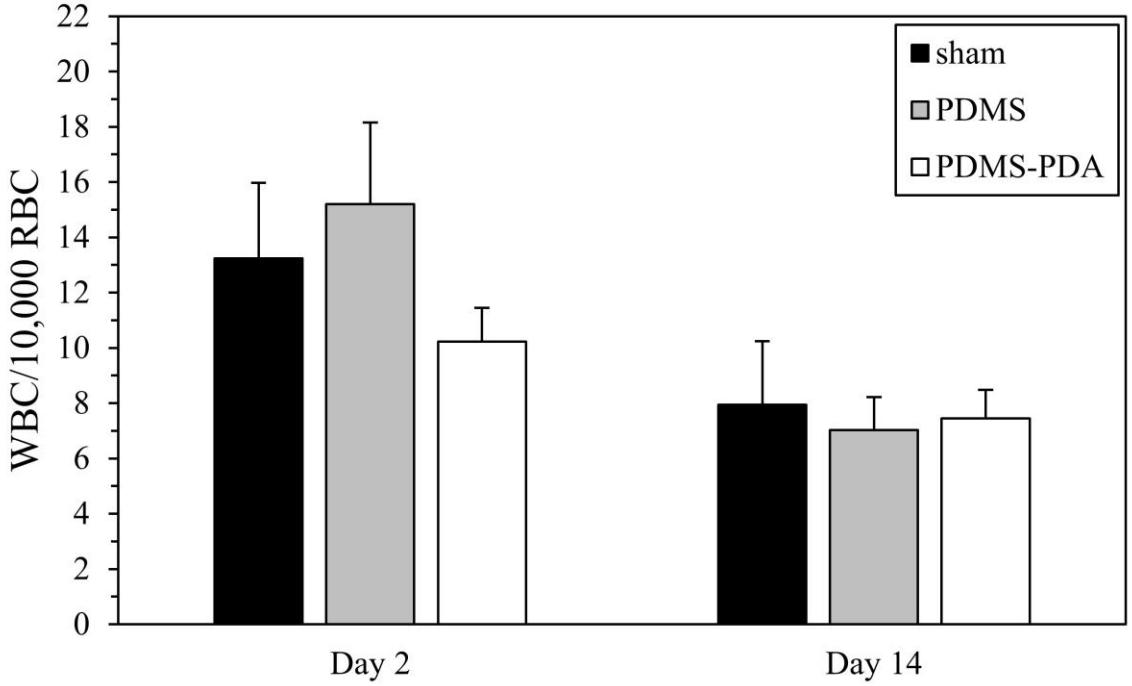

Figure S4.1. Ratio of white blood cells (WBC) to red blood cells (RBC) in systemic blood. PDMS and PDMS-PDA did not cause systemic inflammation. PDMS and PDMS-PDA implants were incubated in mice for 2 and 14 days before whole blood was collected via cardiac puncture. Values represent mean ± SEM for five independent experiments.

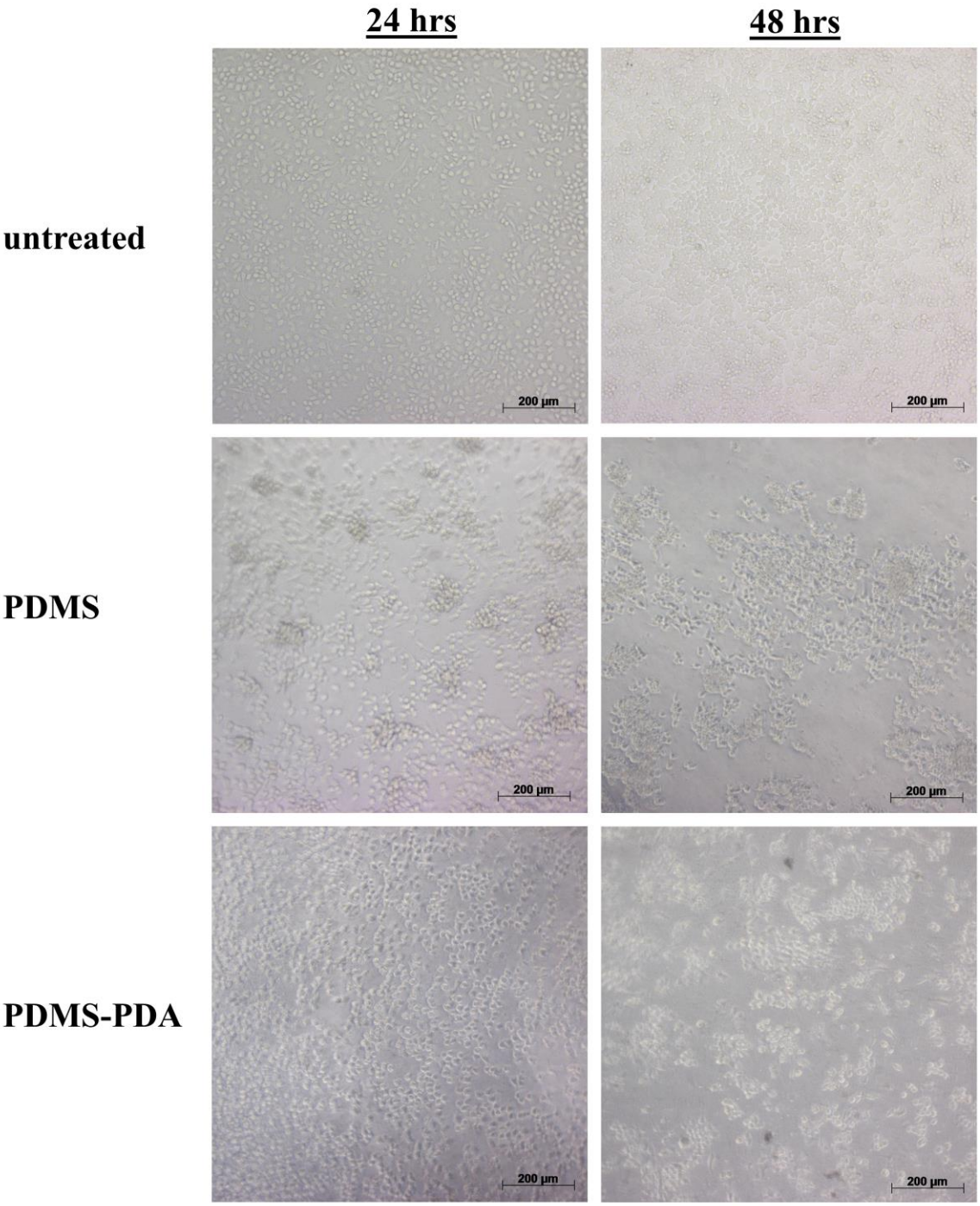

Figure S4.2. RAW 264.7 cells cultured on PDMS and PDMS-PDA films for 24 and 48 hrs. Surface material did not cause a morphology change but it did decrease population density. Micrographs are representative for three independent experiments.

CHAPTER 5: CONCLUSION & FUTURE WORK

PLGA-induced fibrosis was successfully reduced by releasing capsaicin and PGE2 from PLGA carriers in mice. Capsaicin and PGE2 reduced scar tissue formation by 40% and 55%, respectively. Both drugs downregulated the fibrotic response by promoting M2 macrophages to produce anti-inflammatory IL-10 and PGE2 was shown to decrease IL-23 mediated inflammatory responses in peritoneal cells. Release kinetics data indicated that capsaicin would be continuously released for the lifetime of the PLGA implant, but most interesting was the possible permanent effect that PGE2 had on fibrosis. Almost all of the PGE2 was released within 24 hours but the fibrotic layer remained significantly less than the control after 42 days of incubation.

A surprising discovery was made with PDA surface modified PDMS (PDA-PDMS) discs where the fibrotic response from anti-inflammatory macromolecule bound PDA-PDMS discs and PDA-PDMS controls both significantly reduced the cellularity layer compared to unmodified controls. In addition, cellularity around the macromolecule bound PDA-PDMS discs and PDA-PDMS controls were similar, which prompted us to conclude that PDA modification itself has anti-fibrotic effects and reduces fibrosis. Subsequent *in vivo* studies revealed that PDA modification was sufficient to reduce fibrosis development around PDMS implants and significantly reduce scar tissue development by 30%. Interestingly, PDA had no effects on macrophage activity and readily adsorbs fibrinogen but our results show that scar tissue formation is independent of fibrinogen adsorption.

To expand the knowledge gained from this thesis, efforts should be made to quantify the cell types of adherent and peritoneal lavage cells. The genetic response of collected cells was sufficient to determine the overall response but it would be interesting to known which population of cells were present and which were responsible for expressing certain genetic and cytokine markers. Cell type quantification would elucidate the early presence of macrophages when capsaicin and PGE2 was used or if PDA modification had an effect on cell migration and attachment. Additional markers should also be used to identify M2 subtypes and see what role they play in biomaterial-induced fibrosis. Collagen deposition rate would be an interesting topic to investigate as well. We showed that capsaicin, PGE2 and PDA significantly reduced collagen thickness, but how long will it take for modified implants to have a collagen thickness as thick as the untreated controls? This will allow us to determine if the three delay collagen deposition at different rates and to predict how long each compound can extend the efficacy of a biomaterial device, such as a sensor. Another area that needs further investigation is the activation of inflammatory and fibrotic pathways. Now that it has been demonstrated that capsaicin, PGE2 and PDA suppresses fibrosis, the mechanisms and pathways should be investigated to determine if there is crosstalk between cell types or if biomaterials are activating an alternative pathway to induce fibrosis. Lastly, animal numbers should also be increased to decrease variability because most of the data had non-significant treatment effects in ANOVAs indicating that the studies were underpowered.

Overall, capsaicin and PGE2 were demonstrated to have potential as anti-fibrotic agents for long term drug release applications while PDA surface modification revealed

that fibrinogen adsorption and early macrophage response had no effect on biomaterial-induced fibrosis. While the exact mechanisms of how biomaterials induce fibrosis is unknown, this work demonstrates that suppressing overall immune response by promoting IL-10 secretion is an effective strategy to reduce fibrosis.

APPENDIX A

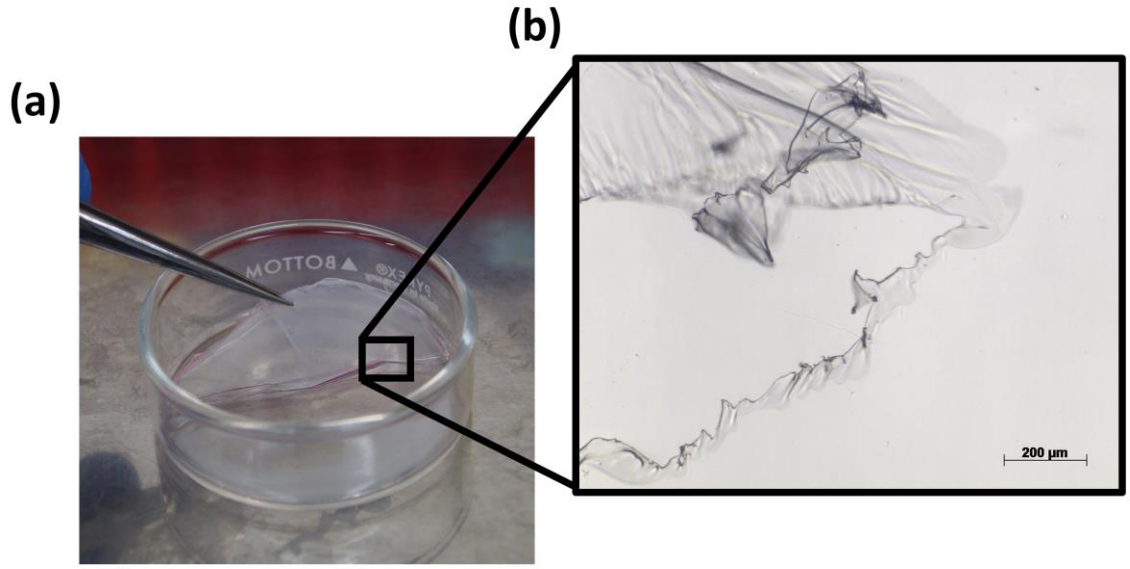

Figure A.1. PLGA films cast in 60 mm glass Petri dishes using solvent casting. (a) The PLGA film weighed 0.01 g and was 0.1729 mm thick. (b) Bright-field microscopy revealed a homogenous layer of PLGA with no openings except for tears that formed when the film was peeled from the surface.

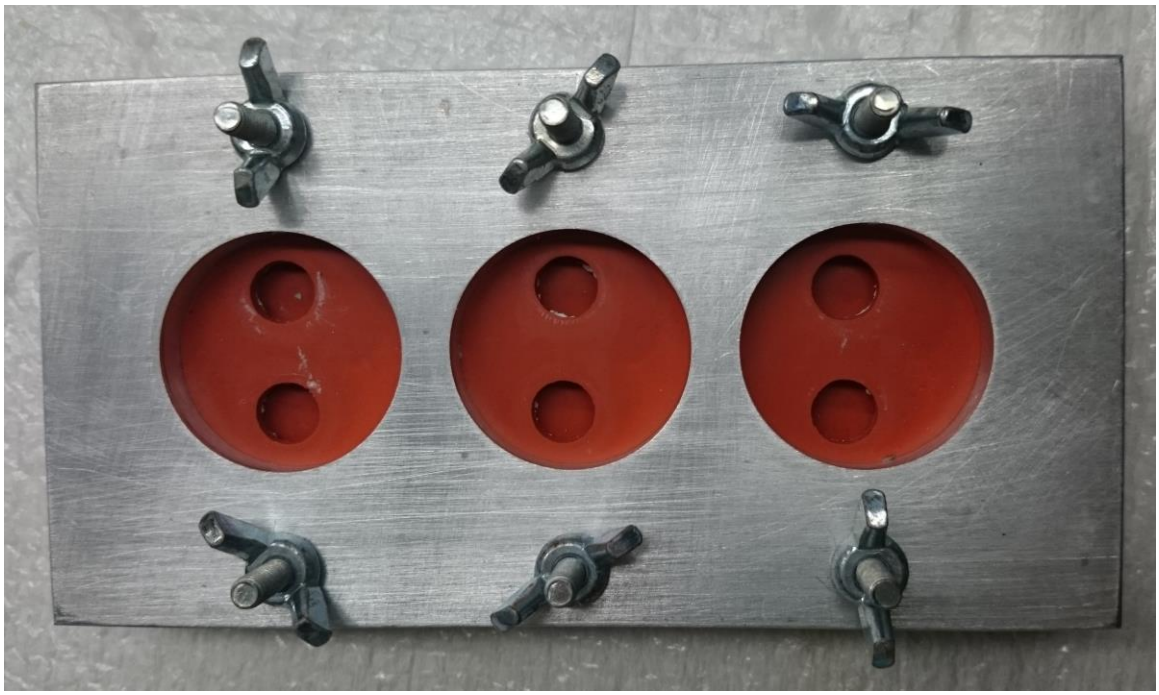

Figure A.2. The custom made silicone and aluminum mold used to cast PLGA implants for *in vivo* studies. Wells were 3/8" in diameter and 1/4" deep.

Figure A.3. PLGA and capsaicin-embedded PLGA discs were stored in sterile Petri dishes prior to being implanted in mice. Implants had a diameter of 1 cm and a thickness of 0.17 mm. Residual PLGA, seen on the outer edge of the disc, was not removed.

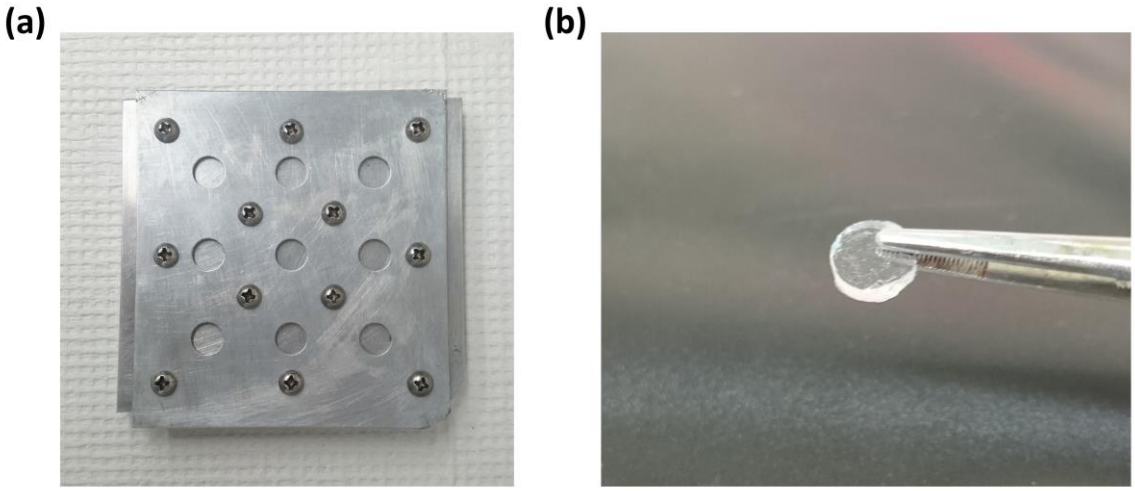

Figure A.4. (a) Stainless steel mold used to cast PDMS discs. Wells are 1 cm in diameter and 1 mm depth. (b) Discs were removed from the mold and autoclaved before undergoing PDA surface modification.

Table A.1. Forward and reverse primer sequences for qPCR assay. Primers were designed using Primer3Plus.

Species	**Gene**	**Forward and reverse primer sequences**
Human	cadherin-1 (E-cadherin, CDH1)	Hs01023894 (ThermoFisher, Burlington)
Mouse	α-smooth muscle actin (α-SMA)	5'- GACGGCTGAGATTTGCTTTC-3' 3'- GTGCAAATGGGTGTGCATAG-5'
Mouse	arginase-1	5'-CAGCTCTTCATTGGCTTTCC-3' 3'-ACCTGGCCTTTGTTGATGTC-5'
Mouse	cadherin-1 (E-cadherin)	5'- TCTGAACATGAGAGCGGATG-3' 3'- TTATCTCCCGGCAACATCTC-5'
Mouse	collagen-1	5'- AGGCATAAAGGGTCATCGTG-3' 3'- TCAGGGTATGGTGGAAAAGG-5'
Mouse	glyceraldehyde-3-phosphate dehydrogenase (GAPDH)	5'-GCTGCTTCCCGAGTAAAATG-3' 3'-TAATGGGGAGAGGTTCGATG-5'
Mouse	inducible nitric oxide synthase (iNOS)	5'-ATGGGTCTGTCCTTGCAAAC-3' 3'-AAGGCCAAACACAGCATACC-5'